國 立 交 通 大 學

電 子 物 理 研 究 所

碩 士 論 文

全電性自旋流量測的研究

A STUDY ON AN ALL-ELECTRIC DETECTION OF SPIN CURRENT

研 究 生：周昆宜

指導教授：朱仲夏教授

中華民國九十八年十月

全電性自旋流量測

A STUDY ON AN ALL-ELECTRIC DETECTION OF SPIN CURRENT

研 究 生：周昆宜　　Student：Kun-Yi Chou

指導教授：朱仲夏教授　　Advisor：Prof. Chon Saar Chu

國 立 交 通 大 學

電 子 物 理 研 究 所

碩 士 論 文

A Thesis
Submitted to Department of Electrophysics
College of Science
National Chiao Tung University
in Partial Fulfillment of the Requirements
for the Degree of
Master
in
Electrophysics

October 2009
Hsinchu, Taiwan, Republic of China

中華民國九十八年十月

全電性自旋流量測的研究

研究生：周昆宜　　　　　　　　　　　　　指導教授：朱仲夏教授

國立交通大學

電子物理研究所

摘要

我們提出了一種全電性量測交流自旋流(alternating spin current)的方法並且理論計算出交流自旋流所產生的電信號。我們的系統主要利用半導體中的自旋軌道交互作用，以平面二維電子氣(two-dimension electron gas)夾在兩個金屬閘極中間作為測量裝置，在這樣結構中的電磁波為波導的模態。我們研究在自旋極化方向與流動方向相互垂直並且躺在二維電子氣平面中的自旋流，這樣的交流自旋流會激發出光子，只有對應於橫向磁場的波導模式(transverse magnetic modes)的光子才被激發。光子在兩個閘極之間產生交替的電位差，而此電位差是可以用實驗去量測的。

A STUDY ON AN ALL-ELECTRIC DETECTION OF SPIN CURRENT

Student: Kun-Yi Chou Advisor：Prof. Chon Saar Chu

Department of Electrophysics
National Chiao Tung University

Abstract

We propose a pure electrical means of detecting an alternating (ac) spin current, and we perform theoretical calculations on the order of magnitude of the expected electrical signal. Our proposed scheme has employed the spin-orbit interaction in semiconductors. The proposed measurement device consists of a two-dimensional electron gas (2DEG) sandwiched between two metallic gates such that the electromagnetic waves in between the gates are waveguide modes. An ac in-plane spin current, with both spin and flow direction orthogonal to each other and in the plane of the 2DEG, passes through the structure is found to excite photons. Only photons corresponding to the transverse magnetic (TM) waveguide modes are excited. These excitations give rise to an ac electrical potential difference between the two metal gates. The potential difference is found to be measurable by present day experimental capability.

致謝

能夠完成碩士學位，我特別感謝朱老師兩年多來的諄諄教誨，不只是在知識上的傳授，更重要的是處事的態度，以及學習的方法。也同樣感謝唐志雄學長、王律堯學長、張榮興學長、江吉偉學長、邱志宣學長，幾位學長都曾多次幫我解答課業與研究上的困難，還有謝謝小明和阿杜兩位同學，我們一起讀書相互勉勵。除此之外更要謝謝爸爸、媽媽、哥哥和朋友的支持與鼓勵。

Contents

List of Figures

Chapter 1

Introduction

To start this first chapter of this thesis, we provide in Sec. 1-1, a general guide to the structure of the thesis. The next two sections of this introductory chapter cover the background and motivation of this thesis. The last section describes our calculation method in this thesis.

1.1 Introductory touring to this thesis

In the first chapter, we introduce the background of spintronics as well as spin-orbit interaction, and we propose the motivation of this issue and the calculation method in this thesis. Chapter 2 describes the geometric structure of our system and the quantization of electromagnetic wave confined by the waveguide. In Chapter 3, we solve two traditional electrodynamics problems with our calculation method, for checking if our method is practical. In Chapter 4, we solve the electric field induced by ac in-plane polarized spin current. Chapter 5 reports that the signal generated by ac in-plane polarized spin current is measurable. Finally, we discuss and take conclusions in this thesis.

1.2 Background and Review

In this review section, we present a brief background on spintronics, on spin current, on spin-orbit interaction, and on the progress in the research on the measurement of spin current.

Spintronics

Spintronics is an area of intense current scientific interests[1]. It is important for information storage and quantum computing. Fundamental studies of spintronics include investigations of spin transport in materials, as well as measurement of spin accumulation, spin relaxation, and spin current. Especially, spin current plays an important role in an spintronic devices. Our work in this thesis focus on measurenent of spin current. We must understand the definition of spin current before our work.

Spin current

In this paragraph, we explain the definition of spin current. An electron carries both charge and spin which may have two components: up and down. In the semi-classical picture, spin can be described by a unit vector. Traditional charge current is a flow of electron which is the sum of flows of up- and down-spin electrons. The spin information may be neglected in charge current. A spin current differs from a charge current. For a simple description, spin current can be recognized as the difference between the flows of up and down spin electrons. A pure spin current means that equivalent up and down spin flows in the opposite direction. There is no net particle transfer across any cross section of the channel. Measuring spin current in solid state systems provides a new tool to investigate the mesoscopic system, and it also give us hopes that it could be applied in spintronics and quantum information processing in the future. We can say that measurement of spin current is an indispensable part in field of spintronics. It has been found that spin-orbit interaction can be a nice tool to measure spin current all electrically. In the following two subsections we will introduce spin-orbit interaction in an atom and in semiconductor respectively.

Spin-orbit interaction in an atom

Spin-orbit interaction is a well-known phenomenon which is caused from the interaction of a particle's spin with its own motion. A particle in an electric field experiences an effective magnetic field in its co-moving frame. For electrons, it brings about lifting of the degeneracy of energy levels of electrons according to their spin states.

In atomic physics, this interaction comes from the electron spin magnetic moment interacting with the magnetic moment due to the orbit motion of the electron. In non-relativistic approximation to Dirac equation, the form of the spin-orbit interaction term in an atom is given by:

$$H_{SO,vac} = -\frac{e\hbar}{4{m_0}^2c^2}\boldsymbol{\sigma}\cdot(\mathbf{p}\times\mathbf{E}), \tag{1.1}$$

where e is the magnitude of electron charge($e > 0$), $\hbar$ is the Plank's constant, m_0 is the mass of a free electron, c is the light speed in vacuum, $\boldsymbol{\sigma} = (\sigma_x, \sigma_y, \sigma_z)$ are the Pauli matrices , $\mathbf{p}$ is the momentum of the spin, and $\mathbf{E}$ is the electric field that the electron travels through in the atom[2].

When the electron velocity is far less than the speed of light and a small electric field is quite small, the Dirac gap $2m_0c^2 \approx 1MeV$ in the denominator of Eq. (1.1) is too large that the spin-orbit interaction in a single atom is quite week.

We may rewrite equation Eq. (1.1) as $H_{SO,vac} = -e\frac{\Lambda_{vac}}{\hbar}\boldsymbol{\sigma}\cdot(\mathbf{p}\times\mathbf{E})$, where $\Lambda_{vac} = \frac{\hbar^2}{4{m_0}^2c^2}$ is the spin-orbit coupling constant in vacuum. Actually, spin-orbit interaction in vacuum or in a single atom has the same coupling constant, but the electric field comes from different sources. In a atom, electric field comes from the atomic nucleus. In vacuum, the electric field comes from the divergence of the potential in space. Even though the spin-orbit coupling in a single atom or in vacuum is very week, it will be magnified in semiconductor.

Spin-orbit interaction in semiconductor

Spin-orbit interaction in solid state physics have the same form as Eq. (1.1) but difference in the spin-orbit coupling due to the energy gap difference. In semiconductor, spin-orbit coupling may be enhanced with several orders. The coupling strength is mostly derived from the electrons with high velocity under the strong electric field near the core of the atoms, rather than the weak velocity movement. Due to the periodicity of crystal, the electron energy spectrum form energy band structure in the reciprocal vector space. If the crystal system does not have the space inversion symmetry, the band gap will be narrower which result in stronger spin orbit coupling. In GaAs, the spin-orbit coupling constant Λ is about 82.5 $\mathring{A}^2$ which is seven order magnitude greater than Λ_{vac}. The perturbing spin-orbit coupling Hamiltonian in GaAs may be written as:

$$H_{SO,sc} = e\frac{\Lambda}{\hbar}\boldsymbol{\sigma} \cdot (\mathbf{p} \times \mathbf{E}), \tag{1.2}$$

where Λ is the spin-orbit coupling constant in GaAs. The strength of spin-orbit interaction un semiconductor is manifestly seven order higher in magnitude than that in vacuum such that it becomes a nice tool to detect spin current electrically. Next, we will introduce kinds of principle means of detection of spin current.

Review of measurement of spin current

Generally, there are three kinds of principle means of detection of spin current. Here, we review some of them.

The first method is mechanical measurement[3, 4]. In 2007, E. B. Sonin demonstrates that an equilibrium spin current in two-dimension electron gas (2DEG) with Rashba interaction which is one kind of spin-orbit interaction will lead to a mechanical torque on a substrate near an edge of the Rashba medium[4]. If the substrate is flexible enough that the torques would distort it, it is a method to detect equilibrium spin currents experimentally that he measure the degree of contortion.

Optical detection is also a general way to measure spin current[5–7]. In 2008, J. Wang, B. F. Zhu, and R. B. Liu described the first non-invasive method of measure pure spin current directly by a polarized light beam [7]. The polarized light beam which act as a 'photon spin current' will interact with spin current due to the spin-orbit coupling without the Rashba or the Dresselhaus effect. The interaction result in linear and circular optical birefringence. They utilized the birefringence effects to measure to pure spin currents.

The third one is electrical detection[8–12]. In 1985, Mark Johnson and R. H. Silsbee performed the experiment in non-magnetic aluminum strip contacted to two ferromagnetic electrodes[11]. They reported that injecting charge current from one of ferromagnetic electrodes into aluminum strip results in non-equilibrium spin accumulation at the interface of aluminum strip and the source ferromagnetic electrode. The spin accumulation defuses away from the interface and forms spin current. If there is a non-equilibrium spin accumulation in the vicinity of the detector, an open-circuit voltage will be developed across the interface. In 2006, S. O. Valenzuela and M. Tinkham demonstrate electrical detection of spin currents in metallic nanostructures. They apply reciprocal spin Hall effect in a diffusive metallic conductor and obtain its spin Hall conductivity. Finally they measure the laterally induced voltage which results from the conversion of the injected spin current into charge imbalance owing to the spin-orbit coupling. There are still Some other means of electrical detection of spin current proposed in resent years including theoretical and experimental proposition. It is worth to mention that in 2004, Qing-feng Sun et al. propose a journal named "spin-current induced electric field" [12]. In that article, the authors investigate properties of the induced electric field of a steady-state spin-current without charge current. They regard one electron spin as a magnetic dipole. Such magnetic dipole current will generate electric field in space. They claim that a spin current with drift velocity $10^{-2}m/s$ flowing in an infinitely long wire with cross section area of 2 $mm \times 2$ mm and the magnetic moment is perpendicular to the current direction.

The spin current causes the potential difference$\sim$ 12 μV at distance -1.1 mm and 1.1 mm on either side of the wire. It is a novel method to measure spin current by measuring the voltage directly induced by spin current. Even though the potential difference their report is measurable, the spin current is up to 640.82 Ampere. That is very giant magnitude of spin current. It is extremely difficult to generate such strong current in the thin wire.

1.3 Motivation

In Sec. 1-2, we mentioned the paper which is proposed by Sun et al.[12] and based on the calculation of electrodynamics and relativity. They utilized the potential difference induced by magnetic dipole current to detect spin current. The spin-orbit interaction strength can be enhanced up to six orders of magnitude in semiconductor rather than in vacuum. We think that if spin current flows in semiconductor, we may think that it could induce more strongly electric field than in vacuum. It may be a power tool to measure spin current by detecting the potential difference induced by spin current. But it is very hard both to take the advantages of spin-orbit interaction in semiconductor and to use the calculation method of electrodynamics simultaneous. We can not find any equation corresponding to the enhanced strength of spin-orbit interaction in electrodynamics. However from the hamiltonian Eq. (1.2), we may take the advantages of spin-orbit interaction in semiconductor and calculate the potential difference induced by ac spin current in semiconductor from the viewpoint of photons.

In addition, from equation Eq. (1.2), we support that the spin polarized direction, the direction of spin flow, and electric field induced by ac spin-polarized current are perpendicular to each other. Therefore, we want to design a device which can detect the ac electrical potential difference generate by ac spin polarized current, and two parallel-planes waveguide is the best choose. The two parallel-planes waveguide is not only easy-fabricated but also measures the electrical potential difference easily. If the spin polarized direction and the ac in-plane spin flow is parallel to the metal gates of waveguide and they are perpendicular to each other, it will generate electric field which is perpendicular to the metal gates of the waveguide. In this thesis, we propose that the ac spin current which flowing in 2DEG which is at the middle of the two metal gates of a two parallel-planes waveguide can induced electrical signal. This signal is measurable if we add appropriate external circuit.

1.4 Introduction to calculation method

Our calculation is based on non-degenerate perturbation theorem. The calculation starts from the perturbing spin-orbit interaction term of the Hamiltonian.

$$H' = e\frac{\Lambda}{\hbar}\boldsymbol{\sigma} \cdot (\mathbf{p} \times \mathbf{E}) \,, \tag{1.3}$$

where e is the magnitude of electron charge ($e > 0$), Λ is the spin-orbit interaction constant in semiconductor, $\hbar$ is the Plank constant, $\boldsymbol{\sigma} = (\sigma_x, \sigma_y, \sigma_z)$ are the Pauli matrices , and $\mathbf{E}$ is the electric field in the waveguide.

While we consider that the second quantization procedure is applied to quantum field theory, the classical field variables become quantum operators [13]. In classical mechanics, the coordinates and momenta of a classical system can specify its state. In ordinary quantum mechanics, the position and the momentum of a single particle promoted to operators because the observables of position and the momentum can be quantized. The ordinary quantum mechanics can only deal with the number of conserved particle systems. However, in relativistic quantum mechanics, particles can be generated and annihilated. The mathematical formulations of ordinary quantum mechanics no longer apply. We must dealing with the creation and annihilation of particles with second quantization which is the establishment of relativistic quantum mechanics and quantum field theory. Second quantization method can deal with natural and simple symmetry of identical particles and anti-symmetry. Essentially, if we can stand in the viewpoint of electron to solve the problem with electromagnetic methods, but it is difficult to calculate. That is why we solve the problem with second quantization method.

When we sandwich the perturbing Hamiltonian H' with the states of the oscillating spin polarized electron state $|\psi\rangle$, we can obtain the equivalent perturbing Hamiltonian H'_{eff} for the photons which emitted by the oscillating spin current between the parallel slabs. The effective Hamiltonian is given by:

$$H'_{eff} = \langle\psi| e\frac{\Lambda}{\hbar}\boldsymbol{\sigma}\cdot(\mathbf{p}\times\mathbf{E})|\psi\rangle . \tag{1.4}$$

Because the momentum $\mathbf{p}$ is an operator for electron, it act on the photon state. And the "$\mathbf{E}$" in Eq. (1.4) is the operator for photons and it does not act on the electron state.

Applying time-dependent perturbation theory, we will obtain the first order perturbation coefficient. That is

$$f^{(1)}_{n\mathbf{k}\lambda} = \frac{-i}{\hbar}\int_{-\infty}^{t}\langle\{0,0,...,0,1_{n\mathbf{k}\lambda},0,...,0\}| H'_{eff}|\{0\}\rangle dt', \tag{1.5}$$

where the subscript $n\mathbf{k}\lambda$ indicate the mode number. And we get the eigenstate state of first order approximation of the photons. It is given by:

$$|\Psi\rangle = |\Psi_0\rangle + \sum_{n\mathbf{k}\lambda} f^{(1)}_{n\mathbf{k}\lambda}|\{0,0,...,0,1_{n\mathbf{k}\lambda},0,...,0\}\rangle , \tag{1.6}$$

where $|\Psi_0\rangle$ is the initial photon state which is one of the eigenststes of unperturbed Hamiltonian. $|\Psi\rangle$ is the new state after the H' is added to our system. It means that the photon state changes from $|\Psi_0\rangle$ to $|\Psi\rangle$ when the ac spin current is applied. The photon eigetstate tells us all information of the photons of our system which we want to know. Then we sandwich the vector potential in the parallel plate capacitor with the the photon state $|\Psi\rangle$.

$$\mathbf{A}(\mathbf{r},t) = \langle\Psi| A^{(op)}|\Psi\rangle \tag{1.7}$$

The result $\mathbf{A}(\mathbf{r}, t)$ is the expectation value of vector potential in the parallel-plates waveguide in the photon state $|\Psi\rangle$. If we choose the transverse gauge, by taking $\mathbf{A}(\mathbf{r}, t)$ partial derivative with respect to t, the electric field between the two parallel slabs could be obtained easily. By integrating the electric field, what we obtain is the ac electrical potential difference between the two metal gates. The potential difference is induced by ac spin current and is also what we want to know.

Chapter 2

Geometric structure of the system we consider

In this chapter, we will introduce the geometric structure of our system and derive the quantized electromagnetic wave in waveguide.

2.1 Structure of our system

In this section, we show the geometric structure of our system. The model of our system is shown as Fig. 2.1. In chapter 5, we will demonstrate that this device can detect electric potential difference induced by ac in-plane polarized spin current by adding appropriate external electric circuit.

At the middle of the device there is an extremely thin layer of 2DEG which is formed at the intersection of two kind of semiconductor with different band gap energies. Two pieces of metal gates sandwich the semiconductor structure and are parallel to the 2DEG. These two metal gates are used to detect the electrical potential difference and they construct a two-parallel-planes waveguide. We can apply two layers with two different ratios of Al to Ga of aluminum gallium arsenide (AlGaAs) as dielectric material between the two metal slabs to form 2DEG, and use aluminum slabs as gate to detect the electrical potential

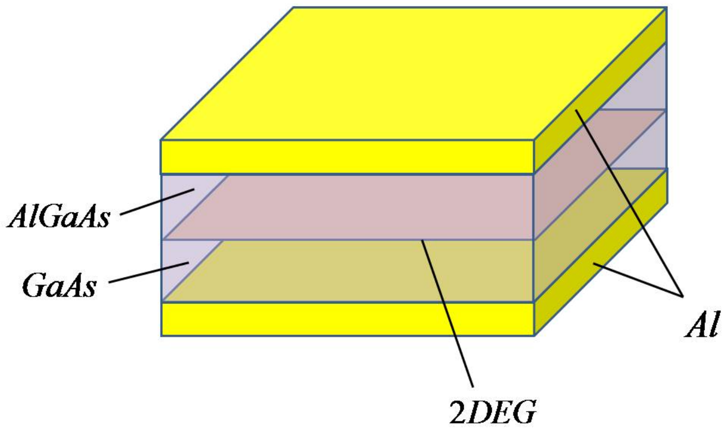

Figure 2.1: An illustration of the geometry of the two parallel-planes waveguide. The 2DEG which is formed at the intersection of two kind of semiconductor with different band gap energies is at the middle of the waveguide.

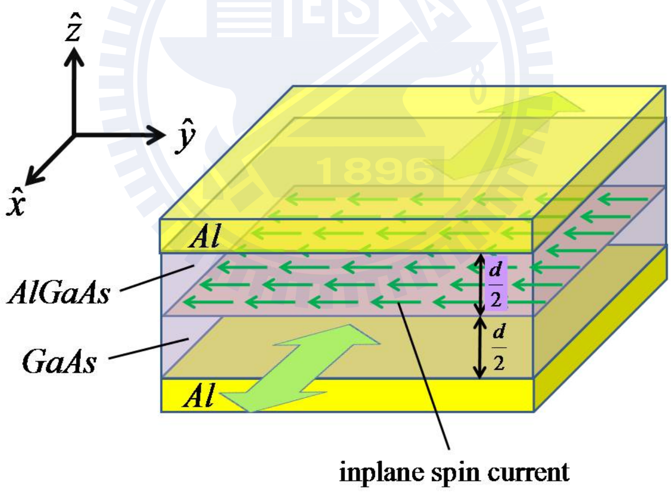

Figure 2.2: If the ac in-plane spin current oscillates toward x-direction on 2DEG and the spin polarized direction toward negative y-direction, it will generate ac electrical potential difference between the two metal gates.

difference.

We had discussed that electric field induced by ac spin-polarized current is perpendicular to the spin polarized direction and the oscillation direction of ac spin current. If we can generate pure ac in-plane polarized spin current on the 2DEG, which the spin polarized direction is towards the negative y-direction, oscillating in x-direction shown as Fig. 2.2, we may measure the ac electrical potential difference between two metallic slabs. The waveguide structure can lead the far field to near field if the thickness of waveguide is comparable with the wave length of field. In our problem here, the propagating direction of the field radiated by ac spin current happens to be parallel to the field direction, because the electric field, spin polarized direction and current direction are perpendicular to each other. Thus we need to use a description different from that for the oscillating electric dipole because near field near field behavior is important. The waveguide modes provide us a naturel and appropriate scheme to describe the near field, which is very important for our case. Furthermore its upper and lower metal gates can also be electrodes to measure the ac electrical potential difference induced by the ac spin current. If we can figure out the correlation between the electrical potential difference and the magnitude of spin current, we may declare that we can detect ac in-plane polarized spin current by electric means.

2.2 Quantization of electromagnetic wave in waveguide

Electromagnetic wave confined by a waveguide is different from that in vacuum. In this section we will deduce the quantization of electromagnetic wave in the waveguide.

Quantization of electromagnetic wave in free space

In chapter1, we discussed why we utilize the second quantization manner to deal with the field induced by ac spin current. The quantization of radiation field in free space is described in many textbooks [14]. The free radiation field is the quantized electromagnetic field inside an optical cavity with dimension L $(L \to \infty)$.

If we want obtain the mathematics form of vector potential, in an intuitive picture, we can start from Maxwell's equations in the absence of currents and charges. Then we can obtain the vector potential in free space in transverse gauge in which the electric scalar potential is equal to zero and the vector potential $\mathbf{A}(\mathbf{r},t)$ is divergence-free. One way to obtain the quantized radiation field in free space is to identify the amplitudes of the vector potential $\mathbf{A}(\mathbf{r},t)$ with the annihilation or creation operators of harmonic oscillators. In interaction representation $\mathbf{A}^{(op)}(\mathbf{r},t)$ develops in time by:

$$\mathbf{A}^{(op)}(\mathbf{r},t)=\sum_{\mathbf{k}\lambda}A_{\mathbf{k}\lambda}^{(op)}\boldsymbol{\lambda}\frac{\exp\left(i\mathbf{k}\cdot\mathbf{r}-i\omega_{\mathbf{k}\lambda}t\right)}{\sqrt{V}}+A_{\mathbf{k}\lambda}^{(op)+}\boldsymbol{\lambda}^{*}\frac{\exp\left(-i\mathbf{k}\cdot\mathbf{r}+i\omega_{\mathbf{k}\lambda}t\right)}{\sqrt{V}}, \quad (2.1)$$

where $V=L^3$ is the free space volume and the vector $\boldsymbol{\lambda}$ is the polarization of the plane wave. $\mathbf{k}$ is the wave vector of the radiation field. $A_{\mathbf{k}\lambda}^{(op)}$ and $A_{\mathbf{k}\lambda}^{(op)+}$ are corresponding to creation and annihilation (raising and lowering) operators respectively. The subscript λ ($\lambda=1$ or 2) of $A_{\mathbf{k}\lambda}^{(op)}$ denotes two orthogonal polarization. When they act on eigenstate of photon, we can write down the relations:

$$A_{\mathbf{k}\lambda}^{(op)}\left|N_{\mathbf{k}_1\lambda_1},N_{\mathbf{k}_2\lambda_2},....,N_{\mathbf{k}\lambda},...\right\rangle=\sqrt{\frac{\hbar}{2\varepsilon_0\omega_{\mathbf{k}\lambda}}}\sqrt{N_{\mathbf{k}\lambda}}\left|N_{\mathbf{k}_1\lambda_1},N_{\mathbf{k}_2\lambda_2},....,N_{\mathbf{k}\lambda}-1,...\right\rangle, \quad (2.2)$$

$$A_{\mathbf{k}\lambda}^{(op)+}\left|N_{\mathbf{k}_1\lambda_1},N_{\mathbf{k}_2\lambda_2},....,N_{\mathbf{k}\lambda},...\right\rangle=\sqrt{\frac{\hbar}{2\varepsilon_0\omega_{\mathbf{k}\lambda}}}\sqrt{N_{\mathbf{k}\lambda}+1}\left|N_{\mathbf{k}_1\lambda_1},N_{\mathbf{k}_2\lambda_2},....,N_{\mathbf{k}\lambda}+1,...\right\rangle, \quad (2.3)$$

where $N_{\mathbf{k}\lambda}$ is the number of photons in the mode $\mathbf{k},\lambda$ and ε_0 is the permittivity in vacuum. When $A_{\mathbf{k}\lambda}^{(op)}$ applies on photon state , it reduces the number of photons in the mode $\mathbf{k}\lambda$ by one. $A_{\mathbf{k}\lambda}^{(op)+}$ applies on photon state , it increase the number of photons in the mode $\mathbf{k}\lambda$ by one.

Quantization of electromagnetic wave in waveguide

Now we will derive the electromagnetic wave in the waveguide which is constructed with two metal plates , and a thick dielectric slab with thickness d and its dielectric constant

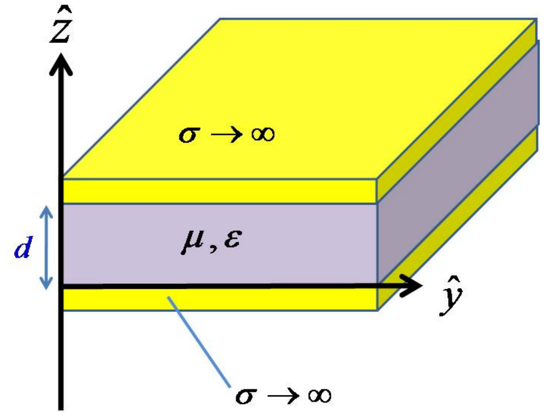

Figure 2.3: The two parallel-planes waveguide consists of a dielectric material with permeability μ and primitivity ε sandwiched by two parallel metal gates with conductivity σ ($\sigma \to \infty$).

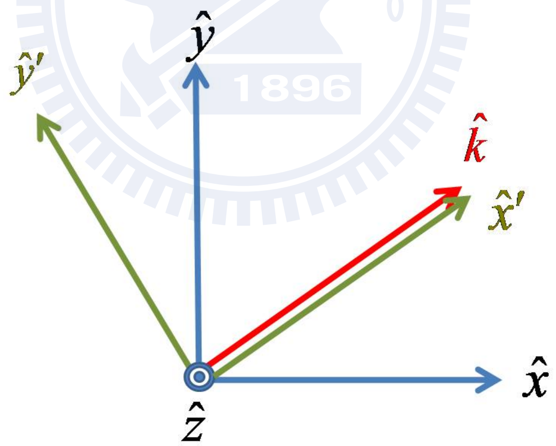

Figure 2.4: The picture shows the relation between $\hat{z}, \hat{x}', \hat{y}'$, and $\hat{k}$.(We set a reference coordinate, $\hat{x}'$-$\hat{y}'$ coordinate, which is in the x-y plane.)

and magnetic permeability are ε and μ respectively. The dielectric slab is sandwiched by the two plates. We assume the metal slabs are perfect conductor. The structure of the waveguide is shown as Fig. 2.3.

We assume that the total electromagnetic wave propagate along the k-direction (note that $\hat{k} = \hat{x}'$) in dielectric layer, and the two metal plates are put $z = 0$ and $z = d$. And we assume $\hat{z} \times \hat{x}' = \hat{y}'$. The relation between $\hat{z}$, $\hat{x}'$, $\hat{y}'$, and $\hat{k}$ is shown in Fig. 2.4.

We just consider about the plane waves, and it means $B \propto e^{-i\omega t}$ and $E \propto e^{-i\omega t}$ where is the angular frequency of incident wave and $\frac{\partial}{\partial y'} \to 0$. From Faraday's law, we can get $\nabla \times \mathbf{E} = -\frac{\partial}{\partial t}\mathbf{B} = i\omega\mathbf{B}$. We may write down the three components of Faraday's law as the following

$$-\frac{\partial}{\partial z}E_{y'} = i\omega B_{x'}, \tag{2.4}$$

$$\frac{\partial}{\partial z}E_{x'} - \frac{\partial}{\partial x'}E_z = i\omega B_{y'}, \tag{2.5}$$

$$\frac{\partial}{\partial x'}E_{y'} = i\omega B_z, \tag{2.6}$$

Considering Ampere's law, we obtain $\nabla \times \mathbf{B} = \mu\varepsilon\frac{\partial}{\partial t}\mathbf{E} = -i\omega\mu\varepsilon\mathbf{E}$. Then we obtain the following three differential equations.

$$-\frac{\partial}{\partial z}B_{y'} = -i\omega\mu\varepsilon E_{x'}, \tag{2.7}$$

$$\frac{\partial}{\partial z}B_{x'} - \frac{\partial}{\partial x'}B_z = -i\omega\mu\varepsilon E_{y'}, \tag{2.8}$$

$$\frac{\partial}{\partial x'}B_{y'} = -i\omega\mu\varepsilon E_z. \tag{2.9}$$

Considering Maxwell equations, for two pieces of slab of waveguide which are made of perfect conductor, we have two boundary condition derived by Faraday's law and divergence free of magnetic field. They are $B_z = 0$ at $z = 0$ and $z = d$ $E_{x'}, E_{y'} = 0$ at $z = 0$ and $z = d$.

The Eq. (2.4), Eq. (2.6), Eq. (2.8) only have variables $E_{y'}$, $B_{x'}$, and B_z. They can construct a wave equation called TE wave equation. The name "TE" means transverse electric field. The wave equation is given by:

$$\left(\frac{\partial^2}{\partial x'^2} + \frac{\partial^2}{\partial z^2} + \omega^2 \mu \varepsilon\right) E_{y'} = 0. \tag{2.10}$$

Solving Eq. (2.10) by separation of variables, finally, we have:

$$E_{y'} = E_0 \sin\left(k_z z\right) e^{ik_{x'} x'},$$

where E_0 is the amplitude of the electric field, $k_{x'}$ is the x'-component wave number, and $k_z = \frac{m\pi}{d}$, $m = 0, 1, 2, 3, ...$

Magnetic field is transverse or perpendicular to the propagation direction. The fields are calculated to be

$$-\frac{\partial}{\partial z} E_{y'} = i\omega B_{x'} \;\rightarrow\; B_{x'} = i\frac{k_z}{\omega} E_0 \sin\left(k_z z\right) e^{ik_{x'} x'},$$

$$\frac{\partial}{\partial x'} E_{y'} = i\omega B_z \;\rightarrow\; B_z = \frac{k_{x'}}{\omega} E_0 \sin\left(k_z z\right) e^{ik_{x'} x'}.$$

m is the mode number which starts from one . k_z and $k_{x'}$ are satisfied with the dispersion relation ${k_z}^2 + {k_{x'}}^2 = \omega^2 \mu \varepsilon$.

The Eq. (2.5), Eq. (2.7), Eq. (2.9) contain variables $E_{x'}$, E_z, and $B_{y'}$. The three differential equations can construct a wave equation called TM wave equation (Magnetic field is transverse or perpendicular to the propagation direction.). The wave equation is:

$$\left(\frac{\partial^2}{\partial x'^2} + \frac{\partial^2}{\partial z^2} + \omega^2 \mu \varepsilon\right) B_{y'} = 0. \tag{2.11}$$

Solving Eq. (2.11), we obtain

$$B_{y'} = B_0 \cos\left(k_z z\right) e^{ik_{x'} x'},$$

where $k_z = \frac{n\pi}{d}$, n=0,1,2,3, ..., $k_{x'}$ is the x'-component wave vector, and B_0 is the amplitude of the magnetic field. Magnetic field is perpendicular to the electric field, and the fields are calculated to be

$$-\frac{\partial}{\partial z}B_{y'} = -i\omega\mu\varepsilon E_{x'} \;\rightarrow\; E_{x'} = i\frac{k_z}{\omega\mu\varepsilon}B_0 \sin\left(k_z z\right) e^{ik_{x'}x'},$$

$$\frac{\partial}{\partial x'}B_{y'} = -i\omega\mu\varepsilon E_z \;\rightarrow\; E_z = -\frac{k_{x'}}{\omega\mu\varepsilon}B_0 \cos\left(k_z z\right) e^{ik_{x'}x'},$$

and we get the dispersion relation${k_z}^2 + {k_{x'}}^2 = \omega^2\mu\varepsilon$. Actually, k_z is the transverse wave vector and k is the effectively longitudinal component of the wave vector.

We already derived electromagnetic wave modes in parallel-plates waveguide. For real physical quantity, we may add its complex conjugate to the fields. Furthermore, we know that the wave in an arbitrary parallel-plate waveguide is not a plane wave, because a plane wave cannot satisfy the appropriate boundary conditions at the waveguide walls. But the modes can be expressed as a sum of plane waves. In general, we decompose the total electric field in the waveguide for different modes and different $\mathbf{k}$ as infinite (Fourier) superposition of all modes as given by

For TE modes:

$$\mathbf{E} = -\sum_{m,\mathbf{k}} \sin\left(\frac{m\pi}{d}z\right)\left\{b_{m\mathbf{k}}e^{i(\mathbf{k}\cdot\boldsymbol{\rho}-\omega_{m\mathbf{k}2}t)} + {b_{m\mathbf{k}}}^* e^{-i(\mathbf{k}\cdot\boldsymbol{\rho}-\omega_{m\mathbf{k}2}t)}\right\}\left(\hat{z}\times\hat{k}\right) \tag{2.12}$$

$$\begin{aligned}\mathbf{B} = \sum_{m,\mathbf{k}} &\left[\frac{1}{\omega_{m\mathbf{k}2}}\left(\frac{m\pi}{d}\right)\cos\left(\frac{m\pi}{d}z\right)\left(-ib_{m\mathbf{k}}e^{i(\mathbf{k}\cdot\boldsymbol{\rho}-\omega_{m\mathbf{k}2}t)} + i{b_{m\mathbf{k}}}^* e^{-i(\mathbf{k}\cdot\boldsymbol{\rho}-\omega_{m\mathbf{k}2}t)}\right)\hat{k}\right. \\ &\left.-\frac{k}{\omega_{m\mathbf{k}2}}\sin\left(\frac{m\pi}{d}z\right)\left(b_{m\mathbf{k}}e^{i(\mathbf{k}\cdot\boldsymbol{\rho}-\omega_{m\mathbf{k}2}t)} + {b_{m\mathbf{k}}}^* e^{-i(\mathbf{k}\cdot\boldsymbol{\rho}-\omega_{m\mathbf{k}2}t)}\right)\hat{z}\right]\end{aligned} \tag{2.13}$$

For TM modes, we have

$$\mathbf{B} = B_{y'}\hat{y}' = -\sum_{n,\mathbf{k}} \cos\left(\frac{n\pi}{d}z\right)\left\{c_{n\mathbf{k}}e^{i(\mathbf{k}\cdot\boldsymbol{\rho}-\omega_{n\mathbf{k}1}t)} + {c_{n\mathbf{k}}}^* e^{-i(\mathbf{k}\cdot\boldsymbol{\rho}-\omega_{n\mathbf{k}1}t)}\right\}\left(\hat{z}\times\hat{k}\right), \tag{2.14}$$

$$\begin{aligned}\mathbf{E} = \sum_{n,\mathbf{k}} \Bigg[&\frac{1}{\mu\varepsilon}\frac{1}{\omega_{n\mathbf{k}1}}\left(\frac{n\pi}{d}\right)\sin\left(\frac{n\pi}{d}z\right)\left(-ic_{n\mathbf{k}}e^{i(\mathbf{k}\cdot\boldsymbol{\rho}-\omega_{n\mathbf{k}1}t)} + i{c_{n\mathbf{k}}}^{*}e^{-i(\mathbf{k}\cdot\boldsymbol{\rho}-\omega_{n\mathbf{k}1}t)}\right)\hat{k} \\ &+ \frac{1}{\mu\varepsilon}\frac{k}{\omega_{n\mathbf{k}1}}\cos\left(\frac{n\pi}{d}z\right)\left(c_{n\mathbf{k}}e^{i(\mathbf{k}\cdot\boldsymbol{\rho}-\omega_{n\mathbf{k}1}t)} + {c_{n\mathbf{k}}}^{*}e^{-i(\mathbf{k}\cdot\boldsymbol{\rho}-\omega_{n\mathbf{k}1}t)}\right)\hat{z}\Bigg]\end{aligned} \quad . \quad (2.15)$$

The dispersion relation is ${k_z}^2 + k^2 = \omega^2\mu\varepsilon$. $b_m(c_n)$ denotes the amplitude of the electric field for the m-th (n-th) mode. The time-dependence is given by putting in the whole plane wave: $e^{i\mathbf{k}\cdot\boldsymbol{\rho}} \rightarrow e^{i(\mathbf{k}\cdot\boldsymbol{\rho}-\omega t)}$. The summation $\mathbf{k}$ contains all direction as well as all magnitude. We also change the notation ω into $\omega_{m\mathbf{k}2}$ ($\omega_{n\mathbf{k}1}$), because the frequency depends on $\hat{k}$-component ($\hat{k} = \hat{x}'$) of wave number and mode number m(n). The other subscript of $\omega_{m\mathbf{k}2}$ ($\omega_{n\mathbf{k}1}$), 1 or 2, indicates TM or TE modes respectively.

The electric field and vector potential respect to the relationship $\mathbf{E} = -\nabla\phi - \frac{\partial\mathbf{A}}{\partial t}$ It's easy to derive the vector potential, if we choose the transverse gauge. For TE modes, the vector potential is given by:

$$\mathbf{A} = -\sum_{m,\mathbf{k}}\frac{1}{i\omega_{m\mathbf{k}2}}\sin\left(\frac{m\pi}{d}z\right)\left\{b_{m\mathbf{k}}e^{i(\mathbf{k}\cdot\boldsymbol{\rho}-\omega_{m\mathbf{k}2}t)} - {b_{m\mathbf{k}}}^{*}e^{-i(\mathbf{k}\cdot\boldsymbol{\rho}-\omega_{m\mathbf{k}2}t)}\right\}\left(\hat{z}\times\hat{k}\right). \quad (2.16)$$

For TM modes, we have:

$$\begin{aligned}\mathbf{A} = \sum_{n,\mathbf{k}}\Bigg[&-\frac{1}{\mu\varepsilon}\frac{1}{{\omega_{n\mathbf{k}1}}^2}\left(\frac{n\pi}{d}\right)\sin\left(\frac{n\pi}{d}z\right)\left(c_{n\mathbf{k}}e^{i(\mathbf{k}\cdot\boldsymbol{\rho}-\omega_{n\mathbf{k}1}t)} + {c_{n\mathbf{k}}}^{*}e^{-i(\mathbf{k}\cdot\boldsymbol{\rho}-\omega_{n\mathbf{k}1}t)}\right)\hat{k} \\ &+\frac{1}{\mu\varepsilon}\frac{k}{{\omega_{n\mathbf{k}1}}^2}\cos\left(\frac{n\pi}{d}z\right)\left(-ic_{n\mathbf{k}}e^{i(\mathbf{k}\cdot\boldsymbol{\rho}-\omega_{n\mathbf{k}1}t)} + i{c_{n\mathbf{k}}}^{*}e^{-i(\mathbf{k}\cdot\boldsymbol{\rho}-\omega_{n\mathbf{k}1}t)}\right)\hat{z}\Bigg].\end{aligned} \quad (2.17)$$

Canonical quantization (also called second quantization) asks that the classical field variable becomes a quantum operator. The amplitude of vector potential $c_{n\mathbf{k}}$ ($b_{m\mathbf{k}}$) or ${c_{n\mathbf{k}}}^{*}$ (${b_{m\mathbf{k}}}^{*}$) is corresponded to annihilation or creation operator respectively. Because ${c_{n\mathbf{k}}}^{*}$ (${b_{m\mathbf{k}}}^{*}$) becomes operator, it may be wrote as ${c_{n\mathbf{k}}}^{+}$ (${b_{m\mathbf{k}}}^{+}$). When $c_{n\mathbf{k}}$ ($b_{m\mathbf{k}}$) acts on the photon state, it will removes one photon with the mode $n\mathbf{k}$ ($m\mathbf{k}$). ${c_{n\mathbf{k}}}^{+}$ (${b_{m\mathbf{k}}}^{+}$) acts on an energy eigenstate, it will increase one photon with the mode $n\mathbf{k}$ ($m\mathbf{k}$) (Here "n" or "m" indicates the n-th mode in TM wave or the m-th mode in TE waves respectively.).

Using $c_{n\mathbf{k}}$ ($b_{m\mathbf{k}}$) or ${c_{n\mathbf{k}}}^{*}$ (${b_{m\mathbf{k}}}^{*}$) to describe the classical electromagnetic energy in a volume V, we find the energy for TE modes inside the volume V is given by:

$$E_{energy} = \int d\mathbf{r} \left[\frac{1}{2}\varepsilon E^2 + \frac{1}{2\mu} B^2 \right] = \varepsilon \sum_{m=1,2,3,...} |b_{m\mathbf{k}}|^2 V. \tag{2.18}$$

By the same way, for TM modes we have

$$E_{energy} = \frac{1}{\mu} \sum_{n=0,1,2,3,...} |c_{n\mathbf{k}}|^2 V. \tag{2.19}$$

Actually, in quantum theory the radiation energy is given by:

$$E_{energy} = N\hbar\omega, \tag{2.20}$$

where N is the number of photons in the volume V, and is the angular frequency of these photons. Combining Eq. (2.18), Eq. (2.19), and Eq. (2.20), we have the dimension of the four coefficients. When they act on the eigenstate of electromagnetic field, we have:

$$b_{m\mathbf{k}} \left| N_{m_1\mathbf{k}_1 2}, N_{m_2\mathbf{k}_2 2}, ..., N_{m\mathbf{k}2}, ... \right\rangle = \sqrt{\frac{\hbar\omega_{m\mathbf{k}2}}{\varepsilon V}} \sqrt{N_{m\mathbf{k}2}} \left| N_{m_1\mathbf{k}_1 2}, N_{m_2\mathbf{k}_2 2}, ..., N_{m\mathbf{k}2} - 1, ... \right\rangle, \tag{2.21}$$

$$b_{m\mathbf{k}}{}^{+} \left| N_{m_1\mathbf{k}_1 2}, N_{m_2\mathbf{k}_2 2}, ..., N_{m\mathbf{k}2}, ... \right\rangle = \sqrt{\frac{\hbar\omega_{m\mathbf{k}2}}{\varepsilon V}} \sqrt{N_{m\mathbf{k}2} + 1} \left| N_{m_1\mathbf{k}_1 2}, N_{m_2\mathbf{k}_2 2}, ..., N_{m\mathbf{k}2} + 1, ... \right\rangle, \tag{2.22}$$

$$c_{n\mathbf{k}} \left| N_{n_1\mathbf{k}_1 1}, N_{n_2\mathbf{k}_2 1}, ..., N_{n\mathbf{k}1}, ... \right\rangle = \sqrt{\mu \frac{\hbar\omega_{n\mathbf{k}1}}{V}} \sqrt{N_{n\mathbf{k}1}} \left| N_{n_1\mathbf{k}_1 1}, N_{n_2\mathbf{k}_2 1}, ..., N_{n\mathbf{k}1} - 1, ... \right\rangle, \tag{2.23}$$

$$c_{n\mathbf{k}}{}^{+} \left| N_{n_1\mathbf{k}_1 1}, N_{n_2\mathbf{k}_2 1}, ..., N_{n\mathbf{k}1}, ... \right\rangle = \sqrt{\mu \frac{\hbar\omega_{n\mathbf{k}1}}{V}} \sqrt{N_{n\mathbf{k}1} + 1} \left| N_{n_1\mathbf{k}_1 1}, N_{n_2\mathbf{k}_2 1}, ..., N_{n\mathbf{k}1} + 1, ... \right\rangle,$$

(2.24)

where $N_{n\kappa 1}$ $(N_{m\mathbf{k2}})$ is the number of photons in the TM (TE) mode $n\,(m)\,,\mathbf{k}$.

We have found out the quantized radiation field in the waveguide. With the result, we can correctly calculate the radiation field generate by spin current or else radiation problem in the waveguide.

2.3 Brief summary

Our system essentially comprises 2DEG which is formed at the AlGaAs/GaAs heterointerface and sandwiched by two piece of Al electrodes outermost. When ac in-plane spin current flows on the 2DEG, we utilize waveguide structure to detect the potential difference induced by the spin current. The quantized field in two-parallel-planes waveguide can be divided into two kinds of modes , TM modes and TE modes. Electric field in TE modes is perpendicular to the propagation direction of the beam and there is no electric field in the direction of propagation. Electric field in TM modes is perpendicular to the propagation direction.

Chapter 3

Examination of the calculation method we consider

In this chapter, we want to check if our calculation method is practical. We propose two problem of electrodynamics to compare the result which is solved by method of classical electrodynamics and the result solved by our method. The first problem is electromagnetic (EM) wave generated by single charge oscillation in free space. The second one is EM wave induced by oscillating charge current carried by an infinite long wire in waveguide.

3.1 Charge oscillation in free space

In electrodynamics, the charge oscillation will generate electromagnetic wave in space. Using the method we proposed in Chapter 1, we calculate electric field generated by the charge oscillation in free space. We can also obtain the EM wave with Jefimenko's equations which describe the behavior of the electric and magnetic fields in terms of the charge and current density at retarded times. Then we compare the result by this method with the result by the method of electrodynamics. If both the results are identical with each other, we confirm that our method is practical. We start from a charge oscillating along the z direction with the frequency Ω and the amplitude "a" in the Cylindrical

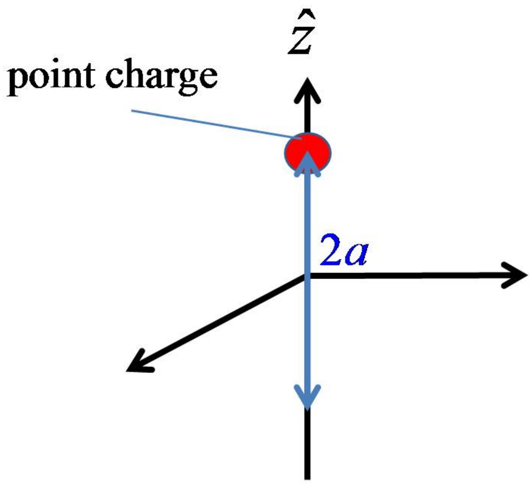

Figure 3.1: The particle carrying electric charge q with is deposited at the origin, and it acts as simple harmonic oscillation with frequancy Ω and amplitude a.

coordinate. The equilibrium point of the charge is deposited at the origin shown as Fig. 3.1. We can write down the time-dependent position of the charge as the following: $\mathbf{r}_p = a\cos(\Omega t)\,\hat{z}$

Effective Hamiltonian of photons

The perturbation operator of charge-photon interaction is given by $H' = -q\mathbf{E}\cdot\mathbf{r}$ where $\mathbf{E}$ is the electric field[14]. If we just consider about the transverse field, the field induced by charge oscillation is the same as dipole oscillation with identical frequency and amplitude. In quantum mechanics, even though we cannot describe both position and momentum of an electron, we still recognize the oscillating charge as a classical particle. If the amplitude "a" is much smaller than the wavelength of the light, the field can be recognize as far field. For relativity far field, because the oscillator is placed at origin, we can replace $\mathbf{E}(\mathbf{r},t)$ by $\mathbf{E}(0,t)$ because the charge oscillating at origin.

$$\begin{aligned} H'_{eff} &= -q\mathbf{E}(0,t)\cdot\mathbf{r}_p \\ &= q\frac{\partial\mathbf{A}(0,t)}{\partial t}\cdot\mathbf{r}_p, \end{aligned} \tag{3.1}$$

where c is the light speed in vacuum , q is the electric charge of the particle, $\mathbf{A}$ is the vector potential in transverses gauge . Incorporating Eq. (2.2) into Eq. (3.1) , and then the perturbing Hamiltonian becomes

$$H'_{eff} = iq \sum_{\mathbf{k}\lambda} \left\{ -ck_{\mathbf{k}\lambda} A^{(op)}_{\mathbf{k}\lambda} \left(\boldsymbol{\lambda} \cdot \mathbf{r}_p\right) \frac{\exp\left(-ick_{\mathbf{k}\lambda}t\right)}{\sqrt{V}} + ck_{\mathbf{k}\lambda} A^{(op)+}_{\mathbf{k}\lambda} \left(\boldsymbol{\lambda}^* \cdot \mathbf{r}_p\right) \frac{\exp\left(+ick_{\mathbf{k}\lambda}t\right)}{\sqrt{V}} \right\}, \tag{3.2}$$

where V is the free space volume and λ is the polarization of the plane wave. $\mathbf{k}$ is the wave vector of the radiation field. $A^{(op)}_{\mathbf{k}\lambda}$ and $A^{(op)+}_{\mathbf{k}\lambda}$ are corresponding to creation and annihilation operators respectively. The subscript λ ($\lambda = 1$ or 2) of $A^{(op)}_{\mathbf{k}\lambda}$ denotes two orthogonal polarization.

The photon eigenstate

For spontaneous emission, the oscillator emits only one photon. The initial state must be $|\Psi_0\rangle = |\{0_{\mathbf{k}_1\lambda_1}, 0_{\mathbf{k}_2\lambda_2}, ..., 0_{\mathbf{k}\lambda}, .., \}\rangle$ (or we can write as$|\{0\}\rangle$) and the final state is $|\{0, 0, ..., 0, 1_{\mathbf{k}\lambda}, 0, ..., 0\}\rangle$. The initial state is also one of the unperturbed eigenstates.

H'_{eff} is identified as time dependant perturbing Hamiltonian. Applying first-order perturbation theory, the first order perturbation coefficient is given by

$$f^{(1)}_{\mathbf{k}\lambda} = \frac{-i}{\hbar} \int_{-\infty}^{t} \langle \{0, ..., 0, 1_{\mathbf{k}\lambda}, 0, ...\}| \, H'_{eff} \, |\{0\}\rangle dt,$$

where $\hbar$ is the Plank constant. Essentially, the strength of perturbing Hamiltonian H' is weak enough, so we can apply perturbation theorem.

Assuming the limit of a very slow switch on, $H'_{eff}e^{\eta t}$ with η which is far smaller than 1, so H'_{eff} switched on very gradually in the past. We can then take the initial time to be $-\infty$, and the first order perturbation coefficient becomes:

$$f^{(1)}_{\mathbf{k}\lambda} = \frac{-i}{\hbar} \int_{-\infty}^{t} \langle \{0, ..., 0, 1_{\mathbf{k}\lambda}, 0, ...\}| \, H'_{eff}e^{\eta t} \, |\{0\}\rangle dt \tag{3.3}$$

We consider one photon emittion. It means the photon state from $|\{0\}\rangle$ to $|\{0,...,0,1_{\mathbf{k}\lambda},0,...\}\rangle$. Substituting equation Eq. (3.2) into Eq. (3.3), we obtain:

$$f_{\mathbf{k}\lambda}^{(1)} = \frac{q}{\hbar}\int_{-\infty}^{t} \langle\{0,...,0,1_{\mathbf{k}\lambda},0,...\}| \sum_{\mathbf{k}'\lambda'} \left\{ ck_{\mathbf{k}'\lambda'} A_{\mathbf{k}'\lambda'}^{(op)+} \left(\boldsymbol{\lambda}'^{*} \cdot \mathbf{r}_p\right) \frac{\exp\left(+ick_{\mathbf{k}'\lambda'}t\right)}{\sqrt{V}} \right\} e^{\eta t} |\{0,...,0\}\rangle dt'. \tag{3.4}$$

Here we used the character of annihilation operator $A_{\mathbf{k}'\lambda'}^{(op)}|\{0,0,...,0\}\rangle = 0$. Solving Eq. (3.4), we can rewrite the first order perturbation coefficient is

$$\begin{aligned} f_{\mathbf{k}\lambda}^{(1)} &= \frac{q}{\hbar}\sqrt{\frac{\hbar\omega_{\mathbf{k}\lambda}}{2\varepsilon_0}} \frac{1}{\sqrt{V}} a\left(\boldsymbol{\lambda}^{*} \cdot \hat{z}\right) \frac{1}{\left(\eta + ick_{\mathbf{k}\lambda}\right)^2 + \Omega^2} \left\{\left(\eta + ick_{\mathbf{k}\lambda}\right)\cos\left(\Omega t\right) + \Omega \sin\left(\Omega t\right)\right\} \\ &\times \exp\left[\left(\eta + ick_{\mathbf{k}\lambda}\right)t\right] \end{aligned} \tag{3.5}$$

The eigenstate of the photon is changed to $|\Psi\rangle$ after we consider about the perturbation of the system H'_{eff}. $|\Psi\rangle$ is given by:

$$|\Psi\rangle = |\{0,0,...,0,...,0\}\rangle + \sum_{\mathbf{k}\lambda} f_{\mathbf{k}\lambda}^{(1)} |\{0,0,...,0,1_{\mathbf{k}\lambda},0,...,0\}\rangle \tag{3.6}$$

The expectation value of vector potential

The photon state describes all information about photons in the waveguide including the vector potential in space. The expectation value of the magnetic vector potential in the state $|\Psi\rangle$ is given by:

$$\begin{aligned} &\mathbf{A}\left(\mathbf{r},t\right) = \langle\Psi|\,\mathbf{A}^{(op)}\,|\Psi\rangle \\ &= \left\{ \langle\{0,0,...,0,...,0\}| + \sum_{\mathbf{k}''\lambda''} f_{\mathbf{k}''\lambda''}^{(1)\,+} \langle\{0,0,...,0,1_{\mathbf{k}''\lambda''},0,...,0\}| \right\} \mathbf{A}^{(op)} \left\{ |\{0,0,...,0,...,0\}\rangle \right. \\ &\quad \left. + \sum_{\mathbf{k}'\lambda'} f_{\mathbf{k}'\lambda'}^{(1)} |\{0,0,...,0,1_{\mathbf{k}'\lambda'},0,...,0\}\rangle \right\} \end{aligned} \tag{3.7}$$

$A^{(op)+}_{\mathbf{k}\lambda}$ is an operator that increases the number of photons in the mode $\mathbf{k}\lambda$ by one. When the operators $A^{(op)}_{\mathbf{k}\lambda}$ and $A^{(op)+}_{\mathbf{k}\lambda}$ are applied to the photon state, they obey the Eq. (2.2) and Eq. (2.3), respectively. And the expectation value of the vector potential of the system becomes

$$\mathbf{A}\left(\mathbf{r},t\right)=\sum_{\mathbf{k}\lambda}\sqrt{\frac{\hbar}{2\omega_{\mathbf{k}\lambda}\varepsilon_0}}\left\{\lambda f^{(1)}_{\mathbf{k}\lambda}\frac{\exp\left(i\mathbf{k}\cdot\mathbf{r}-i\omega_{\mathbf{k}\lambda}t\right)}{\sqrt{V}}+\lambda^* f^{(1)+}_{\mathbf{k}\lambda}\frac{\exp\left(-i\mathbf{k}\cdot\mathbf{r}+i\omega_{\mathbf{k}\lambda}t\right)}{\sqrt{V}}\right\}. \quad (3.8)$$

Putting Eq. (3.5) into Eq. (3.8), the vector potential leads to

$$\begin{aligned}\mathbf{A}\left(\mathbf{r},t\right)=&\sum_{\mathbf{k}\lambda}\frac{qa\left(-i\right)}{4V\varepsilon_0}\exp\left[i\mathbf{k}\cdot\mathbf{r}\right]\lambda_z{}^*\lambda\left\{\frac{\exp\left(i\Omega t\right)}{\Omega+ck-i\eta}+\frac{\exp\left(-i\Omega t\right)}{ck-\Omega-i\eta}\right\}\\&+\sum_{\mathbf{k}\lambda}\frac{qa\left(i\right)}{4V\varepsilon_0}\exp\left[-i\mathbf{k}\cdot\mathbf{r}\right]\lambda_z\lambda^*\left\{\frac{\exp\left(-i\Omega t\right)}{\Omega+ck+i\eta}+\frac{\exp\left(+i\Omega t\right)}{ck-\Omega+i\eta}\right\}.\end{aligned} \quad (3.9)$$

We notice that the second term in above equation is complex conjugate of the first term. Now we take average over polarization. By taking linear polarization, we have $\lambda^*=\lambda$. Then, we have

$$\begin{aligned}\mathbf{A}\left(\mathbf{r},t\right)=&\sum_{\mathbf{k}}\frac{qa\left(-i\right)}{4V\varepsilon_0}\exp\left[i\mathbf{k}\cdot\mathbf{r}\right]\left\{\hat{z}-\left(\hat{k}\cdot\hat{z}\right)\hat{k}\right\}\left\{\frac{\exp\left(i\Omega t\right)}{\Omega+ck-i\eta}+\frac{\exp\left(-i\Omega t\right)}{ck-\Omega-i\eta}\right\}\\&+\sum_{\mathbf{k}}\frac{qa\left(i\right)}{4V\varepsilon_0}\exp\left[-i\mathbf{k}\cdot\mathbf{r}\right]\left\{\hat{z}-\left(\hat{k}\cdot\hat{z}\right)\hat{k}\right\}\left\{\frac{\exp\left(-i\Omega t\right)}{\Omega+ck+i\eta}+\frac{\exp\left(+i\Omega t\right)}{ck-\Omega+i\eta}\right\}.\end{aligned} \quad (3.10)$$

The summation over $\mathbf{k}$ means summing over arbitrary direction and magnitude of wave number $\mathbf{k}$. $\mathbf{k}$ must be continuous, so we may change the representation of the summation to representation of integration. It means

$$\begin{aligned}&\sum_{\mathbf{k}}\rightarrow\sum_{\mathbf{k}}\frac{\Delta k_x}{\Delta k_x}\frac{\Delta k_y}{\Delta k_y}\frac{\Delta k_z}{\Delta k_z}\\&\rightarrow\frac{1}{\left(\Delta k_x\right)\left(\Delta k_y\right)\left(\Delta k_z\right)}\int dk_xdk_ydk_z=\frac{1}{\left(\frac{2\pi}{L_x}\right)\left(\frac{2\pi}{L_y}\right)\left(\frac{2\pi}{L_z}\right)}\int k^2dkd\Omega_{\mathbf{k}}=\frac{V}{\left(2\pi\right)^3}\int k^2dkd\Omega_{\mathbf{k}},\end{aligned}$$

where L_i (i=x,y,z) is length which an quantum state occupies, and $\Omega_{\hat{k}}$ is the solid angle.

$$\begin{aligned}\mathbf{A}(\mathbf{r},t) = &\frac{V}{(2\pi)^3}\int k^2 dk d\Omega_{\mathbf{k}} \frac{qa(-i)}{4V\varepsilon_0}\exp(i\mathbf{k}\cdot\mathbf{r})\left[\hat{z}-\left(\hat{k}\cdot\hat{z}\right)\hat{k}\right] \\ &\times\left\{\frac{\exp(i\Omega t)}{\Omega+ck-i\eta}+\frac{\exp(-i\Omega t)}{ck-\Omega-i\eta}\right\}+\frac{V}{(2\pi)^3}\int k^2 dk d\Omega_{\mathbf{k}}\frac{qa(i)}{4V\varepsilon_0} \\ &\times\exp(-i\mathbf{k}\cdot\mathbf{r})\left[\hat{z}-\left(\hat{k}\cdot\hat{z}\right)\hat{k}\right]\left\{\frac{\exp(-i\Omega t)}{\Omega+ck+i\eta}+\frac{\exp(+i\Omega t)}{ck-\Omega+i\eta}\right\}.\end{aligned} \tag{3.11}$$

We deal with the angular integral $\frac{1}{4\pi}\int d\Omega_{\mathbf{k}}$ first. The detail of calculation is complex, and it will save for Appendix A. After average over direction, the vector potential becomes:

$$\begin{aligned}\mathbf{A}(\mathbf{r},t) = &\frac{V}{2\pi}\frac{qa}{8V\varepsilon_0}\left(\hat{\theta}\sin\theta\right) \\ &\times\left\{\int_{k=0}^{\infty}k^2dk\left(\frac{-\exp[ikr]+\exp[-ikr]}{kr}\right)\left[\frac{\exp(i\Omega t)}{\Omega+ck-i\eta}+\frac{\exp(-i\Omega t)}{ck-\Omega-i\eta}\right]\right. \\ &\left.+\int_{k=0}^{\infty}k^2dk\left(\frac{\exp[ikr]-\exp[-ikr]}{kr}\right)\left[\frac{\exp(-i\Omega t)}{\Omega+ck+i\eta}+\frac{\exp(+i\Omega t)}{ck-\Omega+i\eta}\right]\right\}.\end{aligned} \tag{3.12}$$

Using the relationship $\int_0^a f(x)dx = \int_{-a}^0 f(-x)dx$, and making the change of variables, $u' = ck$ we can obtain :

$$\begin{aligned}\mathbf{A}(\mathbf{r},t) = &\frac{cqa}{16\pi^2\varepsilon_0 c^4}\left(\hat{\theta}\sin\theta\right)\int_{u'=-\infty}^{\infty}u'^2\left[\frac{-\exp\left[iu'\frac{r}{c}\right]}{u'\frac{r}{c}}\frac{\exp(i\Omega t)}{u'+(\Omega-i\eta)}+\frac{-\exp\left[iu'\frac{r}{c}\right]}{u'\frac{r}{c}}\right. \\ &\times\frac{\exp(-i\Omega t)}{u'-(\Omega+i\eta)}+\frac{\exp\left[-iu'\frac{r}{c}\right]}{u'\frac{r}{c}}\frac{\exp(i\Omega t)}{u'+(\Omega-i\eta)} \\ &\left.+\frac{\exp\left[-iu'\frac{r}{c}\right]}{u'\frac{r}{c}}\frac{\exp(-i\Omega t)}{u'-(\Omega+i\eta)}\right]du'\end{aligned} \tag{3.13}$$

Using residue integral method , the vector potential can be derived as :

$$\mathbf{A}(\mathbf{r},t) = -\frac{qa}{4\pi c^2\varepsilon_0}\frac{\Omega}{r}\left(\hat{\theta}\sin\theta\right)\sin\left(\Omega t-\Omega\frac{r}{c}\right) \tag{3.14}$$

The detailed complex integral of equation is preserved in Appendix B. It's easy to obtain the electric field after we get the result of the complex calculation. Because we choose the transverse gauge, the electric scalar potential is equal to zero.

$$\begin{aligned}\mathbf{E}(\mathbf{r},t) &= -\nabla V - \frac{\partial}{\partial t}\mathbf{A} \\ &= \frac{qa}{4\pi c^2\varepsilon_0}\frac{\Omega^2}{r}(\sin\theta)\cos\left(\Omega t - \Omega\frac{r}{c}\right)\hat{\theta}\end{aligned} \tag{3.15}$$

Here, we only consider about the transverse field and neglect Coulomb field. The field is identical with the far electric field induced by dipole antenna. From above equation, we can realize that the frequency of the field is Ω which is the same as the frequency of the oscillating electron. If the charge wiggles back and forth, the higher the frequency, the shorter the waves, because it have less time to get out of the way before the charge changes its direction. This result which we use semi-classical calculation method is the same as the result which we use calculation method of classical electrodynamics. The two results obtained by different calculation methods are the same. It implies our assumption that our oscillating charge radiates light with one photon can match the oscillating charge problem. Also, our method is practical to be use for calculating spin current problem.

3.2 EM wave generated by oscillating line charge current in waveguide

In the same way, we solve the electric field induced by ac line charge current in waveguide with the method we consider, for checking if our calculation method is practical, again. The calculation also gives us a simpler exercise for solving electric field induced by ac in-plane polarized spin current.

When the wave length becomes comparable with the thickness of the waveguide, we should consider the near-field light instead of far-field light. The waveguide structure confines the field and leads far-field into near-field wave. The near-field wave is more complicated than far-field wave. Fortunately, plane wave expansion method is useful method for us to deal with our problem. Therefore, the quantization field in two-parallel-

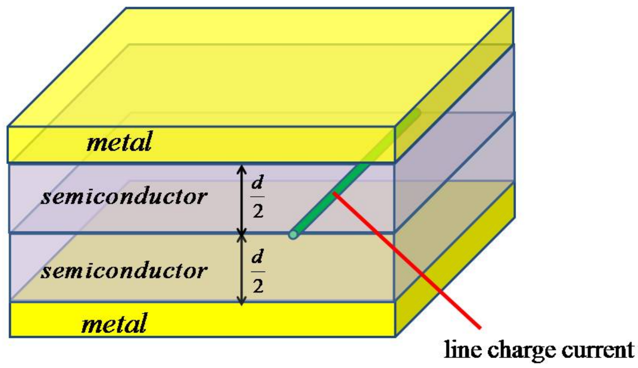

Figure 3.2: An infinite long wire is located at the middle of the waveguide and towards the x-direction.

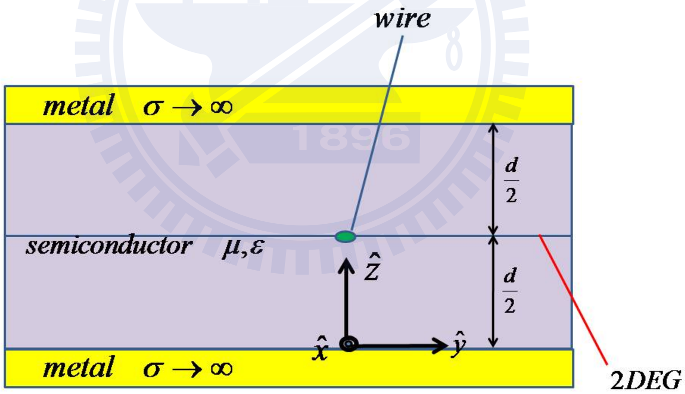

Figure 3.3: The side view of the waveguide structure and the wire. The waveguide is the same as one we discussed in **2.2** which has permeability μ and primitivity ε. The up and down electrode slabs are made of perfect conductor.

planes waveguide we derived in Chapter 2 can be a complete set. The structure of the waveguide we consider about is the same as we discussed in Chapter 2. An infinite long wire parallel with x-axis is located in the middle of two parallel metal gates as shown the following picture.

Assume that the semiconductor between two metal gates has the permittivity ε and permeability μrespectively. The wire is very thin, comparing with the distance d, and this wire carries flow of electron charge $\mathbf{I} = e\lambda_e \frac{\hbar k_e}{m_e}\hat{x}$ where λ_e is the particle density per unit length, m_e is the mass of a free electron, and k_e is the electron wave number, where $\hbar$ is the Plank constant. The wave function of the electrons is

$$\Psi(\mathbf{r}) = \langle \mathbf{r}|\psi\rangle = \sqrt{\lambda_e}\exp\left[ik_e x\right]\varphi(y,z). \tag{3.16}$$

At the beginning, we do not consider about ac current. We will add the oscillating information in the effective Hamiltonian later. The perturbation operator of oscillating line current in the waveguide is given by:

$$H' = \frac{e}{2m_e}(\mathbf{p}\cdot\mathbf{A} + \mathbf{A}\cdot\mathbf{p}) = \frac{e}{m_e}\mathbf{p}\cdot\mathbf{A} = \frac{e}{m_e}\mathbf{A}\cdot\mathbf{p}, \tag{3.17}$$

where $e > 0$. For the transverse gauge $\mathbf{p}\cdot\mathbf{A} - \mathbf{A}\cdot\mathbf{p} = -i\hbar\nabla\cdot\mathbf{A} = 0$. We care about only the transverse field without the longitudinal field. It means that we consider about the field induced by ac charge current without the Coulomb field. Therefore, the perturbing Hamiltonian does not include the Coulomb potential.

Effective Hamiltonian

We sandwich Eq. (3.17) with electron state to get the effective Hamiltonian of the photons in the waveguide which is given by the following:

$$\begin{aligned} H'_{eff} &= \langle\psi| H' |\psi\rangle = \langle\psi| \frac{e}{m_e}\mathbf{A}\cdot\mathbf{p}|\psi\rangle \\ &= k_e\hbar\lambda_e\frac{e}{m_e}\int dx\int dy\int dz\varphi(y,z)A_x\varphi(y,z) - i\hbar\lambda\frac{e}{m_e}\left\{\int dx\int dy\int dz\varphi(y,z)\right. \\ &\times \left. A_y\frac{\partial}{\partial y}\varphi(y,z) + \int dx\int dy\int dz\varphi(y,z)A_z\frac{\partial}{\partial z}\varphi(y,z)\right\}, \end{aligned} \tag{3.18}$$

where A_x, A_y, A_z is the x, y, z-component of vector potential respectively. Vector potential near the position$\left(x, y=0, z=\frac{d}{2}\right)$changes violently, but the wave function of the electron $\varphi\left(y, z\right)$ changes smoothly, so we may take some approximation. Then we have:

$$H'_{eff} = \hbar\lambda_e \frac{e}{m_e}\left\{k_e \int dx A_x\left(x, 0, \tfrac{d}{2}\right) - \frac{1}{2} i \int dx \frac{\partial}{\partial x} A_x\left(x, 0, \tfrac{d}{2}\right)\right\}. \tag{3.19}$$

The detailed derivation from Eq. (3.18) to Eq. (3.19) is left in the Appendix C. Putting Eq. (2.16) and Eq. (2.17) into Eq. (3.19), we obtain:

$$\begin{aligned}
H'_{eff} = \hbar\lambda_e \frac{e}{m_e} \cdot &\left\{k_e\left[-\sum_{m,\mathbf{k}}\left\{\frac{1}{i\omega_{m\mathbf{k}2}} b_{m\mathbf{k}} \sin\left(\frac{m\pi}{2}\right) e^{-i\omega_{m\mathbf{k}2}t} \int dx e^{ik_x x} \; - \frac{1}{i\omega_{m\mathbf{k}2}} {b_{m\mathbf{k}}}^{+}\right.\right.\right. \\
&\times \sin\left(\frac{m\pi}{2}\right) e^{i\omega_{m\mathbf{k}2}t} \int dx e^{-ik_x x} \,\}\left(\hat{z}\times\hat{k}\right)\cdot\hat{x} - \frac{1}{\mu\varepsilon}\frac{1}{{\omega_{n\mathbf{k}1}}^2}\left(c_{n\mathbf{k}}\left(\frac{n\pi}{d}\right)\sin\left(\frac{n\pi}{2}\right)\right. \\
&\times e^{-i\omega_{n\mathbf{k}2}t}\int dx e^{ik_x x} \; + {c_{n\mathbf{k}}}^{+}\left(\frac{n\pi}{d}\right)\sin\left(\frac{n\pi}{2}\right)e^{i\omega_{n\mathbf{k}2}t}\int dx e^{-ik_x x}\Big) k_x\Big] - \frac{1}{2} i \,[\\
&- \sum_{m,\mathbf{k}}\left\{\frac{ik_x}{i\omega_{m\mathbf{k}2}} b_{m\mathbf{k}} \sin\left(\frac{m\pi}{2}\right) e^{-i\omega_{m\mathbf{k}2}t}\int dx e^{ik_x x} + \frac{ik_x}{i\omega_{m\mathbf{k}2}} {b_{m\mathbf{k}}}^{+}\sin\left(\frac{m\pi}{2}\right)\right. \\
&\times e^{i\omega_{m\mathbf{k}2}t}\int dx e^{-ik_x x}\Big\}\left(\hat{z}\times\hat{k}\right)\cdot\hat{x} - \frac{1}{\mu\varepsilon}\frac{1}{{\omega_{n\mathbf{k}1}}^2}\left(ik_x c_{n\mathbf{k}}\left(\frac{n\pi}{d}\right)\sin\left(\frac{n\pi}{2}\right)e^{-i\omega_{n\mathbf{k}2}t}\right. \\
&\times \int dx e^{ik_x x} \; - ik_x {c_{n\mathbf{k}}}^{+}\left(\frac{n\pi}{d}\right)\sin\left(\frac{n\pi}{2}\right)e^{i\omega_{n\mathbf{k}2}t}\int dx e^{-ik_x x}\Big) k_x\Big]\Big\}.
\end{aligned} \tag{3.20}$$

According to Fourier analyze, $\int_{-\infty}^{\infty} e^{ik_x x} dx = 2\pi\delta\left(k_x\right)$. The terms with $k_z\delta\left(k_z\right)$ in the equation above will be vanished after integration overk_x. We can drop it. Then we have

$$\begin{aligned}
H'_{eff} = -e\lambda_e \frac{\hbar k_e}{m_e} 2\pi \sum_{m,\mathbf{k}} &\left[\frac{1}{i\omega_{m\mathbf{k}2}} b_{m\mathbf{k}} \sin\left(\frac{m\pi}{2}\right) e^{-i\omega_{m\mathbf{k}2}t}\delta\left(k_x\right)\right. \\
&\left. - \frac{1}{i\omega_{m\mathbf{k}2}} {b_{m\mathbf{k}}}^{+} \sin\left(\frac{m\pi}{2}\right) e^{i\omega_{m\mathbf{k}2}t}\delta\left(k_x\right)\right]\cos\left(\frac{\pi}{2}+\phi_k\right),
\end{aligned} \tag{3.21}$$

where ϕ_k is the angle between the $\mathbf{k}$ and $\hat{x}$. The relationship between ϕ_k, $\mathbf{k}$, and $\hat{x}$ is shown in Fig. 3.4

"$\delta\left(k_x\right)\cos\left(\frac{\pi}{2}+\phi_k\right)$" in equation above will lead to the form "$-Sgn(k_y)$" after inte-

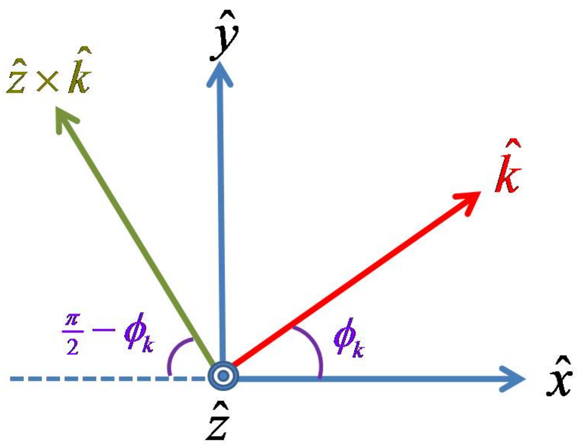

Figure 3.4: The illustration shows the relation between $\phi_k,\ \hat{k},\ and\ \hat{z} \times \hat{k}$.

gration with respect to k_x, so we substitute $\delta(k_x)\cos\left(\frac{\pi}{2}+\phi_k\right)$ to $-\delta(k_x)\,Sgn(k_y)$ to avoid complicated calculation. Actually, the magnitude of electron current is equal to $e\lambda_e\frac{\hbar k_e}{m_e}$ by definition, so that we let $I_0 = e\lambda_e\frac{\hbar k_e}{m_e}$.Then, we have

$$H'_{eff} = 2\pi I_0 \sum_{m,\kappa} \frac{1}{i\omega_{m\mathbf{k}2}} \sin\left(\frac{m\pi}{2}\right)\left\{b_{m\mathbf{k}2}e^{-i\omega_{m\mathbf{k}2}t} - {b_{m\mathbf{k}2}}^{+}e^{i\omega_{m\mathbf{k}2}t}\right\}\delta(k_x)\,Sgn(k_y) \quad (3.22)$$

If we allow the current to oscillate harmonically in time, we can substitute $I_0\cos(\Omega t)$ for I_0 where Ω is the oscillation angular frequency. The perturbation operator becomes:

$$\begin{aligned} H'_{eff} = 2\pi I_0 \cos(\Omega t) \sum_{m,\kappa} \frac{1}{i\omega_{m\mathbf{k}2}} \sin\left(\frac{m\pi}{2}\right)\left\{b_{m\mathbf{k}2}e^{-i\omega_{m\mathbf{k}2}t} - {b_{m\mathbf{k}2}}^{+}e^{i\omega_{m\mathbf{k}2}t}\right\} \\ \times\, \delta(k_x)\,Sgn(k_y) \end{aligned} \quad (3.23)$$

The first order perturbation coefficient

Again, we apply time-dependent perturbation theory to solve the new eigenstate of photon, and the first order perturbation coefficient in H'_{eff} is given by:

$$f^{(1)}_{\mathbf{k}\lambda} = \frac{-i}{\hbar}\int_{-\infty}^{t} \langle\{0,0,...,0,1_{\mathbf{k}\lambda},0,...,0\}|\, H'_{eff}\, |\{0\}\rangle dt. \quad (3.24)$$

We impose the mechanism of adiabatic turn-on to simulate the more realistic system and simplify calculation. Therefore, we put the term $e^{\eta t}$ in the integration form. We consider about one photon emission. It means the photon state from $|\{0\}\rangle$ to $|\{0, 0, ..., 0, 1_{\mathbf{k}\lambda}, 0, ..., 0\}\rangle$

We add a factor of to describe adiabatic turned on . η is a constant smaller than 1 far, switched on very gradually in the past, and we are looking at times much smaller than$\frac{1}{\eta}$. We can then take the initial time to be $-\infty$. For TE modes We have the first order perturbation coefficient by:

$$\begin{aligned} f^{(1)}_{m'\kappa'2} &= \frac{-i}{\hbar}\int_{-\infty}^{t} \langle\{0, 0, ..., 0, 1_{m\mathbf{k}2}, 0, ..., 0\}|\, \frac{e}{m}\mathbf{A}\cdot\mathbf{p}e^{\eta t}\,|\{0\}\rangle dt \\ &= \frac{i}{\hbar}\int_{-\infty}^{t} e^{\eta t}\,\langle\{0, 0, ..., 0, 1_{m\mathbf{k}2}, 0, ..., 0\}|\, I_0\cos(\Omega t)\,2\pi i \\ &\times \sum_{m,\mathbf{k}} \frac{1}{\omega_{m\mathbf{k}2}}\sin\left(\frac{m\pi}{2}\right)\left\{b_{m\mathbf{k}}e^{-i\omega_{m\mathbf{k}2}t} - {b_{m\mathbf{k}}}^{+}e^{i\omega_{m\mathbf{k}2}t}\right\}\delta(k_x)\,Sgn(k_y)\,|\{0\}\rangle\, dt \end{aligned} \tag{3.25}$$

$b_{m\mathbf{k}}$ and ${b_{m\mathbf{k}2}}^{+}$ in Eq. (3.25) is corresponded to the annihilation operator and the creation operator respectively. We use Eq. (2.21) as well as Eq. (2.22) and Simplify Eq. (3.25), so we have:

$$\begin{aligned} f^{(1)}_{m\mathbf{k}2} &= \frac{I_0}{\hbar}2\pi\frac{1}{\omega_{m\mathbf{k}2}}\sqrt{\frac{\hbar\omega_{m\mathbf{k}2}}{\varepsilon V}}\sin\left(\frac{m\pi}{2}\right) \\ &\times \frac{1}{2i}\left\{\frac{\exp\left[i\left(\omega_{m\mathbf{k}2} - i\eta + \Omega\right)t\right]}{\omega_{m\mathbf{k}2} - i\eta + \Omega} + \frac{\exp\left[i\left(\omega_{m\mathbf{k}2} - i\eta - \Omega\right)t\right]}{\omega_{m\mathbf{k}2} - i\eta - \Omega}\right\}\delta(k_x)\,Sgn(k_y) \end{aligned} \tag{3.26}$$

For TM modes

$$f^{(1)}_{n'\mathbf{k}'1} = \frac{-i}{\hbar}\int_{-\infty}^{t} \langle\{0, 0, ..., 0, 1_{n'\mathbf{k}'1}, 0, ..., 0\}|\, {H'}_{eff}\,|\{0\}\rangle dt = 0.$$

The expectation value of vector potential

We are interesting the expectation value of vector potential, because the electric field can be obtained easily after knowing it. The time-dependent expectation value of vector potential in the photon state $|\Psi\rangle$ is given by:

$$\begin{aligned}\mathbf{A}(\mathbf{r},t) &= \langle\Psi|\,\mathbf{A}^{(op)}\,|\Psi\rangle \\ &= \{\langle\{0,0,...,0,...\}| + \sum_{m\mathbf{k}} {f^{(1)}_{m\mathbf{k}2}}^{*}\,\langle\{0,...,0,1_{m\mathbf{k}2},0,...\}|\}\mathbf{A}^{(op)}\{|\{0,0,...,0,...\}\rangle \\ &+ \sum_{m\mathbf{k}} f^{(1)}_{m\mathbf{k}2}\,|\{0,...,0,1_{m\mathbf{k}2},0,...\}\rangle\}.\end{aligned} \tag{3.27}$$

Let's remember that $f^{(1)}_{n\mathbf{k}1}$ is equal to zero, and we already derived $f^{(1)}_{m\mathbf{k}2}$ in Eq. (3.26). We combine Eq. (2.16), Eq. (3.26) and Eq. (3.27), and we get:

$$\begin{aligned}&\mathbf{A}(\mathbf{r},t) \\ &= \sum_{m,\kappa} \frac{I_0}{\hbar}\pi\frac{1}{{\omega^2}_{m\mathbf{k}2}}\frac{\hbar\omega_{m\mathbf{k}2}}{\varepsilon V}\sin\left(\frac{m\pi}{2}\right)\sin\left(\frac{m\pi}{d}z\right)\left\{e^{i(\mathbf{k}\cdot\boldsymbol{\rho}-\omega_{m\mathbf{k}2}t)}\cdot\frac{\exp\left[i\left(\omega_{m\mathbf{k}2}+\Omega\right)t\right]}{\omega_{m\kappa2}-i\eta+\Omega}\right. \\ &+ e^{i(\mathbf{k}\cdot\boldsymbol{\rho}-\omega_{m\mathbf{k}2}t)}\frac{\exp\left[i\left(\omega_{m\mathbf{k}2}-\Omega\right)t\right]}{\omega_{m\mathbf{k}2}-i\eta-\Omega} + e^{-i(\mathbf{k}\cdot\boldsymbol{\rho}-\omega_{m\mathbf{k}2}t)}\frac{\exp\left[-i\left(\omega_{m\mathbf{k}2}+\Omega\right)t\right]}{\omega_{m\mathbf{k}2}+i\eta+\Omega} \\ &\left.+e^{-i(\mathbf{k}\cdot\boldsymbol{\rho}-\omega_{m\mathbf{k}2}t)}\frac{\exp\left[-i\left(\omega_{m\mathbf{k}2}-\Omega\right)t\right]}{\omega_{m\mathbf{k}2}+i\eta-\Omega}\right\}\times\delta\left(k_x\right)Sgn(k_y)\left(\hat{z}\times\hat{k}\right)\end{aligned} \tag{3.28}$$

We can find the first two terms in the curve bracket in above equation is the complex conjugate of the last two terms. It is just like that we add the complex conjugate of electric field in equation, and it keeps the physical quantity be real number. The summation over **k** takes arbitrary directions and arbitrary magnitudes wave number. For arbitrary orientations and magnitudes of **k**, the summation over **k** can be generalized to integration over **k**, just like what we do in Chapter 3.

$$\sum_{\mathbf{k}} \to \sum_{\mathbf{k}} \frac{\Delta k_x}{\Delta k_x}\frac{\Delta k_y}{\Delta k_y} \to \frac{1}{\left(\Delta k_x\right)\left(\Delta k_y\right)}\int dk_x dk_y = \frac{V}{d(2\pi)^2}\int dk_x dk_y$$

Because the z direction is quantized and described by summation over m, it cannot change to representation of integration. The integral only respects to x and y.

$$\begin{aligned}\mathbf{A}(\mathbf{r},t) = I_0\frac{\pi}{\varepsilon d}\left(\frac{1}{2\pi}\right)^2 \sum_{m=1} \sin\left(\frac{m\pi}{2}\right)\sin\left(\frac{m\pi}{d}z\right)\int_{-\infty}^{\infty}dk_x\int_{-\infty}^{\infty}dk_y\frac{1}{\omega_{m\mathbf{k}2}} \\ \times\left\{e^{i(k_x x+k_y y)}\left[\frac{\exp[i\Omega t]}{+\omega_{m\mathbf{k}2}-i\eta+\Omega}+\frac{\exp[-i\Omega t]}{+\omega_{m\mathbf{k}2}-i\eta-\Omega}\right]+e^{-i(k_x x+k_y y)}\right. \\ \times\left.\left[\frac{\exp[-i\Omega t]}{+\omega_{m\mathbf{k}2}+i\eta+\Omega}+\frac{\exp[i\Omega t]}{+\omega_{m\mathbf{k}2}+i\eta-\Omega}\right]\right\}\delta(k_x)\,Sgn(k_y)\,\{-\sin\phi_\kappa\hat{x}+\cos\phi_\kappa\hat{y}\}\end{aligned} \tag{3.29}$$

Substituting the dispersion relation ${k_z}^2+k^2={\omega_{n\mathbf{k}1}}^2\mu\varepsilon$ into above equation, we have:

$$\begin{aligned}\mathbf{A}(\mathbf{r},t) = -\frac{I_0}{4\pi\varepsilon d}\sum_{m=1}\sin\left(\frac{m\pi}{2}\right)\sin\left(\frac{m\pi}{d}z\right)\left\{\exp[i\Omega t]\int_{-\infty}^{\infty}dk_y\frac{e^{i(k_y y)}}{\sqrt{\frac{1}{\mu\varepsilon}\left({k_z}^2+{k_y}^2\right)}}\right. \\ \times\frac{1}{\sqrt{\frac{1}{\mu\varepsilon}\left({k_z}^2+{k_y}^2\right)}-i\eta+\Omega}+\exp[-i\Omega t]\int_{-\infty}^{\infty}dk_y\frac{e^{i(k_y y)}}{\sqrt{\frac{1}{\mu\varepsilon}\left({k_z}^2+{k_y}^2\right)}} \\ \times\frac{1}{\sqrt{\frac{1}{\mu\varepsilon}\left({k_z}^2+{k_y}^2\right)}-i\eta-\Omega}+\exp[-i\Omega t]\int_{-\infty}^{\infty}dk_y\frac{e^{-i(k_y y)}}{\sqrt{\frac{1}{\mu\varepsilon}\left({k_z}^2+{k_y}^2\right)}} \\ \times\frac{1}{\sqrt{\frac{1}{\mu\varepsilon}\left({k_z}^2+{k_y}^2\right)}+i\eta+\Omega}+\exp[i\Omega t]\int_{-\infty}^{\infty}dk_y\frac{e^{-i(k_y y)}}{\sqrt{\frac{1}{\mu\varepsilon}\left({k_z}^2+{k_y}^2\right)}} \\ \times\left.\frac{1}{\sqrt{\frac{1}{\mu\varepsilon}\left({k_z}^2+{k_y}^2\right)}+i\eta-\Omega}\right\}\hat{x}\end{aligned} \tag{3.30}$$

Solving these integrals is not easy. Even though we can apply complex integral methods solve these integrals, the branch cuts make the complex integrals complicated. The detailed derivation is saved for Appendix D. Considering y > 0, we have

$$\mathbf{A}(\mathbf{r},t) = -\frac{I_0}{4\pi\varepsilon d}\sum_{m=1}\sin\left(\frac{m\pi}{2}\right)\sin\left(\frac{m\pi}{d}z\right)\left\{e^{-i\Omega t}2\pi i\frac{\mu\varepsilon\exp\left[i\sqrt{\mu\varepsilon\left(\Omega^2+i2\eta\Omega\right)-{k_z}^2}y\right]}{\sqrt{\mu\varepsilon\left(\Omega^2+i2\eta\Omega\right)-{k_z}^2}}\right.$$
$$\left.-e^{i\Omega t}2\pi i\frac{\mu\varepsilon\exp\left[-i\sqrt{\mu\varepsilon\left(\Omega^2-i2\eta\Omega\right)-{k_z}^2}y\right]}{\sqrt{\mu\varepsilon\left(\Omega^2-i2\eta\Omega\right)-{k_z}^2}}\right\}\hat{x} \tag{3.31}$$

By the same way, we can derive the vector potential for $y < 0$ which is given by:

$$\mathbf{A}(\mathbf{r},t) = -\frac{I_0}{4\pi\varepsilon d}\sum_{m}\sin\left(\frac{m\pi}{2}\right)\sin\left(\frac{m\pi}{d}z\right)\left\{\mathrm{e}^{-i\Omega t}2\pi i\frac{\mu\varepsilon\exp\left[-i\sqrt{\mu\varepsilon\left(\Omega^2+i2\eta\Omega\right)-{k_z}^2}y\right]}{\sqrt{\mu\varepsilon\left(\Omega^2+i2\eta\Omega\right)-{k_z}^2}}\right.$$
$$\left.-\mathrm{e}^{i\Omega t}2\pi i\frac{\mu\varepsilon\exp\left[i\sqrt{\mu\varepsilon\left(\Omega^2-i2\eta\Omega\right)-{k_z}^2}y\right]}{\sqrt{\mu\varepsilon\left(\Omega^2-i2\eta\Omega\right)-{k_z}^2}}\right\}\hat{x} \tag{3.32}$$

From Eq. (3.31) and Eq. (3.32) , we can rewrite the vector potential as following:

$$\mathbf{A}(\mathbf{r},t) = \mathbf{A}^{>}(\mathbf{r},t) + \mathbf{A}^{<}(\mathbf{r},t) \tag{3.33}$$

where $\mathbf{A}^{>}(\mathbf{r},t)$ is vector potential for $\mu\varepsilon\Omega^2 > {k_z}^2$ and $\mathbf{A}^{<}(\mathbf{r},t)$ is vector potential for $\mu\varepsilon\Omega^2 < {k_z}^2$. $\mathbf{A}^{>}(\mathbf{r},t)$ and $\mathbf{A}^{<}(\mathbf{r},t)$ can be written as:

$$\mathbf{A}^{>}(\mathbf{r},t) = \frac{\mu I_0}{d}\sum_{m}\sin\left(\frac{m\pi}{2}\right)\sin\left(\frac{m\pi}{d}z\right)\frac{\sin\left[\sqrt{\mu\varepsilon\Omega^2-{k_z}^2}\,|y|-\Omega t\right]}{\sqrt{\mu\varepsilon\Omega^2-{k_z}^2}}\hat{x} \tag{3.34}$$

and

$$\mathbf{A}^{<}(\mathbf{r},t) = -\frac{\mu I_0}{d}\sum_m \sin\left(\frac{m\pi}{2}\right)\sin\left(\frac{m\pi}{d}z\right)\cos(\Omega t)\frac{\exp\left[-\sqrt{{k_z}^2-\mu\varepsilon\Omega^2}\,|y|\right]}{\sqrt{{k_z}^2-\mu\varepsilon\Omega^2}}\hat{x}. \quad (3.35)$$

$\mu\varepsilon\Omega^2 > {k_z}^2$ means the frequency of the current oscillation beyond the cutoff frequency of the parallel-plates capacitor. The wave is in propagating modes. $\mu\varepsilon\Omega^2 < {k_z}^2$ indicates the frequency of the current oscillation above the cutoff frequency of the parallel-plates capacitor. And the corresponding electric field is given by:

$$\mathbf{E}(\mathbf{r},t) = \mathbf{E}^{>}(\mathbf{r},t) + \mathbf{E}^{<}(\mathbf{r},t) \quad (3.36)$$

where $\mathbf{E}^{>}(\mathbf{r},t)$ is vector potential for $\mu\varepsilon\Omega^2 > {k_z}^2$ and $\mathbf{E}^{<}(\mathbf{r},t)$ is vector potential for $\mu\varepsilon\Omega^2 < {k_z}^2$. They are expressed as:

$$\mathbf{E}^{>}(\mathbf{r},t) = \frac{\mu I_0\Omega}{d}\sum_m \sin\left(\frac{m\pi}{2}\right)\sin\left(\frac{m\pi}{d}z\right)\frac{\cos\left[\sqrt{\mu\varepsilon\Omega^2-\left(\frac{m\pi}{d}\right)^2}\,|y|-\Omega t\right]}{\sqrt{\mu\varepsilon\Omega^2-\left(\frac{m\pi}{d}\right)^2}}\hat{x} \quad (3.37)$$

and

$$\mathbf{E}^{<}(\mathbf{r},t) = -\frac{\mu I_0\Omega}{d}\sum_m \sin\left(\frac{m\pi}{2}\right)\sin\left(\frac{m\pi}{d}z\right)\sin(\Omega t)\frac{\exp\left[-\sqrt{\left(\frac{m\pi}{d}\right)^2-\mu\varepsilon\Omega^2}\,|y|\right]}{\sqrt{\left(\frac{m\pi}{d}\right)^2-\mu\varepsilon\Omega^2}}\hat{x} \quad (3.38)$$

The electric field only couples to TM wave and it only has the x-component field, because the line current oscillates in the x-direction. The direction of the electric field satisfies the expectations of classical electrodynamics. When $\mu\varepsilon\Omega^2 > {k_z}^2 = \left(\frac{m\pi}{d}\right)^2$, the situation will insure wave propagation. When $\mu\varepsilon\Omega^2 < {k_z}^2 = \left(\frac{m\pi}{d}\right)^2$, the wave becomes evanescent mode. An evanescent wave is a nearfield standing wave with an intensity that exhibits exponential decay with distance and it does not propagate. We can see this in Eq. (3.38) which has a term exponentially decaying from $y = 0$.

The electric field is the same as the classical expectation. Again, we prove that our calculation method is practical and the quantization wave in the waveguide we deduce is correct. The detailed calculation process of this problem in classical method is left for Appendix E.

3.3 Brief summary

In previous two sections, we drove the vector potential and electric field induced by oscillating charge in free space and ac line current in waveguide. The electromagnetic wave induced ac line current in waveguide only couples to TM modes. The results of the two different systems solved by our calculation method are identified with the calculation method of classical electrodynamics. We did show that our method is practical.

Chapter 4

The electric field induced by ac spin current

We already know that our calculation method is practical, and we will solve the electric field induced by ac in-plane polarized spin current in the waveguide in this chapter.

4.1 Effective Hamiltonian for photon

We had discussed the structure of the waveguide of our system previously. 2DEG (two dimensional electron gas) in our system is at the middle of the two parallel metal gates as Fig. 2.2. Ac in-plane polarized spin current will generate out-off-plane electric field and we can use a voltmeter to measure the electrical potential difference between the two metal gates.

We will calculate line spin current instead of surface spin current, because the field induced by line spin current is easy to analyze its physical meaning. Moreover, if we directly calculate the field induced by surface current, the field has singularity owing to the waveguide structure. Actually we may decompose the surface spin current into countless line spin currents. We can integrate over the electric field distribution of line spin current into one of surface spin current. Assume that the line spin current flow is parallel to x-axis and this "line" is located at (x,0,d/2). The spin polarization direction is towards the negative y-axis. We do not let this spin current oscillate at first, and the wave function of the spins is given by:

$$\psi(\mathbf{r}) = \langle \mathbf{r}|\psi\rangle = \sqrt{\lambda_s}\exp[ik_s x]\,\varphi(y,z)\begin{bmatrix}\frac{1}{\sqrt{2}}\\ -\frac{i}{\sqrt{2}}\end{bmatrix} \tag{4.1}$$

where λ_s is the line density of the spins and k_s is the wave number of the spins. $\begin{bmatrix}\frac{1}{\sqrt{2}} & -\frac{i}{\sqrt{2}}\end{bmatrix}^T$ is the spin state, whose spin direction always point towards the negative y-axis. In semiconductor, the spin orbit coupling term is given by $H' = e\frac{\Lambda}{\hbar}\sigma \cdot (\mathbf{p}\times\mathbf{E})$, where we discussed in Chapter 1. The effective perturbing Hamiltonian for photons in the system can be obtain by sandwiching H' with electron state as given by:

$$\begin{aligned}
&H'_{eff} = \langle\psi|\,H'\,|\psi\rangle \\
&= \int\left\{\sqrt{\lambda_s}\mathrm{e}^{-ik_s x}\varphi(y,z)\begin{bmatrix}\frac{1}{\sqrt{2}} & \frac{i}{\sqrt{2}}\end{bmatrix}\right\} e\frac{\Lambda}{\hbar}\sigma\cdot(\mathbf{p}\times\mathbf{E})\left\{\sqrt{\lambda_s}\mathrm{e}^{ik_s x}\varphi(y,z)\begin{bmatrix}\frac{1}{\sqrt{2}}\\ -\frac{i}{\sqrt{2}}\end{bmatrix}\right\} d\mathbf{r} \\
&= -e\lambda_s\frac{\Lambda}{\hbar}\int\left\{\mathrm{e}^{-ik_s x}\varphi(y,z)\right\}\left\{-i\hbar\frac{\partial}{\partial z}E_x + i\hbar\frac{\partial}{\partial x}E_z - i\hbar E_x\frac{\partial}{\partial z} + i\hbar E_z\frac{\partial}{\partial x}\right\} \\
&\quad\times\left\{\mathrm{e}^{ik_s x}\varphi(y,z)\right\} d\mathbf{r},
\end{aligned} \tag{4.2}$$

where E_x *and* E_z is the x and z component of the electric field respectively. $\mathbf{p}$ is operator for electron, it operate on the electron state. $\mathbf{E}$ is classical physical quantity for electron. The Eq. (2.12) and Eq. (2.15) lead us to obtain E_x *and* E_z by dot product. Hence, the

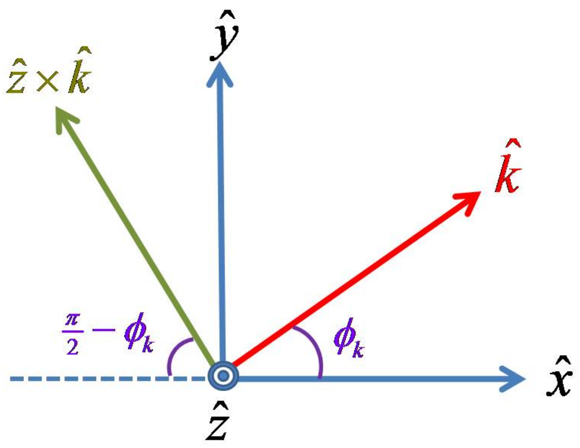

Figure 4.1: The figure shows the relationship between ϕ_k, $\mathbf{k}$, and $\hat{x}$.

perturbing Hamiltonian becomes:

$$
\begin{aligned}
H'_{eff} = -e\lambda\Lambda \int &\left\{ \mathrm{e}^{-ik_s x}\varphi\left(y,z\right)\right\} \left\{ \frac{1}{\mu\varepsilon}\sum_{n,\mathbf{k}} \frac{1}{\omega_{n\mathbf{k}1}}\left(\frac{n\pi}{d}\right)^2 \cos\left(\frac{n\pi}{d}z\right)\left[-c_{n\mathbf{k}}e^{i(k_x x+k_y y-\omega_{n\mathbf{k}1}t)}\right.\right.\\
&\left. + c_{n\mathbf{k}}{}^{+}e^{-i(k_x x+k_y y-\omega_{n\mathbf{k}1}t)}\right]\cos\phi_k - i\sum_{m,\mathbf{k}}\left(\frac{m\pi}{d}\right)\cos\left(\frac{m\pi}{d}z\right)\left[b_{m\mathbf{k}}e^{i(k_x x+k_y y-\omega_{m\mathbf{k}2}t)}\right.\\
&\left. + b_{m\mathbf{k}}{}^{+}e^{-i(k_x x+k_y y-\omega_{m\mathbf{k}2}t)}\right]\sin\phi_k + \frac{1}{\mu\varepsilon}\sum_{n,\mathbf{k}}\frac{k}{\omega_{n\mathbf{k}1}}\cos\left(\frac{n\pi}{d}z\right)\left[-k_x c_{n\mathbf{k}}e^{i(k_x x+k_y y-\omega_{n\mathbf{k}1}t)}\right.\\
&\left.\left. +k_x c_{n\mathbf{k}}{}^{+}e^{-i(k_x x+k_y y-\omega_{n\mathbf{k}1}t)}\right] - iE_x\frac{\partial}{\partial z} + iE_z\frac{\partial}{\partial x}\right\}\left\{\mathrm{e}^{ik_s x}\varphi\left(y,z\right)\right\}d\mathbf{r},
\end{aligned}
\tag{4.3}
$$

where ϕ_k is the angle between the $\mathbf{k}$ and $\hat{x}$. The relationship between ϕ_k, $\mathbf{k}$, and $\hat{x}$ is shown in Fig. 4.1.

Because the cross section of the y-z plane of the line spin current is far smaller than the thickness of the waveguide d, and the electric field near the line current $\left(x, y=0, z=\frac{d}{2}\right)$ change smoothly in the space and the electric field near the line current changes violently in the space, we can write the integration $\int dx \int dy \int dz \varphi\left(y,z\right) E_i \varphi\left(y,z\right)$ $\left(i = x,y,z\right)$ as:

$$\begin{aligned}
&\int dx \int dy \int dz \varphi\left(y,z\right) E_i\left(x,y,z\right) \varphi\left(y,z\right) \\
&= \int dx \int dy \int dz \left|\varphi\left(y,z\right)\right|^2 \int dx E_i\left(x,0,\tfrac{d}{2}\right) \\
&= \int dx E_i\left(x,0,\tfrac{d}{2}\right)
\end{aligned} \tag{4.4}$$

For the same reason, the integration $\int dx \int dy \int dz E_x \varphi\left(y,z\right) \frac{\partial}{\partial z} \varphi\left(y,z\right)$ can be written as:

$$\int dx \int dy \int dz E_x \varphi\left(y,z\right) \frac{\partial}{\partial z} \varphi\left(y,z\right) = -\frac{1}{2} \int dx \int dy \int dz \varphi(y,z)^2 \times \left[\int dx \frac{\partial}{\partial z}\left[E_x\right]\right]\Big|_{y=0,z=\frac{d}{2}} \tag{4.5}$$

We substitute Eq. (4.4) into Eq. (4.5) and express E_x , and E_z in waveguide modes. After simple integral process, the effective perturbing Hamiltonian becomes:

$$\begin{aligned}
H'_{eff} = -e\lambda\Lambda \Bigg\{ &\frac{1}{\mu\varepsilon} \sum_{n,\mathbf{k}} \frac{1}{\omega_{n\mathbf{k}1}} \left(\frac{n\pi}{d}\right)^2 \cos\left(\frac{n\pi}{2}\right) 2\pi\delta\left(k_x\right) \left[-c_{n\mathbf{k}} e^{-i\omega_{n\mathbf{k}1}t} + c_{n\mathbf{k}}{}^{+} e^{i\omega_{n\mathbf{k}1}t}\right] \cos\left(\phi_k\right) \\
&- i \sum_{m,\mathbf{k}} \left(\frac{m\pi}{d}\right) \cos\left(\frac{m\pi}{2}\right) 2\pi\delta\left(k_x\right) \left[b_{m\mathbf{k}} e^{-i\omega_{m\mathbf{k}2}t} + b_{m\mathbf{k}}{}^{+} e^{i\omega_{m\mathbf{k}2}t}\right] \sin\left(\phi_k\right) \\
&+ \frac{1}{\mu\varepsilon} \sum_{n,\mathbf{k}} k_x \frac{k}{\omega_{n\mathbf{k}1}} \cos\left(\frac{n\pi}{2}\right) 2\pi\delta\left(k_x\right) \left[-c_{n\mathbf{k}} e^{-i\omega_{n\kappa1}t} + c_{n\mathbf{k}}{}^{+} e^{i\omega_{n\mathbf{k}1}t}\right] \\
&+ \pi\delta\left(k_x\right) \frac{1}{\mu\varepsilon} \sum_{n,\kappa} \frac{1}{\omega_{n\kappa}} \left(\frac{n\pi}{d}\right)^2 \cos\left(\frac{n\pi}{2}\right) \left[c_{n\mathbf{k}} e^{-i\omega_{n\kappa1}t} - c_{n\mathbf{k}}{}^{*} e^{i\omega_{n\mathbf{k}1}t}\right] \cos\phi_k \\
&+ \pi\delta\left(k_x\right) i \sum_{m,\kappa} \left(\frac{m\pi}{d}\right) \cos\left(\frac{m\pi}{2}\right) \left[b_{m\mathbf{k}} e^{-i\omega_{m\mathbf{k}2}t} + b_{m\mathbf{k}}{}^{*} e^{i\omega_{m\mathbf{k}2}t}\right] \sin\phi_k \\
&- k_s 2\pi\delta\left(k_x\right) \frac{1}{\mu\varepsilon} \sum_{n,\kappa} \frac{k}{\omega_{n\kappa1}} \cos\left(\frac{n\pi}{2}\right) \left[c_{n\kappa} e^{-i\omega_{n\kappa1}t} + c_{n\kappa}{}^{*} e^{i\omega_{n\kappa1}t}\right] \Bigg\}
\end{aligned} \tag{4.6}$$

The first, third, fourth, term in the curve bracket have $\delta\left(\phi_k\right) \cos\left(\phi_k\right)$ or $k_x \delta\left(k_x\right)$ will vanish after integrating over k_x. We drop it to avoid unnecessary calculation. The Hamiltonian of the effective perturbation becomes:

$$H'_{eff} = -e\lambda_s\Lambda \left\{ -\pi i \sum_{m,\mathbf{k}} \left(\frac{m\pi}{d}\right) \cos\left(\frac{m\pi}{2}\right) \left[b_{m\mathbf{k}} e^{-i\omega_{m\mathbf{k}2}t} + b_{m\mathbf{k}}{}^{+} e^{i\omega_{m\mathbf{k}2}t}\right] \delta\left(k_x\right) \sin\phi_k \right.$$
$$\left. -2\pi k_s \frac{1}{\mu\varepsilon} \sum_{n,\mathbf{k}} \frac{k}{\omega_{n\mathbf{k}1}} \cos\left(\frac{n\pi}{2}\right) \left[c_{n\mathbf{k}} e^{-i\omega_{n\mathbf{k}1}t} + c_{n\mathbf{k}}{}^{+} e^{i\omega_{n\mathbf{k}1}t}\right] \delta\left(k_x\right) \right\} \tag{4.7}$$

We divide the effective perturbing Hamiltonian into two parts as $H'_{eff} = H'_{TM} + H'_{TE}$ where

$$H'_{TE} = e\lambda_s\Lambda\pi i \sum_{m,\mathbf{k}} \left(\frac{m\pi}{d}\right) \cos\left(\frac{m\pi}{2}\right) \left[b_{m\mathbf{k}} e^{-i\omega_{m\mathbf{k}2}t} + b_{m\mathbf{k}}{}^{+} e^{i\omega_{m\mathbf{k}2}t}\right] \delta\left(k_x\right) \sin\phi_k$$

$$H'_{TM} = 2\pi e\lambda_s k_s \frac{\Lambda}{\mu\varepsilon} \sum_{n,\mathbf{k}} \frac{k}{\omega_{n\mathbf{k}1}} \cos\left(\frac{n\pi}{2}\right) \left[c_{n\mathbf{k}1} e^{-i\omega_{n\mathbf{k}1}t} + c_{n\kappa 1}{}^{+} e^{i\omega_{n\mathbf{k}1}t}\right] \delta\left(k_x\right)$$

H'_{TE} which contains $b_{m\mathbf{k}}$ and $b_{m\mathbf{k}}{}^{+}$ couples to the TE wave, and H'_{TM} which contains $c_{n\mathbf{k}}$ and $c_{n\mathbf{k}}{}^{+}$ couples to the TM wave. We only care about the z-component of the electric field, because only this component of the electric field distributes the electrical potential difference between the two metal slabs of the waveguide. The z-component electric field is corresponding to the TM wave. ($c_{n\kappa 1}$ or $c_{n\kappa 1}{}^{+}$ couples to photons of TM wave.) Actually, if we keep calculating the vector potential with the perturbing Hamiltonian H'_{TE}, the vector potential of TE modes will be equal to zero. It means that only photons corresponding to the transverse magnetic (TM) waveguide modes are exited. If we allow the spin current to become oscillatory, with an ac frequency Ω, we can incorporate this into our present framework by changing: $k_s \rightarrow k_s \cos(\Omega t)$. Hence, the Hamiltonian of the effective perturbation becomes as the following:

$$H'_{TM} = 2\pi e\lambda_s k_s \cos(\Omega t) \frac{\Lambda}{\mu\varepsilon} \sum_{n,\mathbf{k}} \frac{k}{\omega_{n\mathbf{k}1}} \cos\left(\frac{n\pi}{2}\right) \left[c_{n\mathbf{k}1} e^{-i\omega_{n\mathbf{k}1}t} + c_{n\mathbf{k}1}{}^{+} e^{i\omega_{n\mathbf{k}1}t}\right] \delta\left(k_x\right) \tag{4.8}$$

With the perturbing Hamiltonian for photons, we can obtain the wave function by using perturbation theorem. We will solve the photon state in our system in next section.

4.2 The new photon state in the waveguide

We have obtained the effective Hamiltonian of the system of ac in-plane polarized spin current for TM wave in parallel-planes waveguide. We desire to know the photon state of TM wave in our system. The photon state gives us all information of the wave in the waveguide including the z-component electric field. The photon state of TM wave in our system becomes:

$$\begin{aligned} |\Psi\rangle &= |\Psi_0\rangle + \sum_{n\mathbf{k}1} f^{(1)}_{n\mathbf{k}1} \left|\{0,0,...,0,1_{n\mathbf{k}1},0,...,0\}\right\rangle \\ &= |\{0,0,...,0,...,0\}\rangle + \sum_{n\mathbf{k}1} f^{(1)}_{n\mathbf{k}1} \left|\{0,0,...,0,1_{n\mathbf{k}1},0,...,0\}\right\rangle \end{aligned} \tag{4.9}$$

where $|\Psi_0\rangle$ is the original wave function. $f^{(1)}_{n\mathbf{k}1}$ is the first order perturbation coefficient of H'_{TM}. $f^{(1)}_{n\mathbf{k}1}$ can be solved by:

$$\begin{aligned} f^{(1)}_{n'\mathbf{k}'1} &= \frac{-i}{\hbar}\int_{-\infty}^{t} \langle\{0,0,...,0,1_{n'\mathbf{k}'1},0,...,0\}|\, H'_{eff} e^{\eta t} \,|\{0\}\rangle dt \\ &= \frac{-i}{\hbar}\int_{-\infty}^{t} e^{\eta t} \langle\{0,0,...,0,1_{n'\mathbf{k}'1},0,...,0\}|\, 2\pi e\lambda_s k_s \cos(\Omega t)\, \frac{\Lambda}{\mu\varepsilon} \\ &\times \sum_{n,\kappa} \frac{k}{\omega_{n\mathbf{k}1}} \cos\left(\frac{n\pi}{2}\right) \left[c_{n\mathbf{k}1} e^{-i\omega_{n\mathbf{k}1}t} + {c_{n\mathbf{k}1}}^{+} e^{i\omega_{n\mathbf{k}1}t}\right] \delta(k_x)\, |\{0\}\rangle\, dt \end{aligned} \tag{4.10}$$

After integration, the first order perturbation coefficient becomes:

$$\begin{aligned} f^{(1)}_{n'\mathbf{k}'1} &= \frac{-\pi e\lambda_s k_s}{\hbar} \frac{\Lambda}{\mu\varepsilon} \frac{k}{\omega_{n\mathbf{k}1}} \cos\left(\frac{n\pi}{2}\right) \sqrt{\mu\frac{\hbar\omega_{n\mathbf{k}1}}{V}} \left\{ \frac{\exp\left[i\left(\omega_{n\mathbf{k}1}+\Omega\right)t\right]}{\omega_{n\mathbf{k}1} - i\eta + \Omega} \right. \\ &\left. + \frac{\exp\left[i\left(\omega_{n\mathbf{k}1}-\Omega\right)t\right]}{\omega_{n\mathbf{k}1} - i\eta - \Omega} \right\} \delta(k_x) \end{aligned} \tag{4.11}$$

Since H'_{TM} does not include the $b_{m\mathbf{k}}$ or ${b_{m\mathbf{k}}}^{+}$, H'_{TM} would not couple to the TE wave but TM wave which we care about. From above equation, we know that $f^{(1)}_{n'\mathbf{k}'1}$ vanishes for odd "n" which imply the electric field for TM wave will only couple to even n mode.

Also, we know the photon state of TM wave in our system.

4.3 The expectation value of the vector potential in our system

The expectation value can give us the predicted mean value of the result. In the previous section, we obtained the photon state of TM wave $|\Psi\rangle$. The expectation value of the vector potential of TM wave in the photon state $|\Psi\rangle$ is given by:

$$
\begin{aligned}
&\mathbf{A}_{TM}(\mathbf{r},t) = \langle\Psi| A^{(op)} |\Psi\rangle \\
&= \left\{ \langle\{0,0,....,0\}| + \sum_{m'\mathbf{k}\lambda} {f^{(1)}_{m'\mathbf{k}\lambda}}^{*} \langle\{0,..,0,1_{m'\mathbf{k}\lambda},0,...,0\}| \right\} A^{(op)} \{ |\{0,0,...,0\}\rangle \\
&\quad + \sum_{m'\mathbf{k}\lambda} f^{(1)}_{m'\mathbf{k}\lambda} |\{0,...,0,1_{m'\mathbf{k}\lambda},0,...,0\}\rangle \bigg\}.
\end{aligned} \tag{4.12}
$$

Substituting Eq. (2.17) into Eq. (4.12), we have:

$$
\begin{aligned}
&\mathbf{A}_{TM}(\mathbf{r},t) \\
&= -\frac{1}{\mu\varepsilon} \sum_{n\mathbf{k}} \frac{\left(\frac{n\pi}{d}\right)}{{\omega_{n\mathbf{k}1}}^2} \sin\left(\frac{n\pi}{d}z\right) \sqrt{\mu\frac{\hbar\omega_{n\mathbf{k}1}}{V}} \left\{ f^{(1)}_{n\mathbf{k}1} e^{i(\mathbf{k}\cdot\boldsymbol{\rho}-\omega_{n\mathbf{k}1}t)} + {f^{(1)}_{n\mathbf{k}1}}^{*} e^{-i(\mathbf{k}\cdot\boldsymbol{\rho}-\omega_{n\mathbf{k}1}t)} \right\} \hat{k} \\
&\quad + \frac{1}{\mu\varepsilon} \sum_{n\mathbf{k}} \frac{k}{{\omega_{n\mathbf{k}1}}^2} \cos\left(\frac{n\pi}{d}z\right) \sqrt{\mu\frac{\hbar\omega_{n\mathbf{k}1}}{V}} \left\{ -i f^{(1)}_{n\mathbf{k}1} e^{i(\mathbf{k}\cdot\boldsymbol{\rho}-\omega_{n\mathbf{k}1}t)} + i {f^{(1)}_{n\mathbf{k}1}}^{*} e^{-i(\mathbf{k}\cdot\boldsymbol{\rho}-\omega_{n\mathbf{k}1}t)} \right\} \hat{z}
\end{aligned} \tag{4.13}
$$

From above equation, we notice that the vector potential has two components that are k and z directions. The two directions are the same as the directions of electric field.

Combining above equation Eq. (4.11) and Eq. (4.13), we obtain:

$$\begin{aligned}
\mathbf{A}_{TM}(\mathbf{r},t) &= \frac{\Lambda}{(\mu\varepsilon)^2}\frac{\mu}{V}\pi e\lambda_s k_s \sum_{n\mathbf{k}}\left(\frac{n\pi}{d}\right)\sin\left(\frac{n\pi}{d}z\right) \\
&\times\left\{\frac{k}{{\omega_{n\mathbf{k}1}}^2}\cos\left(\frac{n\pi}{2}\right)\left[\frac{\exp\left[i\left(+\omega_{n\mathbf{k}1}+\Omega\right)t\right]}{\omega_{n\mathbf{k}1}-i\eta+\Omega}+\frac{\exp\left[i\left(+\omega_{n\mathbf{k}1}-\Omega\right)t\right]}{\omega_{n\mathbf{k}1}-i\eta-\Omega}\right]\delta\left(k_x\right)e^{i\left(\mathbf{k}\cdot\boldsymbol{\rho}-\omega_{n\mathbf{k}1}t\right)}\right. \\
&\left.+\frac{k}{{\omega_{n\mathbf{k}1}}^2}\cos\left(\frac{n\pi}{2}\right)\left[\frac{\exp\left[-i\left(\omega_{n\kappa1}+\Omega\right)t\right]}{\omega_{n\kappa1}+i\eta+\Omega}+\frac{\exp\left[-i\left(\omega_{n\mathbf{k}1}-\Omega\right)t\right]}{\omega_{n\mathbf{k}1}+i\eta-\Omega}\right]\delta\left(k_x\right)e^{-i\left(\mathbf{k}\cdot\boldsymbol{\rho}-\omega_{n\mathbf{k}1}t\right)}\hat{k}\right\} \\
&+\frac{\Lambda}{(\mu\varepsilon)^2}\frac{\mu}{V}\pi e\lambda_s k_s \sum_{n\mathbf{k}}\cos\left(\frac{n\pi}{d}z\right) \\
&\times\left\{+i\frac{k^2}{{\omega_{n\mathbf{k}1}}^2}\cos\left(\frac{n\pi}{2}\right)\left[\frac{\exp\left[i\left(\omega_{n\mathbf{k}1}+\Omega\right)t\right]}{\omega_{n\mathbf{k}1}-i\eta+\Omega}+\frac{\exp\left[i\left(\omega_{n\mathbf{k}1}-\Omega\right)t\right]}{\omega_{n\mathbf{k}1}-i\eta-\Omega}\right]\delta\left(k_x\right)e^{i\left(\mathbf{k}\cdot\boldsymbol{\rho}-\omega_{n\mathbf{k}1}t\right)}\right. \\
&\left.-i\frac{k^2}{{\omega_{n\mathbf{k}1}}^2}\cos\left(\frac{n\pi}{2}\right)\left[\frac{\exp\left[-i\left(\omega_{n\mathbf{k}1}+\Omega\right)t\right]}{\omega_{n\mathbf{k}1}+i\eta+\Omega}+\frac{\exp\left[-i\left(\omega_{n\mathbf{k}1}-\Omega\right)t\right]}{\omega_{n\mathbf{k}1}+i\eta-\Omega}\right]\delta\left(k_x\right)e^{-i\left(\mathbf{k}\cdot\boldsymbol{\rho}-\omega_{n\mathbf{k}1}t\right)}\hat{z}\right\}
\end{aligned} \tag{4.14}$$

For arbitrary orientation and arbitrary magnitude of wave number $\mathbf{k}$, We can generalize the summation to representation of integration for continuous $\mathbf{k}$. It means $\sum_{\mathbf{k}}\to\sum_{\mathbf{k}}\frac{\Delta k_x}{\Delta k_x}\frac{\Delta k_y}{\Delta k_y}\to\frac{1}{(\Delta k_x)(\Delta k_y)}\int dk_x dk_y=\frac{V}{d(2\pi)^2}\int dk_x dk_y$. Because the z direction is quantized and described by summation m, it may not change to representation of integration. The integral only respects to x and y. Then we get

$$\begin{aligned}
\mathbf{A}_{TM}(\mathbf{r},t) &= \frac{\Lambda}{(\mu\varepsilon)^2}\frac{\mu}{d}\pi e\lambda_s k_s\left(\frac{1}{2\pi}\right)^2\sum_{n=0}\left(\frac{n\pi}{d}\right)\sin\left(\frac{n\pi}{d}z\right)\cos\left(\frac{n\pi}{2}\right) \\
&\times\int_{-\infty}^{\infty}dk_x\int_{-\infty}^{\infty}dk_y\left\{\frac{k}{{\omega_{n\mathbf{k}1}}^2}\left[\frac{\exp\left[i\Omega t\right]}{+\omega_{n\mathbf{k}1}-i\eta+\Omega}+\frac{\exp\left[-i\Omega t\right]}{+\omega_{n\mathbf{k}1}-i\eta-\Omega}\right]\delta\left(k_x\right)e^{i\left(k_x x+k_y y\right)}\right. \\
&\left.+\frac{k}{{\omega_{n\mathbf{k}1}}^2}\left[\frac{\exp\left[-i\Omega t\right]}{+\omega_{n\mathbf{k}1}+i\eta+\Omega}+\frac{\exp\left[i\Omega t\right]}{+\omega_{n\mathbf{k}1}+i\eta-\Omega}\right]\delta\left(k_x\right)e^{-i\left(k_x x+k_y y\right)}\right\}\hat{k} \\
&+\frac{\Lambda}{(\mu\varepsilon)^2}\frac{\mu}{d}\pi e\lambda_s k_s\left(\frac{1}{2\pi}\right)^2\sum_{n=0}\cos\left(\frac{n\pi}{d}z\right)\cos\left(\frac{n\pi}{2}\right) \\
&\times\int_{-\infty}^{\infty}dk_x\int_{-\infty}^{\infty}dk_y\left\{i\frac{k^2}{{\omega_{n\mathbf{k}1}}^2}\left[\frac{\exp\left[i\Omega t\right]}{+\omega_{n\mathbf{k}1}-i\eta+\Omega}+\frac{\exp\left[-i\Omega t\right]}{+\omega_{n\mathbf{k}1}-i\eta-\Omega}\right]\delta\left(k_x\right)e^{i\left(k_x x+k_y y\right)}\right. \\
&\left.-i\frac{k^2}{{\omega_{n\mathbf{k}1}}^2}\left[\frac{\exp\left[-i\Omega t\right]}{+\omega_{n\mathbf{k}1}+i\eta+\Omega}+\frac{\exp\left[i\Omega t\right]}{+\omega_{n\mathbf{k}1}+i\eta-\Omega}\right]\delta\left(k_x\right)e^{-i\left(k_x x+k_y y\right)}\right\}\hat{z}.
\end{aligned} \tag{4.15}$$

We use the dispersion relation ${k_z}^2 + k^2 = {\omega_{n\mathbf{k}}}^2 \mu\varepsilon$ and replace $\omega_{n\mathbf{k}1}$ by $\sqrt{\frac{1}{\mu\varepsilon}\left({k_y}^2 + {k_z}^2\right)}$. "$\delta\left(k_x\right)$" in above equation make the integration with respect to k_x easy. Then the vector potential becomes:

$$\begin{aligned}\mathbf{A}_{TM}\left(\mathbf{r},t\right) = &\frac{\Lambda}{\left(\mu\varepsilon\right)^2}\frac{\mu}{d}\pi e\lambda_s k_s\left(\frac{1}{2\pi}\right)^2\sum_{n=0}\left(\frac{n\pi}{d}\right)\sin\left(\frac{n\pi}{d}z\right)\cos\left(\frac{n\pi}{2}\right)\left\{F_1+F_2+F_3+F_4\right\}\hat{y}\\&+i\frac{\Lambda}{\left(\mu\varepsilon\right)^2}\frac{\mu}{d}\pi e\lambda_s k_s\left(\frac{1}{2\pi}\right)^2\sum_{n=0}\cos\left(\frac{n\pi}{d}z\right)\cos\left(\frac{n\pi}{2}\right)\left\{G_1+G_2-G_3-G_4\right\}\hat{z},\end{aligned} \tag{4.16}$$

where

$$F_1 = \int_{-\infty}^{\infty} dk_y \frac{\mu\varepsilon k_y}{{k_y}^2+{k_z}^2} \times \frac{\exp\left[i\Omega t\right]}{\sqrt{\frac{1}{\mu\varepsilon}\left({k_y}^2+{k_z}^2\right)} - i\eta + \Omega} e^{ik_y y}$$

$$F_2 = \int_{-\infty}^{\infty} dk_y \frac{\mu\varepsilon k_y}{{k_y}^2+{k_z}^2} \times \frac{\exp\left[-i\Omega t\right]}{\sqrt{\frac{1}{\mu\varepsilon}\left({k_y}^2+{k_z}^2\right)} - i\eta - \Omega} e^{ik_y y}$$

$$F_3 = \int_{-\infty}^{\infty} dk_y \frac{\mu\varepsilon k_y}{{k_y}^2+{k_z}^2} \times \frac{\exp\left[-i\Omega t\right]}{\sqrt{\frac{1}{\mu\varepsilon}\left({k_y}^2+{k_z}^2\right)} + i\eta + \Omega} e^{-ik_y y}$$

$$F_4 = \int_{-\infty}^{\infty} dk_y \frac{\mu\varepsilon k_y}{{k_y}^2+{k_z}^2} \times \frac{\exp\left[i\Omega t\right]}{\sqrt{\frac{1}{\mu\varepsilon}\left({k_y}^2+{k_z}^2\right)} + i\eta - \Omega} e^{-ik_y y}$$

$$G_1 = \int_{-\infty}^{\infty} dk_y \frac{\mu\varepsilon {k_y}^2}{{k_y}^2+{k_z}^2} \times \frac{\exp\left[i\Omega t\right]}{\sqrt{\frac{1}{\mu\varepsilon}\left({k_y}^2+{k_z}^2\right)} - i\eta + \Omega} e^{ik_y y}$$

$$G_2 = \int_{-\infty}^{\infty} dk_y \frac{\mu\varepsilon {k_y}^2}{{k_y}^2+{k_z}^2} \times \frac{\exp\left[-i\Omega t\right]}{\sqrt{\frac{1}{\mu\varepsilon}\left({k_y}^2+{k_z}^2\right)} - i\eta - \Omega} e^{ik_y y}$$

$$G_3 = \int_{-\infty}^{\infty} dk_y \frac{\mu\varepsilon {k_y}^2}{{k_y}^2+{k_z}^2} \times \frac{\exp\left[-i\Omega t\right]}{\sqrt{\frac{1}{\mu\varepsilon}\left({k_y}^2+{k_z}^2\right)} + i\eta + \Omega} e^{-ik_y y}$$

$$G_4 = \int_{-\infty}^{\infty} dk_y \frac{\mu\varepsilon {k_y}^2}{{k_y}^2+{k_z}^2} \times \frac{\exp\left[i\Omega t\right]}{\sqrt{\frac{1}{\mu\varepsilon}\left({k_y}^2+{k_z}^2\right)} + i\eta - \Omega} e^{-ik_y y}$$

We find that F_1 , F_2 , G_1 , G_2 is the complex conjugate of F_3 , F_4 , G_3 , G_4. When we deal with vector potential induced by charge oscillation or ac line current problem in Chapter 3, we ever both experience this condition. The integrals in Eq. (4.16) seem not easy. We have to consider about the situation for $y > 0$ and $y < 0$. Complex integral methods can simplify this problem. Using Complex integral method, we must choose different contours for the corresponded integral. The detailed derivation is saved for Appendix F. We instead $\lambda\frac{\hbar k_s}{m^*}$ to I_{sc}. I_{sc} is the magnitude of spin current in unit of Ampere.

After the complex contour integration, the vector potential can be divided by two part.

$$A_{TM}(\mathbf{r},t) = \mathbf{A}_{TM}^{>}(\mathbf{r},t) + \mathbf{A}_{TM}^{<}(\mathbf{r},t) \tag{4.17}$$

$\mathbf{A}_{TM}^{>}(\mathbf{r},t)$ is the vector potential in the situation $\mu\varepsilon\Omega^2 > {k_z}^2$. For $\mu\varepsilon\Omega^2 < {k_z}^2$, the vector potential is $\mathbf{A}_{TM}^{<}(\mathbf{r},t)$. $\mathbf{A}_{TM}^{>}(\mathbf{r},t)$ and $\mathbf{A}_{TM}^{<}(\mathbf{r},t)$ is given by:

$$\begin{aligned}\mathbf{A}_{TM}^{>}(\mathbf{r},t) = \frac{\Lambda}{\varepsilon d} e \frac{m^*}{\hbar} I_{sc} \frac{1}{\Omega} \sum_n \cos\left(\frac{n\pi}{2}\right) \Bigg\{ \left(\frac{n\pi}{d}\right) \sin\left(\frac{n\pi}{d} z\right) \Bigg[-e^{-\frac{n\pi}{d}|y|} \sin(\Omega t) \\ - \sin\left(\sqrt{\mu\varepsilon\Omega^2 - \left(\tfrac{n\pi}{d}\right)^2}\,|y| - \Omega t\right)\Bigg] \hat{k} + \cos\left(\frac{n\pi}{d} z\right) \Bigg[\left(\frac{n\pi}{d}\right) e^{-\frac{n\pi}{d}|y|} \\ \times \sin(\Omega t) - \sqrt{\mu\varepsilon\Omega^2 - \left(\tfrac{n\pi}{d}\right)^2} \cos\left(\sqrt{\mu\varepsilon\Omega^2 - \left(\tfrac{n\pi}{d}\right)^2}\,|y| - \Omega t\right)\Bigg] \hat{z} \Bigg\}\end{aligned} \tag{4.18}$$

and

$$\begin{aligned}\mathbf{A}_{TM}^{<}(\mathbf{r},t) = \frac{\Lambda}{\varepsilon d} e \frac{m^*}{\hbar} I_{sc} \frac{1}{\Omega} \sum_n \cos\left(\frac{n\pi}{2}\right) \Bigg\{ \left(\frac{n\pi}{d}\right) \sin\left(\frac{n\pi}{d} z\right) \Bigg[-e^{-\frac{n\pi}{d}|y|} \sin(\Omega t) \\ + \exp\left(-\sqrt{\left(\tfrac{n\pi}{d}\right)^2 - \mu\varepsilon\Omega^2}\,|y|\right) \sin(\Omega t)\Bigg] \hat{k} + \cos\left(\frac{n\pi}{d} z\right) \Bigg[\left(\frac{n\pi}{d}\right) e^{-\frac{n\pi}{d}|y|} \\ \times \sin(\Omega t) - \sqrt{\left(\tfrac{n\pi}{d}\right)^2 - \mu\varepsilon\Omega^2} \exp\left(-\sqrt{\left(\tfrac{n\pi}{d}\right)^2 - \mu\varepsilon\Omega^2}\,|y|\right) \sin(\Omega t)\Bigg] \hat{z} \Bigg\}\end{aligned} \tag{4.19}$$

For $y > 0$, $\hat{y} = \hat{k}$; for $y > 0$, $-\hat{y} = \hat{k}$. Remember that k_z is equal to $\frac{n\pi}{d}$. We choose the transverse gauge in which the scalar potential vanishes. The electric field is given by

$\mathbf{E} = -\frac{\partial A(\mathbf{r},t)}{\partial t}$. Therefore, the electric field for TM modes can be shown as:

$$\mathbf{E}_{TM}(\mathbf{r},t) = \mathbf{E}_{TM}^{>}(\mathbf{r},t) + \mathbf{E}_{TM}^{<}(\mathbf{r},t) \tag{4.20}$$

where $\mathbf{E}_{TM}^{>}(\mathbf{r},t)$ is the electric field in the situation $\mu\varepsilon\Omega^2 > \left(\frac{n\pi}{d}\right)^2$ and $\mathbf{E}_{TM}^{<}(\mathbf{r},t)$ is the electric field in the situation $\mu\varepsilon\Omega^2 < \left(\frac{n\pi}{d}\right)^2$. They are given by:

$$\begin{aligned}\mathbf{E}_{TM}^{>}(\mathbf{r},t) = {} & \frac{\Lambda}{\varepsilon d} e \frac{m^*}{\hbar} I_{sc} \sum_n \cos\left(\frac{n\pi}{2}\right) \left\{ \left(\frac{n\pi}{d}\right) \sin\left(\frac{n\pi}{d} z\right) \left[e^{-\frac{n\pi}{d}|y|} \cos(\Omega t) \right.\right. \\ & \left. - \cos\left(\sqrt{\mu\varepsilon\Omega^2 - \left(\tfrac{n\pi}{d}\right)^2} |y| - \Omega t \right) \right] \hat{k} - \cos\left(\frac{n\pi}{d} z\right) \left[\left(\frac{n\pi}{d}\right) e^{-\frac{n\pi}{d}|y|} \right. \\ & \left.\left. \times \cos(\Omega t) - \sqrt{\mu\varepsilon\Omega^2 - \left(\tfrac{n\pi}{d}\right)^2} \sin\left(\sqrt{\mu\varepsilon\Omega^2 - \left(\tfrac{n\pi}{d}\right)^2} |y| - \Omega t \right) \hat{z} \right\}\end{aligned} \tag{4.21}$$

and

$$\begin{aligned}\mathbf{E}_{TM}^{<}(\mathbf{r},t) = {} & \frac{\Lambda}{\varepsilon d} e \frac{m^*}{\hbar} I_{sc} \sum_n \cos\left(\frac{n\pi}{2}\right) \left\{ \left(\frac{n\pi}{d}\right) \sin\left(\frac{n\pi}{d} z\right) \left[e^{-\frac{n\pi}{d}|y|} \cos(\Omega t) \right.\right. \\ & \left. - \exp\left(-\sqrt{\left(\tfrac{n\pi}{d}\right)^2 - \mu\varepsilon\Omega^2} |y| \right) \cos(\Omega t) \right] \hat{k} - \cos\left(\frac{n\pi}{d} z\right) \left[\left(\frac{n\pi}{d}\right) e^{-\frac{n\pi}{d}|y|} \right. \\ & \left.\left. \times \cos(\Omega t) - \sqrt{\left(\tfrac{n\pi}{d}\right)^2 - \mu\varepsilon\Omega^2} \exp\left(-\sqrt{\left(\tfrac{n\pi}{d}\right)^2 - \mu\varepsilon\Omega^2} |y| \right) \cos(\Omega t) \right] \hat{z} \right\}\end{aligned} \tag{4.22}$$

After complicated calculations we finally get the electric field induced by ac spin-polarized current in the waveguide. "$\sum\limits_{n=0} \cos\left(\frac{n\pi}{2}\right)$" in Eq. (4.21) and Eq. (4.22) ask that only the even modes of electric field exist. It is different from the electric field that is induced by charge current in the waveguide we discussed in Chapter 3 only and couples to odd modes.

The electric field has the term $\exp\left(-\frac{n\pi}{d}|y|\right)$ which decays in the positive y-axis and negative y-axis from the $y = 0$, even though we do not understand that it's physical meaning, we find that the result is extremely different with the ac charge current. From mathematics view point, the ac in-plane polarized spin current couples to TM wave which the electric field is proportional to $\frac{1}{\omega_{n\mathbf{k}1}}$. But charge current oscillation which couples to the TE wave is not. This difference results that the final residue integral methods generate difference number of poles, so that the electric field induced by the ac in-plane polarized spin current exists the decay terms. From Eq. (4.22), we notice that the electric field vanishes if the oscillation frequency is equal to zero. This checks with the ac nature of our results in this work. We will explain in next chapter that only the n=0 waveguide mode will contribute to the potential difference between the two metal gates of the waveguide.

4.4 Brief summary

We drove electric field induced by ac spin current in waveguide and coupling to TM modes. The electric field only couple to even mode and has exponential decaying terms. With the electric field, we can calculate the ac electrical potential difference induced by ac spin current.

Chapter 5

Result and discussion

In the last chapter, we will discuss the final result of the ac electrical potential difference induced by as in-plane polarized spin current and explain the signal is measurable if we add a film bulk acoustic-wave resonator in the measuring circuit.

5.1 Discussion

In this section, we deduce the magnitude of the electrical potential difference induced by ac in-plane polarized spin current and discuss the result. The potential difference induced by the ac spin current can be deduced from equation by integrating the z-component of the electric field over the thickness of the waveguide. Then the ac electrical potential difference is given by

$$V_z = \int_0^d E_z dz = \frac{\Lambda}{\varepsilon} e \frac{m^*}{\hbar} I_{sc} \left\{ \sqrt{\mu\varepsilon\Omega^2} \sin\left(\sqrt{\mu\varepsilon\Omega^2} y - \Omega t \right) \right\} \tag{5.1}$$

Only the mode $n = 0$ wave distributes the potential difference, because the electric field of every mode of the wave oscillates in the z direction and is canceled by integrating over the thickness of the waveguide except the ground mode. We notice that the electrical potential difference is independent from the thickness of the waveguide d. It is good news for us, because we neglect the skin effect in our calculation.

Skin depth

Skin depth, also known as classical skin depth, is the depth to which electromagnetic radiation can penetrate the surface of a conductor. It will cause energy loss or change of the field. Under the condition that the electronic mean free path becomes comparable with or greater than the classically calculated skin depth, we should consider about anomalous skin depth instead of classical skin depth [15]. The anomalous skin depth is given by:

$$\delta = \left(\frac{l}{2\pi f' a\mu\sigma}\right)^{1/3} \frac{2}{\sqrt{3}}$$

where "a" is a real coefficient of the order of unity, l is the mean free path in material, μ is permeability in material, f' is the frequency of incident electromagnetic wave, σ is the conductivity of material. The higher frequency gives the less anomalous skin depth.

If the thickness of slabs is longer than the skin depth, we do not worry about this problem. Essentially, for any material the ratio of electronic mean free path l to absolute conductivity σ is a constant independent of temperature. For aluminum and gigahertz of incident electromagnetic wave, the skin depth is about $0.5\mu m$. If the thickness of slabs is more than $0.5\mu m$, we do not worry about the impact of skin effect.

Surface spin current

The electric field in Eq. (4.20) is induced by the ac line spin current in the waveguide. Actually spin current should flow though the 2DEG. We can calculate the total distribution of surface spin current on the 2DEG by integration over the y-direction. That is

$$E_z(r,t) = \frac{\Lambda}{\varepsilon d} e \frac{m^*}{\hbar} I_{sc} \cos\left(\frac{n\pi}{d} z\right) \times \sqrt{\mu\varepsilon\Omega^2} \int dy' \sin\left(\sqrt{\mu\varepsilon\Omega^2}\,(y-y') - \Omega t\right) \quad (5.2)$$

where we only consider about the ground mode. If the oscillation frequency is about gigahertz, when we integrate the electric field with respect to y', the wave length $2\pi/\sqrt{\mu\varepsilon\Omega^2}$ for mode $n = 0$ is long enough not to cancel total electric field induced by surface ac spin current in the z direction. And the electrical potential difference is almost the same when we think that the line spin current or surface spin current carries the same magnitude of in-plane polarized spin current with the same oscillation frequency.

The potential difference

For we must be sure whether the electrical signal generated by ac in-plane polarized spin current is measurable, we estimate the electrical potential difference between two slabs of the waveguide from Eq. (5.1). The effective electron mass in GaAs $m^* = 0.068m_0 \sim 6.1 \times 10^{-32}$kg [16] where m_0 is the electron mass in free space; the spin orbit coupling constant $\Lambda \sim 8.25 \times 10^{-19} m^2$; the relative permittivity in GaAs is about 12.95. The estimated value of the electrical potential difference $V_z \sim 2.9 \times 10^{-13} \times I_{spin\ \mathrm{current}} \times f$ in the unit of Volt, $I_{spin\ \mathrm{current}}$ is the magnitude of spin current in the unit of Ampere, f is the oscillation frequency of spin current in the unit of Hertz.

Electronic filter

If we can generate 50 nA of ac in-plane polarized spin current with oscillating frequency 10^9 Hertz, the induced electrical potential difference is not high enough to detect. Some microstructure or electronic filters which can reach high quality factor Q and high operation frequency could enhance the signal by four order in magnitude.[17]. By apply these kinds of microstructure, we can set our device as Fig. 5.1. If we generate 50 nA of ac spin current with oscillating frequency 500 MHz , the maximum potential difference between the resonant induced by ac spin current in system is about 725×10^{-10} volt which is measurable.

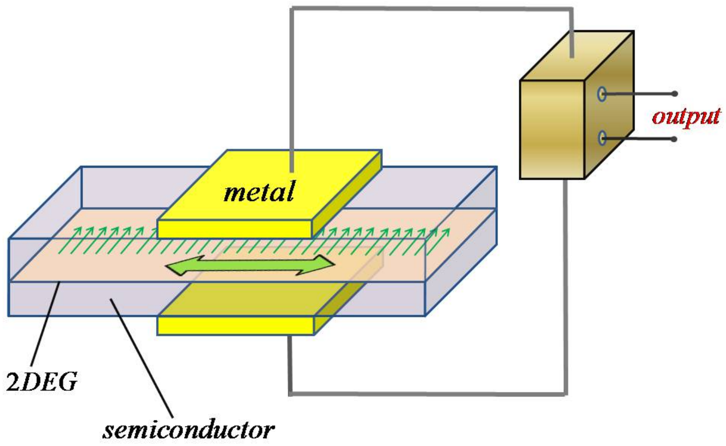

Figure 5.1: The spin current is injected from the both sides of the waveguide. We apply an external electronic filter with high quality vector Q to increase the output signal by several order.

5.2 Injection of in-plane AC spin current

Even thought we already know the electrical potential difference between the two metal gates induced by ac in-plane polarized spin current, the generation of ac in-plane spin current is still a challenge now. Here we propose a few means to generating in-plane ac spin current.

Optical spin injection

A photon is a boson and its helicity is $\pm\hbar$. These two spin components correspond to the classical concepts of right-handed and left-handed circularly polarized light. If we drive the circular polarization electromagnetic wave to illuminate the 2DEG normally on a spot, it will generate spin accumulation on this spot. These spins will diffuse away due to concentration imbalance and cause spin current. When we drive right- and left-hand alternating circular polarized electromagnetic wave to illuminate the 2DEG normally on a spot, it will generate ac spin current. But the spin polarization direction of the spin current is out of plane of 2DEG. we can redesign the waveguide as shown as Fig. 5.2.

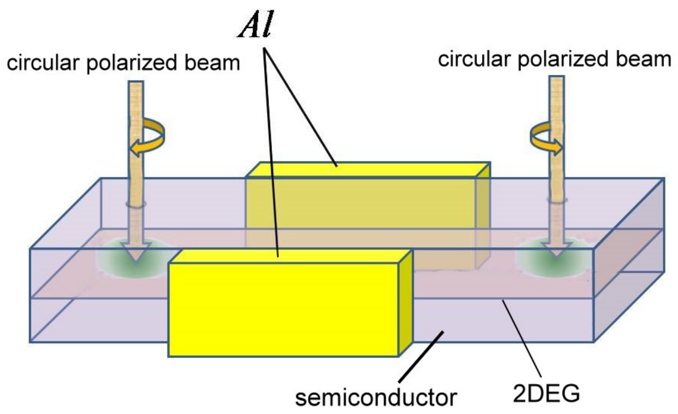

Figure 5.2: The illustration of the optical spin injection for our system. Right- or left-hand circular polarized electromagnetic wave to illuminate the 2DEG normally and then generate spin accumulation.Spins will diffuse away due to concentration imbalance and cause spin current. Right- and left-hand alternating circular can drive ac spin current diffusing away. The metal gates of waveguide are deposited at both side of the device and detect the electrical potential difference. The two beams with opponent right- and left-hand alternating circular polarization on the left and right side of the system can enhance the spin current.

There two beams with opponent right- and left-hand alternating circular polarization on the left and right side of the system in order to enhance the spin current. The metal gates of waveguide are deposited at both side of the device. The spin current flows on the 2DEG. Thought the spin current flows not only through the middle of the two slabs but also the neighborhood of it, the ac electrical potential difference induced by ac spin current flowing through the neighborhood of the middle of the waveguide is the same as the potential difference induced by spin current flowing in the middle of the waveguide. It is because of this that only ground mode of electromagnetic wave will distribute the potential difference. surface spin current can be decomposed into numerous "line spin current" the and the electric field of the ground mode of wave is independent of relative distance form the "line" spin current to two metal gates.

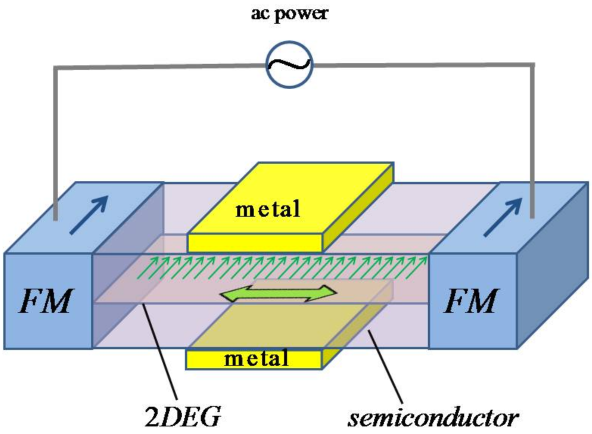

Figure 5.3: The ac charge current is injected from the both terminals, and the charge current with spin-polarization flows through the waveguide. These spin-polarized electrons originate from the ferromagnetic probes.

Ferromagnetic spin injection

The second method is ferromagnetic spin injection [18]. We can construct a ferromagnet/semiconductor/ferromagnet device which is shown in Fig. 5.3. we inject ac charge current through ferromagnetic probe to polarize the spins of the electrons. It can generate in-plane polarized spin current by apply external magnetic field to the ferromagnetic probe. The external magnetic field applied on the ferromagnetic probe is used to tile the magnetization in ferromagnetic probe and the spin polarized direction of the current will be aligned. But the injected current not only include the spin current but also charge current. Ac charge current can also generate electric field in a waveguide. Even though the ferromagnetic spin injection could inject more spin current, the signal induced by charge current may interfere the measurement.

Non-local spin injection

The third one is non-local spin injection. For non-local spin injection, our system could be set up as Fig. 5.4. The FM1 and FM2 are ferromagnets which are use to align the

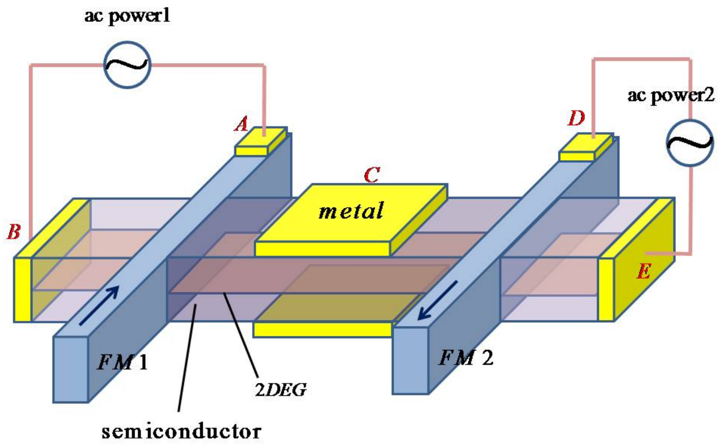

Figure 5.4: When we drive charge current between A,B and D,E, it will resulting in nonequilibrium spin accumulation in the ferromagnets that diffused away from the injection point. If we drive ac charge current, it will drive ac spin current into the waveguide structure.

electron spin and their magnetization directions ate out of the 2DEG plane with opposite directions. There is a waveguide at the middle of the system used to detect the potential difference induced by spin current. If we drive the charge current flowing between the electrode A and B, it will generate spin-polarized current diffusing away from FM1 into the 2DEG. And spin-polarized current will flow into the waveguide structure and no net charge current flows into the waveguide. When an ac power drives the charge current, the ac spin current will flow though the waveguide structure. The another set of ferromagnet FM2 with anti-direction of magnetization and ac power can increase the spin current. The non-local detection can avoid interfering signal. We can detect the electrical potential difference at the waveguide.

5.3 Conclusion

This work demonstrates a new method to calculate spin-current induced field. The induced ac electrical potential difference and ac spin current have the relation:

$$\boxed{V_z \sim 2.9 \times 10^{-13} \times I_{spin\,\mathrm{current}} \times f \quad \text{in Volt}}$$

, where $I_{spin\,\mathrm{current}}$ is the magnitude of spin current in Ampere, f is the oscillation frequency of spin current in Hertz. Even the strength of the induced electrical potential difference is not enough to be detected. It shows that electrical signal generated by ac spin current is measurable, if we set up appropriate external electronic filter. Comparing with Sun et al. [12], we have reasonable magnitude of spin current, and the electric field is not screened by the charge of the conduction electrons [19].

Appendix A

Average over direction

In this appendix, we will show the derivation from Eq. (3.9) to Eq. (3.11). By taking linear polarization, we have $\boldsymbol{\lambda}^* = \boldsymbol{\lambda}$. For $\boldsymbol{\lambda}^* = \boldsymbol{\lambda}$, we can assume $\mathbf{k}$ to be along $\hat{z}''$, the $\boldsymbol{\lambda}$ is in the $\hat{x}''$-$\hat{y}''$plane. The Fig. A.1 show the relationship of $\mathbf{k}$, $\hat{x}''$, $\hat{y}''$, and $\hat{z}''$.

We focus on the term $\sum_{\lambda} \exp\left[i\mathbf{k}\cdot\mathbf{r}\right]\boldsymbol{\lambda}\lambda_z{}^*$ in Eq. (3.9) which is related to polarization direction. λ_z is the z-component polarization direction and $\sum_{\lambda} \boldsymbol{\lambda}\lambda_z$ can rewrite as $\boldsymbol{\lambda}\lambda_z = \hat{x}''\sin\left(\theta_1\right) = \left(\hat{k}\times\hat{z}\right)\times\hat{k}$. Therefore,

$$\begin{aligned}&\sum_{\lambda} \exp\left[i\mathbf{k}\cdot\mathbf{r}\right]\boldsymbol{\lambda}\lambda_z{}^* \\ =&\sum_{\lambda} \exp\left[i\mathbf{k}\cdot\mathbf{r}\right]\boldsymbol{\lambda}\lambda_z = \exp\left[i\mathbf{k}\cdot\mathbf{r}\right]\left(\hat{k}\times\hat{z}\right)\times\hat{k}\end{aligned}$$

Using the vector relation $\left(\hat{k}\times\hat{z}\right)\times\hat{k} = \hat{z} - \left(\hat{k}\cdot\hat{z}\right)\hat{k}$, we get:

$$\sum_{\lambda} \exp\left[i\mathbf{k}\cdot\mathbf{r}\right]\boldsymbol{\lambda}\lambda_z{}^* = \exp\left[i\mathbf{k}\cdot\mathbf{r}\right]\left\{\hat{z} - \left(\hat{k}\cdot\hat{z}\right)\hat{k}\right\} \tag{A.1}$$

From Eq. (A.1), we can derive Eq. (3.10) from Eq. (3.9). Then we will derive Eq. (3.11). Assume that the angle between $\mathbf{k}$ and $\mathbf{r}$ is θ_2. And the average over direction

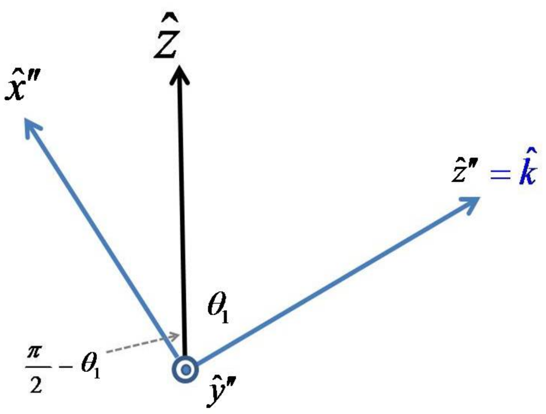

Figure A.1: The figure shows the relationship of $\hat{k}$, $\hat{z}''$, $\hat{x}''$, $\hat{y}''$, $\hat{z}$. $\hat{k} = \hat{z}''$, and the $\boldsymbol{\lambda}$ is in the $\hat{x}''$-$\hat{y}''$ plane. $\hat{y}''$ is normal to the $\hat{x}''$-$\hat{z}''$ plane.

of "$\exp\left[i\mathbf{k}\cdot\mathbf{r}\right]\hat{z}$ " is given by:

$$\begin{aligned}
&\frac{1}{4\pi}\int \exp\left[i\mathbf{k}\cdot\mathbf{r}\right]\hat{z}d\Omega_{\hat{k}} \\
&= \frac{1}{4\pi}\hat{z}\int_{\phi=0}^{2\pi}\int_{\theta_2=0}^{\pi}\exp\left[i\mathbf{k}\cdot\mathbf{r}\right]\sin\theta_2 d\theta_2 d\phi \\
&= \frac{1}{kr}\sin\left[kr\right]\hat{z}
\end{aligned}$$

It is more convenient to us to construct a coordinate to illustrate the relationship between $\hat{k}$, $\hat{z}$, and $\hat{r}$ as Fig. A.2. From Fig. A.2, we know that $\hat{k} = \sin\theta'\cos\phi'\hat{x}' + \sin\theta'\sin\phi'\hat{y}' + \cos\theta'\hat{z}'$. The average over direction of "$-\exp\left[i\mathbf{k}\cdot\mathbf{r}\right]\left(\hat{k}\cdot\hat{z}\right)\hat{k}$" is given by:

$$\begin{aligned}
&-\frac{1}{4\pi}\int \exp\left[i\mathbf{k}\cdot\mathbf{r}\right]\left(\hat{k}\cdot\hat{z}\right)\hat{k}d\Omega_{\hat{k}} \\
&= -\frac{1}{4\pi}\int_{\theta'=0}^{\theta'=\pi}\int_{\phi'=0}^{\phi'=2\pi}\exp\left[ikr\cos\theta'\right]\left\{\left(\sin^2\theta'\cos\phi'\sin\phi'\sin\theta + \cos\theta'\cos\theta\sin\theta'\cos\phi'\right)\hat{x}'\right. \\
&+ \left(\sin^2\theta'\sin^2\phi'\sin\theta + \cos\theta'\sin\theta'\cos\theta\sin\phi'\right)\hat{y}' \\
&+ \left.\left(\sin\theta'\sin\phi'\sin\theta\cos\theta' + \cos^2\theta'\cos\theta\right)\hat{z}'\right\}d\phi'\sin\theta' d\theta'
\end{aligned}$$

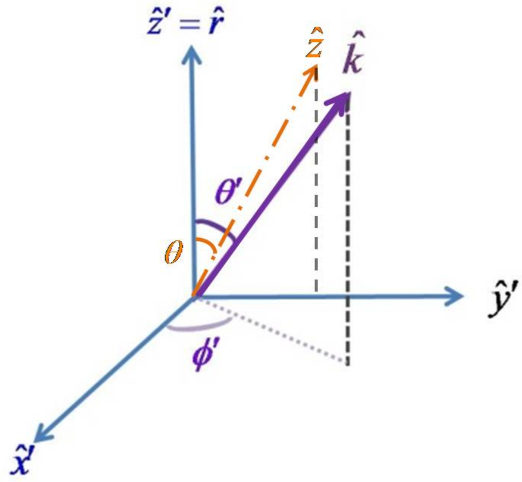

Figure A.2: The figure shown the relation of $\hat{y}'$, $\hat{x}'$, $\hat{z}'$, and $\hat{r}$. The $\hat{z}$ direction is in the $\hat{y}'$-$\hat{z}'$ plane and θ is the angle between $\hat{r}$ and $\hat{z}$.

Because $\int_{\phi'=0}^{\phi'=2\pi} \cos\phi' d\phi' = 0$ and $\int_{\phi'=0}^{\phi'=2\pi} \sin\phi' d\phi' = 0$, we obtain:

$$\begin{aligned}
&-\frac{1}{4\pi}\int \exp\left[i\mathbf{k}\cdot\mathbf{r}\right]\left(\hat{k}\cdot\hat{z}\right)\hat{k}d\Omega_{\hat{k}} \\
&=\frac{1}{4}\hat{y}'\sin\theta\int_{\cos\theta'=1}^{\cos\theta'=-1}\exp\left[ikr\left(\cos\theta'\right)\right]\left[1-\left(\cos\theta'\right)^2\right]d\left(\cos\theta'\right) \\
&+\frac{1}{2}\hat{z}'\cos\theta\int_{\cos\theta'=1}^{\cos\theta'=-1}\exp\left[ikr\left(\cos\theta'\right)\right]\left(\cos\theta'\right)^2 d\left(\cos\theta'\right)
\end{aligned} \tag{A.2}$$

where the first term in Eq. (A.2) can be solved as:

$$\begin{aligned}
&\frac{1}{4}\hat{y}'\sin\theta\int_{\cos\theta'=1}^{\cos\theta'=-1}\exp\left[ikr\left(\cos\theta'\right)\right]\left[1-\left(\cos\theta'\right)^2\right]d\left(\cos\theta'\right) \\
&=-\frac{1}{2kr}\hat{y}'\sin\theta\sin(kr)+\frac{1}{4}\hat{y}'\sin\theta\left\{-\frac{\partial^2}{\partial(kr)^2}\left(\frac{2\sin\left(kr\right)}{kr}\right)\right\}
\end{aligned} \tag{A.3}$$

The second term in Eq. (A.2) can be written as:

$$
\begin{aligned}
&\frac{1}{2}\hat{z}'\cos\theta\int_{\cos\theta'=1}^{\cos\theta'=-1}\exp\left[ikr\left(\cos\theta'\right)\right]\left(\cos\theta'\right)^2 d\left(\cos\theta'\right)\\
&=-\frac{1}{2}\hat{z}'\cos\theta\left\{\frac{2}{kr}\sin\left(kr\right)+\frac{4}{\left(kr\right)^2}\cos\left(kr\right)-\frac{4}{\left(kr\right)^3}\sin(kr)\right\}\\
&=-\frac{1}{2}\hat{z}'\cos\theta\left\{-\frac{\partial^2}{\partial(kr)^2}\left(\frac{2\sin\left(kr\right)}{kr}\right)\right\},
\end{aligned}
\tag{A.4}
$$

We combine Eq. (A.2), Eq. (A.3), and Eq. (A.4), $\frac{1}{4\pi}\int\exp\left[i\mathbf{k}\cdot\mathbf{r}\right]\left\{\hat{z}-\left(\hat{k}\cdot\hat{z}\right)\hat{k}\right\}d\Omega_{\hat{k}}$ can be write as:

$$
\begin{aligned}
&\frac{1}{4\pi}\int\exp\left[i\mathbf{k}\cdot\mathbf{r}\right]\left\{\hat{z}-\left(\hat{k}\cdot\hat{z}\right)\hat{k}\right\}d\Omega_{\hat{k}}\\
&=\frac{1}{kr}\sin\left[kr\right]\hat{z}-\frac{1}{2}\hat{y}'\sin\theta\left\{\frac{\sin(kr)}{kr}\right\}+\frac{1}{4}\hat{y}'\sin\theta\left\{-\frac{\partial^2}{\partial(kr)^2}\left(\frac{2\sin\left(kr\right)}{kr}\right)\right\}\\
&\quad-\frac{1}{2}\hat{z}'\cos\theta\left\{-\frac{\partial^2}{\partial(kr)^2}\left(\frac{2\sin\left(kr\right)}{kr}\right)\right\}\\
&=\frac{1}{2}\hat{z}\left\{\frac{\sin\left[kr\right]}{kr}-\frac{\partial^2}{\partial(kr)^2}\left(\frac{\sin\left(kr\right)}{kr}\right)\right\}+\frac{1}{2}\hat{r}\cos\theta\left\{\frac{\sin(kr)}{kr}+3\frac{\partial^2}{\partial(kr)^2}\left(\frac{\sin\left(kr\right)}{kr}\right)\right\}
\end{aligned}
\tag{A.5}
$$

Dropping terms smaller than $\left(\frac{1}{kr}\right)$, we have:

$$
\begin{aligned}
&\frac{1}{4\pi}\int\exp\left[i\mathbf{k}\cdot\mathbf{r}\right]\left\{\hat{z}-\left(\hat{k}\cdot\hat{z}\right)\hat{k}\right\}d\Omega_{\hat{k}}\\
&\approx\frac{1}{2}\hat{z}\left\{\frac{\sin\left[kr\right]}{kr}+\left(\frac{\sin\left(kr\right)}{kr}\right)\right\}+\frac{1}{2}\hat{r}\cos\theta\left\{\frac{\sin(kr)}{kr}-3\left(\frac{\sin\left(kr\right)}{kr}\right)\right\}\\
&=\left(\frac{\sin\left[kr\right]}{kr}\right)\left(\hat{z}-\hat{r}\cos\theta\right).
\end{aligned}
\tag{A.6}
$$

Utilizing above equation, we can get Eq. (3.11).

Appendix B

The complex integral I

Eq. (3.13) in Chapter 3 will be derived in this Appendix.

Using residue integral method, the first term of the integral in the bracket can be derived as:

$$\int_{u'=-\infty}^{\infty} u'^2 du' \left[\frac{-\exp\left[iu'\frac{r}{c}\right]}{u'\frac{r}{c}} \frac{\exp(i\Omega t)}{u' + (\Omega - i\eta)} \right].$$

Let $u' = u'_R + iu'_I$, where u'_R is the real part of u' and u'_I is the imaginary part of u'. The pole of

$$u' \frac{-\exp\left(iu'\frac{r}{c}\right)}{\frac{r}{c}} \times \frac{\exp(i\Omega t)}{u' + (\Omega - i\eta)}$$

is located at $u' = -\Omega + i\eta$ on the complex plane. Because

$$\exp\left[iu'\frac{r}{c}\right] = \exp\left[i\left(u'_R + iu'_I\right)\frac{r}{c}\right] = \exp\left[iu'_R\frac{r}{c}\right]\exp\left[-u'_I\frac{r}{c}\right],$$

we may take a contour which closes the upper half-plane as Fig. B.1. There is a pole inside the contour. We use the Jordan's lemma theorem [20] , we obtain:

$$\begin{aligned}
&\int_{u'=-\infty}^{\infty} u'^2 du' \left[\frac{-\exp\left[iu'\frac{r}{c}\right]}{u'\frac{r}{c}} \frac{\exp(i\Omega t)}{u' + (\Omega - i\eta)} \right] \\
&= -\lim_{R\to\infty} \frac{c}{r} \oint_{contour} u' \exp\left[iu'\frac{r}{c}\right] \frac{\exp(i\Omega t)}{u' + (\Omega - i\eta)} du' \\
&= -2\pi i \frac{c}{r} \left[\underset{u'\to-\Omega+i\eta}{\operatorname{Re} s} \left(u' \exp\left[iu'\frac{r}{c}\right] \frac{\exp(i\Omega t)}{u' + (\Omega - i\eta)} \right) \right] \\
&\approx 2\pi i \frac{c}{r} \Omega \exp\left[-i\Omega\frac{r}{c}\right] \exp(i\Omega t) .
\end{aligned}$$

We neglect η since it is very small. For the same reason we may solve the other three integrations.

$$\int_{u'=-\infty}^{\infty} u'^2 du' \left[\frac{-\exp\left[iu'\frac{r}{c}\right]}{u'\frac{r}{c}} \frac{\exp(-i\Omega t)}{u' - (\Omega + i\eta)} \right] \approx -2\pi i \frac{c}{r} \left[\Omega \exp\left[i\Omega\frac{r}{c}\right] \exp(-i\Omega t) \right],$$

$$\int_{u'=-\infty}^{\infty} u'^2 du' \left[\frac{\exp\left[-iu'\frac{r}{c}\right]}{u'\frac{r}{c}} \frac{\exp(i\Omega t)}{u' + (\Omega - i\eta)} \right] = 0,$$

$$\int_{u'=-\infty}^{\infty} u'^2 du' \left[\frac{\exp\left[-iu'\frac{r}{c}\right]}{u'\frac{r}{c}} \frac{\exp(-i\Omega t)}{u' - (\Omega + i\eta)} \right] = 0.$$

For the last two integrals, we may take contours which close the lower half-plane, because $\exp\left[-iu'r/c\right]$ is convergent at u' approaching negative infinite. The contours do not close any pole, so the integrals are equal to zero.

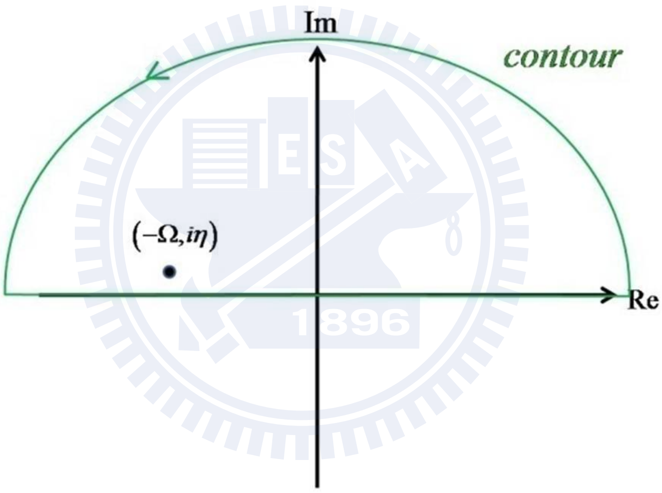

Figure B.1: The counter-clockwise contour we choose closes the upper half plane and has one pole at $(-\Omega, i\eta)$ in it.

Appendix C

Approximation between wave function of current and vector potential

Here we will derive the detailed calculation from Eq. (3.18) to Eq. (3.19).

The first term in Eq. (3.18), $k_e \hbar\lambda_e \frac{e}{m_e} \int dx \int dy \int dz \varphi(y,z) A_x \varphi(y,z)$, is equal to

$$\hbar\lambda_e \frac{e}{m_e} k_e \int dx A_x \left(x, 0, \tfrac{d}{2}\right) \int dy \int dz \varphi^2(y,z), \tag{C.1}$$

because the vector potential near the position$\left(x, y=0, z=\frac{d}{2}\right)$changes violently, but the wave function of the electron $\varphi(y,z)$ changes smoothly. And the integral $\int dy \int dz \varphi^2(y,z)$ is equal to 1 due to the normalization of wave function.

Then we solve the second and third integrals in Eq. (3.18).That is

$$\int dx \int dy \int dz \varphi(y,z) A_y \frac{\partial}{\partial y} \varphi(y,z) + \int dx \int dy \int dz \varphi(y,z) A_z \frac{\partial}{\partial z} \varphi(y,z).$$

Now if we apply the relationship for integration by parts, we have

$$\begin{aligned}
&\int dx \int dy \int dz \varphi\left(y,z\right) A_y \frac{\partial}{\partial y}\varphi\left(y,z\right) + \int dx \int dy \int dz \varphi\left(y,z\right) A_z \frac{\partial}{\partial z}\varphi\left(y,z\right) \\
&= \left[\int dx \int dz \varphi\left(y,z\right) A_y \varphi\left(y,z\right)\right]\Bigg|_{\substack{\textit{the } y-\textit{direction} \\ \textit{boudary value of} \\ \textit{the current density}}} - \int dx \int dy \int dz \varphi\left(y,z\right) \frac{\partial}{\partial y}\left[A_y \varphi\left(y,z\right)\right] \\
&+ \left[\int dx \int dz \varphi\left(y,z\right) A_z \varphi\left(y,z\right)\right]\Bigg|_{\substack{\textit{the } z-\textit{direction} \\ \textit{boudary value of} \\ \textit{the current density}}} - \int dx \int dy \int dz \varphi\left(y,z\right) \frac{\partial}{\partial z}\left[A_z \varphi\left(y,z\right)\right]
\end{aligned}$$

The boundary conditions ask that the wave function of the current is equal to zero at the edge of cross-section of the wire. We deal with the derivative first, and we get:

$$\begin{aligned}
&\int dx \int dy \int dz \varphi\left(y,z\right) A_y \frac{\partial}{\partial y}\varphi\left(y,z\right) + \int dx \int dy \int dz \varphi\left(y,z\right) A_z \frac{\partial}{\partial z}\varphi\left(y,z\right) \\
&= -\int dx \int dy \int dz \varphi\left(y,z\right) A_y \frac{\partial}{\partial y}\varphi\left(y,z\right) - \int dx \int dy \int dz \varphi^2\left(y,z\right) \frac{\partial}{\partial y} A_y \\
&\quad - \int dx \int dy \int dz \varphi\left(y,z\right) A_z \frac{\partial}{\partial z}\varphi\left(y,z\right) - \int dx \int dy \int dz \varphi^2\left(y,z\right) \frac{\partial}{\partial z} A_z
\end{aligned} \tag{C.2}$$

we rewrite Eq. (C.2):

$$\begin{aligned}
&\int dx \int dy \int dz \varphi\left(y,z\right) A_y \frac{\partial}{\partial y}\varphi\left(y,z\right) + \int dx \int dy \int dz \varphi\left(y,z\right) A_z \frac{\partial}{\partial z}\varphi\left(y,z\right) \\
&= -\frac{1}{2}\left\{\int dx \int dy \int dz \varphi^2\left(y,z\right) \frac{\partial}{\partial y} A_y + \int dx \int dy \int dz \varphi^2\left(y,z\right) \frac{\partial}{\partial z} A_z\right\} \\
&= -\frac{1}{2}\int dx \int dy \int dz \varphi^2\left(y,z\right) \nabla \cdot \mathbf{A} + \frac{1}{2}\int dx \int dy \int dz \varphi^2\left(y,z\right) \frac{\partial}{\partial x} A_x
\end{aligned} \tag{C.3}$$

For transverse gauge, in which the vector potential is divergence-free, we can write down: $\nabla \cdot \mathbf{A} = 0$. The Eq. (C.3) becomes:

$$\begin{aligned}
&\int dx \int dy \int dz \varphi\left(y,z\right) A_y \frac{\partial}{\partial y}\varphi\left(y,z\right) + \int dx \int dy \int dz \varphi\left(y,z\right) A_z \frac{\partial}{\partial z}\varphi\left(y,z\right) \\
&= \frac{1}{2}\int dx \int dy \int dz \varphi^2\left(y,z\right) \frac{\partial}{\partial x} A_x
\end{aligned}$$

A-vector near the position$\left(x, y=0, z=\frac{d}{2}\right)$changes violently, and the wave function of the electron $\varphi\left(y,z\right)$changes smoothly. Therefore, we have:

$$\begin{aligned}
&\int dx\int dy\int dz\varphi\left(y,z\right)A_y\frac{\partial}{\partial y}\varphi\left(y,z\right)+\int dx\int dy\int dz\varphi\left(y,z\right)A_z\frac{\partial}{\partial z}\varphi\left(y,z\right)\\
&=\frac{1}{2}\int dx\int dy\int dz\varphi^2\left(y,z\right)\frac{\partial}{\partial x}A_x\\
&\approx\frac{1}{2}\int dx\frac{\partial}{\partial x}A_x\left(x,0,\tfrac{d}{2}\right)
\end{aligned}\tag{C.4}$$

Combing Eq. (C.1), Eq. (C.4),and Eq. (3.18), we can obtain Eq. (3.19).

Appendix D

The complex integral II

Now , we derive the first integral in the curve bracket of Eq. (3.30)

$$\int_{-\infty}^{\infty} dk_y \frac{e^{i(k_y y)}}{\sqrt{\frac{1}{\mu\varepsilon}\left({k_z}^2 + {k_y}^2\right)}} \frac{1}{\sqrt{\frac{1}{\mu\varepsilon}\left({k_z}^2 + {k_y}^2\right)} - i\eta + \Omega}. \tag{D.1}$$

Let $k_y = z'$, Eq. (D.1) becomes:

$$\int_{-\infty}^{\infty} dz' \frac{e^{iz'y}}{\sqrt{\frac{1}{\mu\varepsilon}\left({k_z}^2 + z'^2\right)}} \frac{1}{\sqrt{\frac{1}{\mu\varepsilon}\left({k_z}^2 + z'^2\right)} - i\eta + \Omega}$$

$\frac{e^{iz'y}}{\sqrt{\frac{1}{\mu\varepsilon}\left({k_z}^2+z'^2\right)}} \frac{1}{\sqrt{\frac{1}{\mu\varepsilon}\left({k_z}^2+z'^2\right)}-i\eta+\Omega}$ has two branch point on the complex plane which are located at $z = ik_z$ and $z = -ik_z$. The branch point will complicate the integration. The contour does not close any branch point and branch cuts and we should define the branch cuts.

For $y > 0$, we take our contour and the cut line as Fig. D.1, and the two red arrows are the branch cuts that we choose. The section of contour , C_R, is a semicircle with infinite long radius and the integral along C_R approaches zero. The integral along C_r also approaches zero, because the point $z = ik_z$ on the complex plane is not a pole, but a branch point.

$\frac{e^{iz'y}}{\sqrt{\frac{1}{\mu\varepsilon}\left({k_z}^2+z'^2\right)}} \frac{1}{\sqrt{\frac{1}{\mu\varepsilon}\left({k_z}^2+z'^2\right)}-i\eta+\Omega}$ does not have any pole on the complex plane. So we

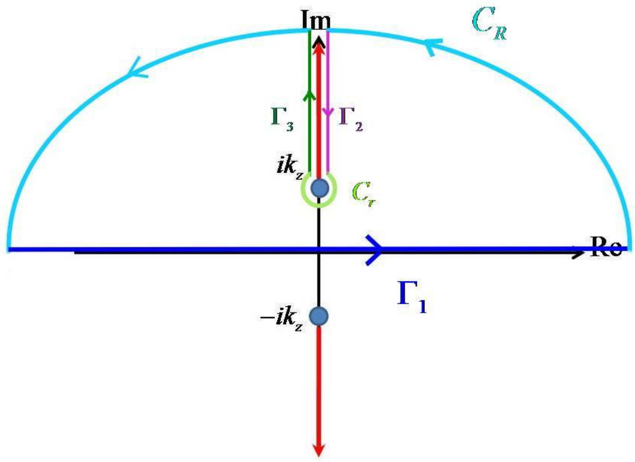

Figure D.1: The contour we separate into five section closes the upper-half plane except the branch point at $z' = ik_z$ and the branch cut (red arrow).

have:

$$\oint_{C_R+\Gamma_1+\Gamma_2+C_r+\Gamma_3} dz' \frac{e^{iz'y}}{\sqrt{\frac{1}{\mu\varepsilon}\left({k_z}^2 + z'^2\right)}} \frac{1}{\sqrt{\frac{1}{\mu\varepsilon}\left({k_z}^2 + z'^2\right)} - i\eta + \Omega} = 0 \tag{D.2}$$

We solve the integral first: $\int\limits_{\Gamma_2} dz' \frac{e^{iz'y}}{\sqrt{\frac{1}{\mu\varepsilon}\left({k_z}^2+z'^2\right)}} \frac{1}{\sqrt{\frac{1}{\mu\varepsilon}\left({k_z}^2+z'^2\right)}-i\eta+\Omega}$

Let $z' - ik_z = r_1 e^{i\theta_1}$, $z' + ik_z = r_2 e^{i\theta_2}$; $z = ip$ and then $dz' = idp$ $-\frac{3}{2}\pi \le \theta_1 < \frac{1}{2}\pi$; $-\frac{\pi}{2} \le \theta_2 < \frac{3}{2}\pi$.

For the integration path $\theta_1 = \frac{1}{2}\pi$,$\theta_2 = \frac{1}{2}\pi$, and $z' = ip$. Hence, $z' - ik_z = r_1 e^{i\theta_1} \Rightarrow$

$i\left(p-k_z\right)=r_1 e^{i\frac{1}{2}\pi} \Rightarrow r_1=p-k_z$. For the same reason, $r_2=p+k_z$. The integral becomes

$$\begin{aligned}
&\int\limits_{\Gamma_2} dz' \frac{e^{iz'y}}{\sqrt{\frac{1}{\mu\varepsilon}\left({k_z}^2+z'^2\right)}} \frac{1}{\sqrt{\frac{1}{\mu\varepsilon}\left({k_z}^2+z'^2\right)}-i\eta+\Omega} \\
&=\int\limits_{\Gamma_2} dz' \frac{e^{iz'y}}{\sqrt{\frac{1}{\mu\varepsilon}r_1 e^{i\theta_1} r_2 e^{i\theta_2}}} \frac{1}{\sqrt{\frac{1}{\mu\varepsilon}r_1 e^{i\theta_1} r_2 e^{i\theta_2}}-i\eta+\Omega} \\
&=\int\limits_{\Gamma_2} dz' \frac{e^{iz'y}}{\frac{1}{\mu\varepsilon}\left(p^2-{k_z}^2\right) e^{i\left(\frac{\pi}{2}+\frac{\pi}{2}\right)}+\Omega\sqrt{\frac{1}{\mu\varepsilon}}\sqrt{\left(p^2-{k_z}^2\right)} e^{i\left(\frac{\pi}{2}+\frac{\pi}{2}\right)/2}} \\
&=i\int_{\infty}^{k_z} dp \frac{e^{-py}}{-\frac{1}{\mu\varepsilon}\left(p^2-{k_z}^2\right)+i\Omega\sqrt{\frac{1}{\mu\varepsilon}}\sqrt{\left(p^2-{k_z}^2\right)}}
\end{aligned} \tag{D.3}$$

We neglect η in the denominator in Eq. (D.3).

Then we look at the integral:

$$\int\limits_{\Gamma_3} dz' \frac{e^{iz'y}}{\sqrt{\frac{1}{\mu\varepsilon}\left({k_z}^2+z'^2\right)}} \frac{1}{\sqrt{\frac{1}{\mu\varepsilon}\left({k_z}^2+z'^2\right)}-i\eta+\Omega}$$

Let $z'-ik_z=r_1 e^{i\theta_1}$, $z'+ik_z=r_2 e^{i\theta_2}$, $z'=ip$, $dz'=idp$, $-\frac{3}{2}\pi\leq\theta_1<\frac{1}{2}\pi$; $-\frac{\pi}{2}\leq\theta_2<\frac{3}{2}\pi$, and η is so small that we neglect it.

For the integration path Γ_3: $\theta_1=-\frac{3}{2}\pi$,$\theta_2=\frac{1}{2}\pi$, $z'-ik_z=r_1 e^{i\theta_1} \Rightarrow i\left(p-k_z\right)=r_1 e^{-i\frac{3}{2}\pi} \Rightarrow$ $r_1=p-k_z$, and $z'+ik_z=r_2 e^{i\theta_2} \Rightarrow i\left(p+k_z\right)=r_2 e^{i\frac{\pi}{2}} \Rightarrow r_2=p+k_z$

$$\begin{aligned}
&\int\limits_{\Gamma_3} dz' \frac{e^{iz'y}}{\sqrt{\frac{1}{\mu\varepsilon}\left({k_z}^2+z'^2\right)}} \frac{1}{\sqrt{\frac{1}{\mu\varepsilon}\left({k_z}^2+z'^2\right)}-i\eta+\Omega} \\
&=\int\limits_{\Gamma_3} dz' \frac{e^{iz'y}}{\sqrt{\frac{1}{\mu\varepsilon}r_1 e^{i\theta_1} r_2 e^{i\theta_2}}} \frac{1}{\sqrt{\frac{1}{\mu\varepsilon}r_1 e^{i\theta_1} r_2 e^{i\theta_2}}-i\eta+\Omega} \\
&=\int\limits_{\Gamma_3} dz' \frac{e^{iz'y}}{\frac{1}{\mu\varepsilon}r_1 e^{-i\frac{3\pi}{2}} r_2 e^{i\frac{\pi}{2}}+\Omega\sqrt{\frac{1}{\mu\varepsilon}}\left(r_1 r_2\right)^{1/2} e^{i\left(-\frac{3\pi}{2}+\frac{\pi}{2}\right)/2}} \\
&=-i\int_{k_z}^{\infty} dp \frac{e^{-py}}{\frac{1}{\mu\varepsilon}\left(p^2-{k_z}^2\right)+i\Omega\sqrt{\frac{1}{\mu\varepsilon}}\sqrt{p^2-{k_z}^2}}
\end{aligned} \tag{D.4}$$

Therefore, combining the Eq. (D.2), Eq. (D.3), and Eq. (D.4), we have

$$\int_{-\infty}^{\infty} dk_y \frac{e^{i(k_y y)}}{\sqrt{\frac{1}{\mu\varepsilon}\left({k_z}^2+{k_y}^2\right)}} \frac{1}{\sqrt{\frac{1}{\mu\varepsilon}\left({k_z}^2+{k_y}^2\right)}-i\eta+\Omega}\ (y>0)$$
$$=\int_{\Gamma_1} dk_y \frac{e^{i(k_y y)}}{\sqrt{\frac{1}{\mu\varepsilon}\left({k_z}^2+{k_y}^2\right)}} \frac{1}{\sqrt{\frac{1}{\mu\varepsilon}\left({k_z}^2+{k_y}^2\right)}-i\eta+\Omega}$$
$$=i\int_{\infty}^{k_z} dp \frac{e^{-py}}{+\frac{1}{\mu\varepsilon}\left(p^2-{k_z}^2\right)-i\Omega\sqrt{\frac{1}{\mu\varepsilon}}\sqrt{\left(p^2-{k_z}^2\right)}}+i\int_{k_z}^{\infty} dp \frac{e^{-py}}{\frac{1}{\mu\varepsilon}\left(p^2-{k_z}^2\right)+i\Omega\sqrt{\frac{1}{\mu\varepsilon}}\sqrt{p^2-{k_z}^2}} \tag{D.5}$$

Then we solve this integral $\int_{-\infty}^{\infty} dk_y \frac{e^{i(k_y y)}}{\sqrt{\frac{1}{\mu\varepsilon}\left({k_z}^2+{k_y}^2\right)}} \frac{1}{\sqrt{\frac{1}{\mu\varepsilon}\left({k_z}^2+{k_y}^2\right)}-i\eta-\Omega}$, for $y>0$. Let $f(z')=\frac{e^{iz'y}}{\sqrt{\frac{1}{\mu\varepsilon}\left({k_z}^2+z'^2\right)}} \frac{1}{\sqrt{\frac{1}{\mu\varepsilon}\left({k_z}^2+z'^2\right)}-i\eta-\Omega}$. $f(z')$ has two poles at $\pm\sqrt{\mu\varepsilon\left(\Omega^2+i2\eta\Omega\right)-{k_z}^2}$ and it also has two branch point at $\pm ik_z$.

We take our contour and the cut line the same as Fig. D.1, and the two red lines are the branch cuts that we choose. Using the Jordan's lemma theorem [20], we have:

$$\oint_{C_R+\Gamma_1+\Gamma_2+C_r+\Gamma_3} dz' \frac{e^{iz'y}}{\sqrt{\frac{1}{\mu\varepsilon}\left({k_z}^2+z'^2\right)}} \frac{1}{\sqrt{\frac{1}{\mu\varepsilon}\left({k_z}^2+z'^2\right)}-i\eta-\Omega}=2\pi i \underset{z'\to+\sqrt{\mu\varepsilon\Omega^2-{k_z}^2}}{\operatorname{Re}s}\left(f(z')\right) \tag{D.6}$$

Then

$$\int_{-\infty}^{\infty} dz' \frac{e^{iz'y}}{\sqrt{\frac{1}{\mu\varepsilon}\left({k_z}^2+z'^2\right)}} \frac{1}{\sqrt{\frac{1}{\mu\varepsilon}\left({k_z}^2+z'^2\right)}-i\eta-\Omega}$$
$$=-\int_{\Gamma_2+C_r+\Gamma_3} dz' \frac{e^{iz'y}}{\sqrt{\frac{1}{\mu\varepsilon}\left({k_z}^2+z'^2\right)}} \frac{1}{\sqrt{\frac{1}{\mu\varepsilon}\left({k_z}^2+z'^2\right)}-i\eta-\Omega}+2\pi i \underset{z'\to+\sqrt{\mu\varepsilon\Omega^2-{k_z}^2}}{\operatorname{Re}s}\left(f(z')\right) \tag{D.7}$$

The section of contour C_R is an infinite semicircle and the integral along C_R approach zero. The integral along C_r also approaches zero. The calculation method of Eq. (D.7) is the same as what we do from Eq. (D.1) to Eq. (D.4). But there is a pole inside the integral contour. We should find out the residue of $f(z')$. That is

$$
\begin{aligned}
&\operatorname*{Re s}_{z' \to \sqrt{\mu\varepsilon(\Omega^2+i2\eta\Omega)-{k_z}^2}} (f(z')) \\
&= \lim_{z' \to \sqrt{\mu\varepsilon(\Omega^2+i2\eta\Omega)-{k_z}^2}} \frac{e^{iz'y}}{\sqrt{\frac{1}{\mu\varepsilon}\left({k_z}^2+z'^2\right)}} \left(z' - \sqrt{\mu\varepsilon\left(\Omega^2+i2\eta\Omega\right)-{k_z}^2}\right) \\
&\quad \times \frac{1}{\sqrt{\frac{1}{\mu\varepsilon}\left({k_z}^2+z'^2\right)}-i\eta-\Omega} \\
&= \frac{\mu\varepsilon \exp\left[i\sqrt{\mu\varepsilon\left(\Omega^2+i2\eta\Omega\right)-{k_z}^2}y\right]}{\sqrt{\mu\varepsilon\left(\Omega^2+i2\eta\Omega\right)-{k_z}^2}}
\end{aligned}
\tag{D.8}
$$

The Eq. (D.7) can be write as:

$$
\begin{aligned}
&\int_{-\infty}^{\infty} dk_y \frac{e^{i(k_y y)}}{\sqrt{\frac{1}{\mu\varepsilon}\left({k_z}^2+{k_y}^2\right)}} \frac{1}{\sqrt{\frac{1}{\mu\varepsilon}\left({k_z}^2+{k_y}^2\right)}-i\eta-\Omega} \; (y>0) \\
&= i\int_{\infty}^{k_z} dp \frac{e^{-py}}{\frac{1}{\mu\varepsilon}\left(p^2-{k_z}^2\right)+i\Omega\sqrt{\frac{1}{\mu\varepsilon}}\sqrt{\left(p^2-{k_z}^2\right)}} + i\int_{k_z}^{\infty} dp \frac{e^{-py}}{+\frac{1}{\mu\varepsilon}\left(p^2-{k_z}^2\right)-i\Omega\sqrt{\frac{1}{\mu\varepsilon}}\sqrt{p^2-{k_z}^2}} \\
&+ 2\pi i \frac{\mu\varepsilon \exp\left[i\sqrt{\mu\varepsilon\left(\Omega^2+i2\eta\Omega\right)-{k_z}^2}y\right]}{\sqrt{\mu\varepsilon\left(\Omega^2+i2\eta\Omega\right)-{k_z}^2}}.
\end{aligned}
\tag{D.9}
$$

By the same way, we can obtain:

$$
\begin{aligned}
&\int_{-\infty}^{\infty} dk_y \frac{e^{-i(k_y y)}}{\sqrt{\frac{1}{\mu\varepsilon}\left({k_z}^2+{k_y}^2\right)}} \frac{1}{\sqrt{\frac{1}{\mu\varepsilon}\left({k_z}^2+{k_y}^2\right)}+i\eta+\Omega} \; (y>0) \\
&= -\left\{ i\int_{\infty}^{k_z} dp \frac{e^{-py}}{\frac{1}{\mu\varepsilon}\left(p^2-{k_z}^2\right)+i\Omega\sqrt{\frac{1}{\mu\varepsilon}}\sqrt{p^2-{k_z}^2}} + i\int_{k_z}^{\infty} dp \frac{e^{-py}}{\frac{1}{\mu\varepsilon}\left(p^2-{k_z}^2\right)-i\Omega\sqrt{\frac{1}{\mu\varepsilon}}\sqrt{p^2-{k_z}^2}} \right\},
\end{aligned}
\tag{D.10}
$$

$$\int_{-\infty}^{\infty} dk_y \frac{e^{-i(k_y y)}}{\sqrt{\frac{1}{\mu\varepsilon}\left({k_z}^2+{k_y}^2\right)}} \frac{1}{\sqrt{\frac{1}{\mu\varepsilon}\left({k_z}^2+{k_y}^2\right)}+i\eta-\Omega}\ (y>0)$$
$$= -\left\{ i\int_{\infty}^{k_z} dp \frac{e^{-py}}{\frac{1}{\mu\varepsilon}\left(p^2-{k_z}^2\right)-i\Omega\sqrt{\frac{1}{\mu\varepsilon}}\sqrt{p^2-{k_z}^2}} + i\int_{k_z}^{\infty} dp \frac{e^{-py}}{\frac{1}{\mu\varepsilon}\left(p^2-{k_z}^2\right)+i\Omega\sqrt{\frac{1}{\mu\varepsilon}}\sqrt{p^2-{k_z}^2}} \right\}$$
$$-2\pi i\mu\varepsilon \frac{\exp\left[-i\sqrt{\mu\varepsilon\left(\Omega^2-i2\eta\Omega\right)-{k_z}^2}y\right]}{\sqrt{\mu\varepsilon\left(\Omega^2-i2\eta\Omega\right)-{k_z}^2}}. \tag{D.11}$$

Substituting the Eq. (D.5), Eq. (D.9), Eq. (D.10), and Eq. (D.11), into equation, we have

$$\mathbf{A}\left(\mathbf{r},t\right)$$
$$= -\frac{I_0}{4\pi\varepsilon d}\sum_m \sin\left(\frac{m\pi}{2}\right)\sin\left(\frac{m\pi}{d}z\right)\left\{ e^{-i\Omega t}2\pi i \frac{\mu\varepsilon\exp\left[i\sqrt{\mu\varepsilon\left(\Omega^2+i2\eta\Omega\right)-{k_z}^2}y\right]}{\sqrt{\mu\varepsilon\left(\Omega^2+i2\eta\Omega\right)-{k_z}^2}}\right.$$
$$\left. -e^{i\Omega t}2\pi i \frac{\mu\varepsilon\exp\left[-i\sqrt{\mu\varepsilon\left(\Omega^2-i2\eta\Omega\right)-{k_z}^2}y\right]}{\sqrt{\mu\varepsilon\left(\Omega^2-i2\eta\Omega\right)-{k_z}^2}}\right\}\hat{x}$$

The above equation is Eq. (3.31).

Appendix E

The derivation of electric field induced by ac line current in classical calculation

Here, we will derive the electric field induced by ac line charge current in parallel-plane waveguide with the means of classical electrodynamics. The system is the same as section 3-2 in this thesis. The infinite long wire carries ac electric current $\mathbf{I} = -I_0 \cos(\Omega t)\,\hat{x}$. We start with Jefimeko's equation:

$$\mathbf{E} = \frac{1}{4\pi\varepsilon_0} \int d\mathbf{r}' \left(\rho_c(\mathbf{r}', t_r) \frac{\mathbf{r}-\mathbf{r}'}{|\mathbf{r}-\mathbf{r}'|^3} + \frac{1}{c} \frac{\partial \rho_c(\mathbf{r}', t_r)}{\partial t} \frac{\mathbf{r}-\mathbf{r}'}{|\mathbf{r}-\mathbf{r}'|^2} - \frac{1}{c^2} \frac{1}{|\mathbf{r}-\mathbf{r}'|} \frac{\partial \mathbf{J}(\mathbf{r}', t_r)}{\partial t} \right), \tag{E.1}$$

where $t_r \equiv t - \frac{|\mathbf{r}-\mathbf{r}'|}{c}$ is the retarded time, $\rho_c(\mathbf{r}', t_r)$ is the charge density at $\mathbf{r} = \mathbf{r}'$ at $t = t_r$, $\mathbf{J}(\mathbf{r}', t_r)$ is the current density at $\mathbf{r} = \mathbf{r}'$ and $t = t_r$, c is the light speed.

We utilize image current to calculate the electric field in the waveguide. For simplifying the calculation, we assume the wire is deposited along x-axis. If the wire is in free space, the electric field is given by:

$$
\begin{aligned}
\mathbf{E}'_0 &= \frac{1}{4\pi\varepsilon_0}\int d\mathbf{r}'\left(\rho_c(\mathbf{r}',t_r)\frac{\mathbf{r}-\mathbf{r}'}{|\mathbf{r}-\mathbf{r}'|^3}+\frac{1}{c}\frac{\partial\rho_c(\mathbf{r}',t_r)}{\partial t}\frac{\mathbf{r}-\mathbf{r}'}{|\mathbf{r}-\mathbf{r}'|^2}-\frac{1}{c^2}\frac{1}{|\mathbf{r}-\mathbf{r}'|}\frac{\partial\mathbf{J}(\mathbf{r}',t_r)}{\partial t}\right)\\
&= \frac{1}{4\pi\varepsilon_0}\int dx'\left(\frac{1}{c^2}\frac{I_0}{|\mathbf{r}-\mathbf{r}'|}\frac{\partial\cos(\Omega t_r)}{\partial t}\hat{x}\right)\\
&= \frac{1}{4\varepsilon_0}\frac{1}{c^2}I_0\Omega\left\{\sin(\Omega t)\,Y_0\left(\frac{\Omega}{c}\rho\right)+\cos(\Omega t)\,J_0\left(\frac{\Omega}{c}\rho\right)\right\}\hat{x}
\end{aligned}
\tag{E.2}
$$

where $\rho=\sqrt{y^2+z^2}$. If the wire is located at $(x,0,d/2)$, the field becomes

$$
\begin{aligned}
\mathbf{E}_0 = \frac{1}{4\varepsilon_0}\frac{I_0}{c^2}\Omega\Bigg\{&\sin(\Omega t)\,Y_0\left(\frac{\Omega}{c}\sqrt{y^2+\left(z-\frac{3}{2}d\right)^2}\right)\\
&+\cos(\Omega t)\,J_0\left(\frac{\Omega}{c}\sqrt{y^2+\left(z-\frac{3}{2}d\right)^2}\right)\Bigg\}\hat{x}
\end{aligned}
\tag{E.3}
$$

The electric field we solve Eq. (E.3) is induced by ac line charge current in free space. If we put two metal gates at $z=0$ and $z=d$, we must add the field induced by its image current. the total field is:

$$
\begin{aligned}
\mathbf{E}(\mathbf{r},t) = \sum_{n=-\infty}^{\infty}(-1)^n\frac{1}{4\varepsilon_0}\frac{I_0}{c^2}\Omega\Bigg\{&\sin(\Omega t)\,Y_0\left(\frac{\Omega}{c}\sqrt{y^2+\left(z-\frac{1+2n}{2}d\right)^2}\right)\\
&+\cos(\Omega t)\,J_0\left(\frac{\Omega}{c}\sqrt{y^2+\left(z-\frac{1+2n}{2}d\right)^2}\right)\Bigg\}\hat{x}
\end{aligned}
\tag{E.4}
$$

Applying Poisson summation formula, Eq. (E.4) becomes:

For $\frac{\Omega}{c}>\frac{m\pi}{d}$

$$
\mathbf{E}^{>}(\mathbf{r},t)=\frac{\mu I_0\Omega}{d}\sin\left(\frac{m\pi}{2}\right)\sin\left(\frac{m\pi}{d}z\right)\sum_{\substack{m>0\\ m=odd}}\left\{\frac{\cos\left(\sqrt{\mu\varepsilon\Omega^2-\left(\frac{m\pi}{d}\right)^2}\,|y|-\Omega t\right)}{\sqrt{\mu\varepsilon\Omega^2-\left(\frac{m\pi}{d}\right)^2}}\right\}\hat{x};
\tag{E.5}
$$

for $\frac{\Omega}{c} < \frac{m\pi}{d}$

$$\mathbf{E}^{>}(\mathbf{r},t) = -\frac{\mu I_0 \Omega}{d} \sum_{m=0}^{\infty} \sin\left(\frac{m\pi}{2}\right) \sin\left(\frac{m\pi}{d} z\right) \left\{ \frac{\exp\left(-\sqrt{\left(\frac{m\pi}{d}\right)^2 - \mu\varepsilon\Omega^2}\,|y|\right)}{\sqrt{\left(\frac{m\pi}{d}\right)^2 - \mu\varepsilon\Omega^2}} \sin(\Omega t) \right\}. \tag{E.6}$$

The total electric field is $\mathbf{E}(\mathbf{r},t) = \mathbf{E}^{>}(\mathbf{r},t) + \mathbf{E}^{<}(\mathbf{r},t)$. The Eq. (E.5) and Eq. (E.6) are the same as the calculation in Eq. (3.37) and Eq. (3.38) which are solved by semi-classical method.

Appendix F

The complex integral III

In this appendix, we derive Eq. (4.18) and Eq. (4.19) from Eq. (4.16) briefly. Let's solve the first integral term $F_1 = \int_{-\infty}^{\infty} dk_y \frac{\mu\varepsilon k_y}{{k_y}^2+{k_z}^2} \frac{\exp[i\Omega t]}{\sqrt{\frac{1}{\mu\varepsilon}\left({k_y}^2+{k_z}^2\right)}-i\eta+\Omega} e^{ik_y y}$.

Let $k_y = z'$. For $y > 0$, $\frac{z'}{z'^2+{k_z}^2} \frac{\exp[i\Omega t]}{\sqrt{\frac{1}{\mu\varepsilon}\left(z'^2+{k_z}^2\right)}-i\eta+\Omega}$ has two branch points located at $z' = ik_z$ and $z' = -ik_z$ respectively on the complex plane. The contour must not close any branch point and branch cuts. We take the contour and the cut lines as Fig. F.1, and the two red arrows are the branch cut that we choose.

The contour we choose closes no pole on the complex plane. So we have:

$$\mu\varepsilon \oint_{C_R+\Gamma_1+\Gamma_2+C_r+\Gamma_3} dz' \frac{z'}{z'^2+{k_z}^2} \times \frac{\exp\left[i\Omega t\right]}{\sqrt{\frac{1}{\mu\varepsilon}\left(z'^2+{k_z}^2\right)}-i\eta+\Omega} e^{iz'y} = 0 \tag{F.1}$$

The section of the contour C_R is a semicircle with infinite radius and the integral along C_R approaches zero. Then Eq. (F.1) can be rewrite as

$$\begin{aligned} &\int_{-\infty}^{\infty} dz' \frac{\mu\varepsilon z'}{z'^2+{k_z}^2} \frac{\exp\left[i\Omega t\right]}{\sqrt{\frac{1}{\mu\varepsilon}\left(z'^2+{k_z}^2\right)}-i\eta+\Omega} e^{iz'y} \\ &= -\int\limits_{\Gamma_2+C_r+\Gamma_3} dz' \frac{\mu\varepsilon z'}{z'^2+{k_z}^2} \frac{\exp\left[i\Omega t\right]}{\sqrt{\frac{1}{\mu\varepsilon}\left(z'^2+{k_z}^2\right)}-i\eta+\Omega} e^{iz'y} \end{aligned} \tag{F.2}$$

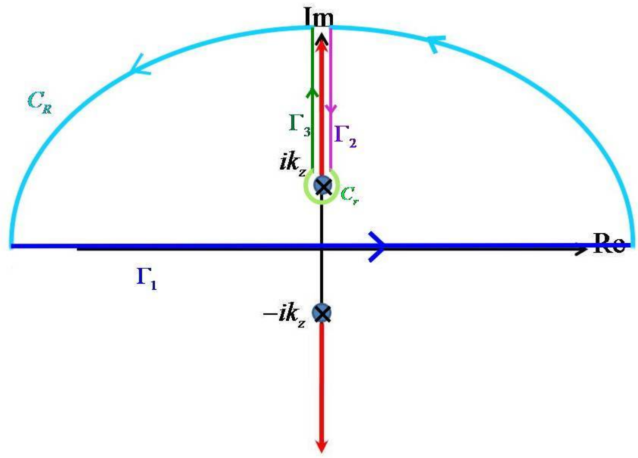

Figure F.1: The illustration shows the contour we choose in Eq. (F.1) on the complex plane of z'. The contour can be separated with five sections, Γ_1, Γ_2, Γ_3, C_r, C_R. $\frac{z'}{z'^2+k_z{}^2}\frac{\exp[i\Omega t]}{\sqrt{\frac{1}{\mu\varepsilon}\left(z'^2+k_z{}^2\right)-i\eta+\Omega}}$ has two branch points located at $z'=ik_z$ and $z'=-ik_z$ respectively on the complex plane. The red allows are the branch cuts we choose.

There are three path integral in Eq. (F.2). We solve the integral $\int_{\Gamma_2} dz' \frac{z'}{z'^2+k_z{}^2}\frac{1}{\sqrt{\frac{1}{\mu\varepsilon}}\sqrt{z'^2+k_z{}^2}-i\eta+\Omega}e^{iz'y}$ first. Let $z'-ik_z=r_1e^{i\theta_1}$, $z'=ip$; $dz'=idp$.

We already chosen the branch cuts on the complex plane, so we have$-\frac{3}{2}\pi \leq \theta_1 < \frac{1}{2}\pi$ and $-\frac{\pi}{2} \leq \theta_2 < \frac{3}{2}\pi$. For the integration path Γ_2: $\theta_1 = \frac{1}{2}\pi$, $\theta_2=\frac{1}{2}\pi$, and $z'=ip$. Therefore, $z'-ik_z=r_1e^{i\theta_1} \Rightarrow i\left(p-k_z\right)=r_1e^{i\frac{1}{2}\pi} \Rightarrow r_1=p-k_z$. For the same reason, $z'+ik_z=r_2e^{i\theta_2} \Rightarrow i\left(p+k_z\right)=r_2e^{i\frac{\pi}{2}} \Rightarrow r_2=p+k_z$

$$\begin{aligned}
&\int_{\Gamma_2} dz'\frac{z'}{z'^2+k_z{}^2}\times\frac{1}{\sqrt{\frac{1}{\mu\varepsilon}}\sqrt{z'^2+k_z{}^2}-i\eta+\Omega}e^{iz'y}\\
&=\int_{\Gamma_2} dz'\frac{z'}{r_1e^{i\theta_1}r_2e^{i\theta_2}}\times\frac{1}{\sqrt{\frac{1}{\mu\varepsilon}}\sqrt{r_1r_2}e^{i(\theta_1+\theta_2)/2}-i\eta+\Omega}e^{iz'y}\\
&=\int_{\infty}^{k_z} dp\frac{p}{\left(p^2-k_z{}^2\right)}\times\frac{1}{\Omega+i\sqrt{\frac{1}{\mu\varepsilon}}\sqrt{p^2-k_z{}^2}}e^{-py}
\end{aligned} \tag{F.3}$$

Then we solve the integral $\int_{\Gamma_3} dz' \frac{z'}{z'^2+{k_z}^2} \times \frac{1}{\sqrt{\frac{1}{\mu\varepsilon}}\sqrt{z'^2+{k_z}^2}-i\eta+\Omega} e^{iz'y}$. Let $z' - ik_z = r_1 e^{i\theta_1}$, $z' + ik_z = r_2 e^{i\theta_2}$, $z' = ip$, and $dz' = idp$.

For the branch cuts we choose: $-\frac{3}{2}\pi \le \theta_1 < \frac{1}{2}\pi$, $-\frac{\pi}{2} \le \theta_2 < \frac{3}{2}\pi$. η is small enough to be neglected. For the integration path $\theta_1 = -\frac{3}{2}\pi$

$$z' - ik_z = r_1 e^{i\theta_1} \;\Rightarrow\; r_1 = p - k_z.$$

For the same reason $\theta_2 = \frac{1}{2}\pi$

$$z' + ik_z = r_2 e^{i\theta_2} \;\Rightarrow\; i\left(p + k_z\right) = r_2 e^{i\frac{\pi}{2}} \;\Rightarrow\; r_2 = p + k_z.$$

$$\begin{aligned}
&\int_{\Gamma_3} dz' \frac{z'}{z'^2+{k_z}^2} \times \frac{1}{\sqrt{\frac{1}{\mu\varepsilon}}\sqrt{z'^2+{k_z}^2}-i\eta+\Omega} e^{iz'y} \\
&= \int_{\Gamma_2} dz' \frac{z'}{r_1 e^{i\theta_1} r_2 e^{i\theta_2}} \times \frac{1}{\sqrt{\frac{1}{\mu\varepsilon}}\sqrt{r_1 r_2} e^{i(\theta_1+\theta_2)/2}-i\eta+\Omega} e^{iz'y} \\
&= \int_{k_z}^{\infty} dp \frac{p}{\left(p^2-{k_z}^2\right)} \times \frac{1}{\Omega - i\sqrt{\frac{1}{\mu\varepsilon}}\sqrt{p^2-{k_z}^2}} e^{-py}
\end{aligned} \tag{F.4}$$

Then we solve the integral

$$\int_{C_r} dz' \frac{z'}{z'^2+{k_z}^2} \frac{1}{\sqrt{\frac{1}{\mu\varepsilon}}\sqrt{z'^2+{k_z}^2}-i\eta+\Omega} e^{iz'y}$$

. Let $z' - ik_z = \varepsilon e^{i\theta_1} \Rightarrow z' = ik_z + \varepsilon e^{i\theta_1} \Rightarrow dz' = i\varepsilon e^{i\theta_1} d\theta_1$ and $z' + ik_z = r_2 e^{i\theta_2}$, where ε is positive real number which approach to zero. We define :$-\frac{3}{2}\pi \le \theta_1 < \frac{1}{2}\pi$ and $-\frac{\pi}{2} \le \theta_2 < \frac{3}{2}\pi$. For the integration path C_r: $-\frac{3}{2}\pi \le \theta_1 < \frac{1}{2}\pi$F$\theta_2 = \frac{1}{2}\pi$ and $r_2 = 2k_z$. The

η in the denominator is small enough to be neglected and $\theta_2 = \frac{1}{2}\pi$.

$$\begin{aligned}
&\int_{C_r} dz' \frac{z'}{z'^2 + {k_z}^2} \times \frac{1}{\sqrt{\frac{1}{\mu\varepsilon}}\sqrt{z'^2 + {k_z}^2} - i\eta + \Omega} e^{iz'y} \\
&= \int_{C_r} i\varepsilon e^{i\theta_1} d\theta_1 \frac{ik_z + \varepsilon e^{i\theta_1}}{\varepsilon r_2 e^{i\theta_1} e^{i\theta_2}} \times \frac{1}{\sqrt{\frac{1}{\mu\varepsilon}}\sqrt{\varepsilon r_2} e^{i(\theta_1+\theta_2)/2} - i\eta + \Omega} \exp\left[i\left(ik_z + \varepsilon e^{i\theta_1}\right) y\right] \\
&= \int_{\theta_1 = \frac{\pi}{2}}^{-\frac{3}{2}\pi} i\varepsilon e^{i\theta_1} d\theta_1 \frac{ik_z}{i\varepsilon r_2 e^{i\theta_1}} \times \frac{1}{-i\eta + \Omega} \exp\left[-k_z y\right] \\
&= -\pi i \frac{1}{\Omega} \exp\left[-k_z y\right]
\end{aligned} \tag{F.5}$$

Substituting Eq. (F.3), Eq. (F.4), Eq. (F.5), into Eq. (F.2), we obtain:

$$\begin{aligned}
F_1 &= \int_{-\infty}^{\infty} dz \frac{\mu\varepsilon z}{z^2 + {k_z}^2} \frac{\exp\left[i\Omega t\right]}{\sqrt{\frac{1}{\mu\varepsilon}\left(z^2 + {k_z}^2\right)} - i\eta + \Omega} e^{izy} \quad (y > 0) \\
&= -\mu\varepsilon \exp\left[i\Omega t\right] \left\{ \int_{\infty}^{k_z} dp \frac{p}{\left(p^2 - {k_z}^2\right)} \times \frac{1}{\Omega + i\sqrt{\frac{1}{\mu\varepsilon}}\sqrt{p^2 - {k_z}^2}} e^{-py} \right. \\
&\quad \left. + \int_{k_z}^{\infty} dp \frac{p}{\left(p^2 - {k_z}^2\right)} \times \frac{1}{\Omega - i\sqrt{\frac{1}{\mu\varepsilon}}\sqrt{p^2 - {k_z}^2}} e^{-py} - \pi i \frac{1}{\Omega} \exp\left[-k_z y\right] \right\}
\end{aligned} \tag{F.6}$$

Then we deal with the integral

$$F_2 = \int_{-\infty}^{\infty} dk_y \frac{\mu\varepsilon k_y}{{k_y}^2 + {k_z}^2} \frac{\exp\left[-i\Omega t\right]}{\sqrt{\frac{1}{\mu\varepsilon}\left({k_y}^2 + {k_z}^2\right)} - i\eta - \Omega} e^{ik_y y} \ .$$

The contour we choose and the steps of calculation is the same as we work out F_1, except that there is a pole in the contour of F_2 we choose. Let

$$f'\left(k_y\right) = \frac{\mu\varepsilon k_y}{{k_y}^2 + {k_z}^2} \frac{\exp\left[-i\Omega t\right]}{\sqrt{\frac{1}{\mu\varepsilon}\left({k_y}^2 + {k_z}^2\right)} - i\eta - \Omega} e^{ik_y y}.$$

We choose the contour for F_2 which is shown as Fig. F.2 and the contour closes a pole at $\sqrt{\mu\varepsilon\left(\Omega^2 + i2\eta\Omega\right) - {k_z}^2}$. We get the following equation, using Jordan's lemma theorem.

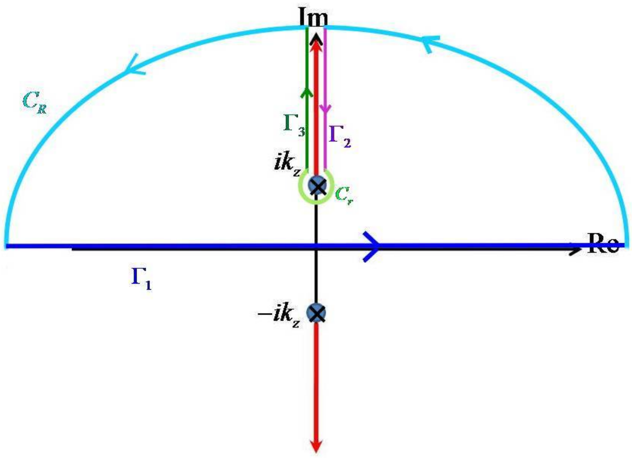

Figure F.2: There are still two poles at $\pm\sqrt{\mu\varepsilon\left(\Omega^2+i2\eta\Omega\right)-{k_z}^2}$ which we do not show here. The section of integral Γ_1 is the integral from negative infinity to infinity x. The two red arrows are the cut lines which are from the points ik_z and $-ik_z$ respectively to infinity and negative infinity.

$$\begin{aligned}&\oint_{C_R+\Gamma_1+\Gamma_2+C_r+\Gamma_3} dk_y \frac{\mu\varepsilon k_y}{{k_y}^2+{k_z}^2}\times\frac{\exp\left[-i\Omega t\right]}{\sqrt{\frac{1}{\mu\varepsilon}\left({k_y}^2+{k_z}^2\right)}-i\eta-\Omega}e^{ik_y y}\\&=2\pi i \underset{k_y\to+\sqrt{\mu\varepsilon\Omega^2-{k_z}^2}}{\operatorname{Re}s}\left(f'\left(k_y\right)\right)\end{aligned} \tag{F.7}$$

The integral

$$\oint_{C_R} dk_y \frac{\mu\varepsilon k_y}{{k_y}^2+{k_z}^2}\times\frac{\exp\left[-i\Omega t\right]}{\sqrt{\frac{1}{\mu\varepsilon}\left({k_y}^2+{k_z}^2\right)}-i\eta-\Omega}e^{ik_y y}$$

is equal to zero, because $\frac{\mu\varepsilon k_y}{{k_y}^2+{k_z}^2}\times\frac{\exp[-i\Omega t]}{\sqrt{\frac{1}{\mu\varepsilon}\left({k_y}^2+{k_z}^2\right)}-i\eta-\Omega}$ will vanish for $|k_y|\to\infty$ on the upper half-plane.

$$
\begin{aligned}
&\int_{-\infty}^{\infty} dk_y \frac{\mu\varepsilon k_y}{{k_y}^2+{k_z}^2} \times \frac{\exp\left[-i\Omega t\right]}{\sqrt{\frac{1}{\mu\varepsilon}\left({k_y}^2+{k_z}^2\right)}-i\eta-\Omega} e^{ik_y y} \\
&= -\mu\varepsilon \int\limits_{\Gamma_2+C_r+\Gamma_3} dk_y \frac{k_y}{{k_y}^2+{k_z}^2} \times \frac{\exp\left[-i\Omega t\right]}{\sqrt{\frac{1}{\mu\varepsilon}\left({k_y}^2+{k_z}^2\right)}-i\eta-\Omega} e^{ik_y y} \\
&\quad + 2\pi i \operatorname*{Re s}_{k_y\to+\sqrt{\mu\varepsilon\Omega^2-{k_z}^2}} \left(f'\left(k_y\right)\right)
\end{aligned}
\tag{F.8}
$$

The residue of $f'\left(k_y\right)$ can be written as:

$$
\begin{aligned}
&\operatorname*{Re s}_{k_y\to\sqrt{\mu\varepsilon\left(\Omega^2+i2\eta\Omega\right)-{k_z}^2}} \left(f'\left(k_y\right)\right) \\
&= \lim_{k_y\to\sqrt{\mu\varepsilon\left(\Omega^2+i2\eta\Omega\right)-{k_z}^2}} \left(k_y-\sqrt{\mu\varepsilon\left(\Omega^2+i2\eta\Omega\right)-{k_z}^2}\right) \frac{\mu\varepsilon k_y}{{k_y}^2+{k_z}^2} \\
&\times \frac{\exp\left[-i\Omega t\right]}{\sqrt{\frac{1}{\mu\varepsilon}\left({k_y}^2+{k_z}^2\right)}-i\eta-\Omega} e^{ik_y y} \\
&= \frac{\mu\varepsilon}{\Omega} \exp\left[i\left(\sqrt{\mu\varepsilon\left(\Omega^2+i2\eta\Omega\right)-{k_z}^2} y-\Omega t\right)\right]
\end{aligned}
$$

We can solve the path integral the same as we deal with F_1. Hence, we obtain

$$
\begin{aligned}
F_2 &= \int_{-\infty}^{\infty} dk_y \frac{\mu\varepsilon k_y}{{k_y}^2+{k_z}^2} \frac{\exp\left[-i\Omega t\right]}{\sqrt{\frac{1}{\mu\varepsilon}\left({k_y}^2+{k_z}^2\right)}-i\eta-\Omega} e^{ik_y y} \quad (y>0) \\
&= -\mu\varepsilon \exp\left[-i\Omega t\right] \left\{ -\int_{\infty}^{k_z} dp \frac{p}{\left(p^2-{k_z}^2\right)} \times \frac{1}{\Omega - i\sqrt{\frac{1}{\mu\varepsilon}}\sqrt{p^2-{k_z}^2}} e^{-py} \right. \\
&\quad \left. -\int_{k_z}^{\infty} dp \frac{p}{\left(p^2-{k_z}^2\right)} \times \frac{1}{\Omega + i\sqrt{\frac{1}{\mu\varepsilon}}\sqrt{p^2-{k_z}^2}} e^{-py} + \pi i \frac{1}{\Omega}\exp\left[-k_z y\right] \right\} \\
&\quad + 2\pi i \left(\frac{\mu\varepsilon}{\Omega} \exp\left[i\left(\sqrt{\mu\varepsilon\left(\Omega^2+i2\eta\Omega\right)-{k_z}^2} y-\Omega t\right)\right]\right)
\end{aligned}
\tag{F.9}
$$

By the same way, we can solve $F_3,\ F_4,\ G_1,\ G_2,\ G_3,\ G_4,$:

$$
\begin{aligned}
F_3 &= \int_{-\infty}^{\infty} dk_y \frac{\mu\varepsilon k_y}{{k_y}^2+{k_z}^2} \frac{\exp\left[-i\Omega t\right]}{\sqrt{\frac{1}{\mu\varepsilon}\left({k_y}^2+{k_z}^2\right)}+i\eta+\Omega} e^{-ik_y y} \quad (y>0) \\
&= -\mu\varepsilon \exp\left[-i\Omega t\right] \left\{ \int_{\infty}^{k_z} dp \frac{p}{\left(p^2-{k_z}^2\right)} \times \frac{1}{\Omega - i\sqrt{\frac{1}{\mu\varepsilon}\left(p^2-{k_z}^2\right)}} e^{-py} \right. \\
&\quad \left. + \int_{k_z}^{\infty} dp \frac{p}{\left(p^2-{k_z}^2\right)} \times \frac{1}{\Omega + i\sqrt{\frac{1}{\mu\varepsilon}\left(p^2-{k_z}^2\right)}} e^{-py} + \pi i \frac{1}{\Omega} e^{-k_z y} \right\}
\end{aligned} \tag{F.10}
$$

$$
\begin{aligned}
F_4 &= \int_{-\infty}^{\infty} dk_y \frac{\mu\varepsilon k_y}{{k_y}^2+{k_z}^2} \frac{\exp\left[i\Omega t\right]}{\sqrt{\frac{1}{\mu\varepsilon}\left({k_y}^2+{k_z}^2\right)}+i\eta-\Omega} e^{-ik_y y} \quad (y>0) \\
&= -\mu\varepsilon \exp\left[i\Omega t\right] \left\{ -\int_{\infty}^{k_z} dp \frac{p}{\left(p^2-{k_z}^2\right)} \times \frac{1}{\Omega + i\sqrt{\frac{1}{\mu\varepsilon}\left(p^2-{k_z}^2\right)}} e^{-py} \right. \\
&\quad \left. - \int_{k_z}^{\infty} dp \frac{p}{\left(p^2-{k_z}^2\right)} \times \frac{1}{\Omega - i\sqrt{\frac{1}{\mu\varepsilon}\left(p^2-{k_z}^2\right)}} e^{-py} - \pi i \frac{1}{\Omega} e^{-k_z y} \right\} \\
&\quad - 2\pi i \frac{\mu\varepsilon}{\Omega} \exp\left(-i\sqrt{\mu\varepsilon\left(\Omega^2 - i2\eta\Omega\right) - {k_z}^2} y + i\Omega t\right)
\end{aligned} \tag{F.11}
$$

$$
\begin{aligned}
G_1 &= \int_{-\infty}^{\infty} dk_y \frac{\mu\varepsilon {k_y}^2}{{k_y}^2+{k_z}^2} \times \frac{\exp\left[+i\Omega t\right]}{\sqrt{\frac{1}{\mu\varepsilon}\left({k_y}^2+{k_z}^2\right)}-i\eta+\Omega} e^{ik_y y} \\
&= -\mu\varepsilon \exp\left[i\Omega t\right] \left\{ i \int_{\infty}^{k_z} dp \frac{p^2}{\left(p^2-{k_z}^2\right)} \times \frac{1}{\Omega + i\sqrt{\frac{1}{\mu\varepsilon}}\sqrt{p^2-{k_z}^2}} e^{-py} \right. \\
&\quad \left. + i \int_{k_z}^{\infty} dp \frac{p^2}{\left(p^2-{k_z}^2\right)} \times \frac{1}{\Omega - i\sqrt{\frac{1}{\mu\varepsilon}}\sqrt{p^2-{k_z}^2}} e^{-py} + \pi k_z \times \frac{1}{\Omega} e^{-k_z y} \right\}
\end{aligned} \tag{F.12}
$$

$$G_2 = \int_{-\infty}^{\infty} dk_y \frac{\mu\varepsilon {k_y}^2}{{k_y}^2 + {k_z}^2} \times \frac{\exp\left[-i\Omega t\right]}{\sqrt{\frac{1}{\mu\varepsilon}\left({k_y}^2 + {k_z}^2\right)} - i\eta - \Omega} e^{ik_y y}$$
$$= -\mu\varepsilon \exp\left[-i\Omega t\right] \left\{ -i \int_{\infty}^{k_z} dp \frac{p^2}{\left(p^2 - {k_z}^2\right)} \times \frac{1}{\Omega - i\sqrt{\frac{1}{\mu\varepsilon}}\sqrt{p^2 - {k_z}^2}} e^{-py} \right.$$
$$\left. -i \int_{k_z}^{\infty} dp \frac{p^2}{\left(p^2 - {k_z}^2\right)} \times \frac{1}{\Omega + i\sqrt{\frac{1}{\mu\varepsilon}}\sqrt{p^2 - {k_z}^2}} e^{-py} - \pi k_z \times \frac{1}{\Omega} \exp\left[-k_z y\right] \right\}$$
$$+ 2\pi i \frac{\mu\varepsilon}{\Omega} \sqrt{\mu\varepsilon\left(\Omega^2 + i2\eta\Omega\right) - {k_z}^2} \exp\left[i\left(\sqrt{\mu\varepsilon\left(\Omega^2 + i2\eta\Omega\right) - {k_z}^2} y - \Omega t\right)\right] \tag{F.13}$$

$$G_3 = \int_{-\infty}^{\infty} dk_y \frac{\mu\varepsilon {k_y}^2}{{k_y}^2 + {k_z}^2} \times \frac{\exp\left[-i\Omega t\right]}{\sqrt{\frac{1}{\mu\varepsilon}\left({k_y}^2 + {k_z}^2\right)} + i\eta + \Omega} e^{-ik_y y}$$
$$= -\mu\varepsilon \exp\left[-i\Omega t\right] \left\{ -i \int_{\infty}^{k_z} dp \frac{p^2}{\left(p^2 - {k_z}^2\right)} \times \frac{1}{\Omega - i\sqrt{\frac{1}{\mu\varepsilon}\left(p^2 - {k_z}^2\right)}} e^{-py} \right.$$
$$\left. - i \int_{k_z}^{\infty} dp \frac{p^2}{\left(p^2 - {k_z}^2\right)} \times \frac{1}{\Omega + i\sqrt{\frac{1}{\mu\varepsilon}\left(p^2 - {k_z}^2\right)}} e^{-py} + \pi k_z \times \frac{1}{\Omega} e^{-k_z y} \right\} \tag{F.14}$$

$$G_4 = \int_{-\infty}^{\infty} dk_y \frac{\mu\varepsilon {k_y}^2}{{k_y}^2 + {k_z}^2} \times \frac{\exp\left[i\Omega t\right]}{\sqrt{\frac{1}{\mu\varepsilon}\left({k_y}^2 + {k_z}^2\right)} + i\eta - \Omega} e^{-ik_y y}$$
$$= -\mu\varepsilon \exp\left[i\Omega t\right] \left\{ i \int_{\infty}^{k_z} dp \frac{p^2}{\left(p^2 - {k_z}^2\right)} \times \frac{1}{\Omega + i\sqrt{\frac{1}{\mu\varepsilon}\left(p^2 - {k_z}^2\right)}} e^{-py} \right.$$
$$\left. +i \int_{k_z}^{\infty} dp \frac{p^2}{\left(p^2 - {k_z}^2\right)} \times \frac{1}{\Omega - i\sqrt{\frac{1}{\mu\varepsilon}\left(p^2 - {k_z}^2\right)}} e^{-py} - \pi k_z \times \frac{1}{\Omega} e^{-k_z y} \right\}$$
$$- 2\pi i \frac{\mu\varepsilon}{\Omega} \sqrt{\mu\varepsilon\left(\Omega^2 - i2\eta\right) - {k_z}^2} \exp\left[-i\left(\sqrt{\mu\varepsilon\left(\Omega^2 - i2\eta\Omega\right) - {k_z}^2} y - \Omega t\right)\right] \tag{F.15}$$

where $\mu\varepsilon\Omega^2 > {k_z}^2 \;\Rightarrow\; \sqrt{\mu\varepsilon\left(\Omega^2 + i2\eta\Omega\right) - {k_z}^2} \approx \sqrt{\mu\varepsilon\Omega^2 - {k_z}^2}$

; if $\mu\varepsilon\Omega^2 < {k_z}^2 \Rightarrow \sqrt{\mu\varepsilon\left(\Omega^2 + i2\eta\Omega\right) - {k_z}^2} \approx i\sqrt{{k_z}^2 - \mu\varepsilon\Omega^2}$

; if $\mu\varepsilon\Omega^2 > {k_z}^2 \Rightarrow \sqrt{\mu\varepsilon\left(\Omega^2 + i2\eta\Omega\right) - {k_z}^2} \approx \sqrt{\mu\varepsilon\Omega^2 - {k_z}^2}$

; if $\mu\varepsilon\Omega^2 < {k_z}^2 \Rightarrow \sqrt{\mu\varepsilon\left(\Omega^2 - i2\eta\Omega\right) - {k_z}^2} \approx -i\sqrt{{k_z}^2 - \mu\varepsilon\Omega^2}$.

Bibliography

[1] Igor Zutic, Jaroslav Fabian, and S. Das Sarma, Rev. Mod. Phys. 76, No. 2 (2004)

[2] *Spin-Orbit Coupling in Two-Dimensional Electron and Hole systems*, Roland Winkler (Springer, 2003).

[3] P. Mohanty, G. Zolfagharkhani, S. Kettemann, and P. Fulde, Phys. Rev. B 70, 195301 (2004)

[4] E. B. Sonin, Phys. Rev. Lett. 99, 266602 (2007)

[5] Brian A. Ruzicka, Karl Higley, Lalani K. Werake, and Hui Zhao, Phys. Rev. B 78, 045314 (2008)

[6] Jiang-Tao Liu and Kai Chang, Phys. Rev. B 78, 113304 (2008)

[7] Jing Wang, Bang-Fen Zhu, and Ren-Bao Liu, Phys. Rev. Lett. 100, 086603 (2008).

[8] Gerd Bergmann, Phys. Rev. B 63, 193101 (2001)

[9] R.M. Potok, J. A. Folk, C.M. Marcus, and V. Umansky, Phys. Rev. Lett. 99, 266602 (2002)

[10] A. G. Malshukov, C. S. Tang, C. S. Chu, and K. A. Chao, B 68, 233307 (2003)

[11] M. Johnson and R. H. Silsbee, Phys. Rev. Lett. 55, 1790 (1985).

[12] Q. F. Sun, H. Guo, and J. Wang, Phys. Rev. B 69, 054409 (2004).

[13] *An introduction to quantum field theory*, M.E. Peskin and H.D. Schroeder.

[14] *Lectures on quantum mechanics*, Gordon Baym (1969)

[15] *Fundamentals of the theory of metals*, A.A. Abrikosov (1988)

[16] *CRC Handbook of Chemistry and Physics 63RD Edition,19* David R. Lide (1982).

[17] K. M. Lakin and J. S. Wang, Appl. Phys. Lett. 38, no. 3, pp. 125-127, (1981).

[18] V. F. Motsnyi, J. De Boeck, J. Das, W. Van Roy, G. Borghs, E. Goovaerts, and V. I. Safarov, Appl. Phys. Lett. 81, 265 (2002)

[19] Amanda Fournier, Gerd Bergmann, and Richard S. Thompson, Phys. Rev. B 75, 233101 (2007)

[20] *Mathematical methods for physicists 5ed.*, Arfken G.B., Weber H.J (2001)